

Project Number: HXA 1503

Rehabilitative Adult Tricycle

A Major Qualifying Project Report

Submitted to the Faculty

of the

WORCESTER POLYTECHNIC INSTITUTE

in partial fulfillment of the requirements for the

Degree of Bachelor of Science

in Mechanical Engineering

by

Eric Correia
Jaime Espinola
James Gruenbaum
John Papa

Date: April 28, 2016

Advisors:



WPI

Professor Holly Ault
Professor Allen Hoffman

This report represents the work of WPI undergraduate students. It has been submitted to the faculty as evidence of completion of a degree requirement. WPI publishes these reports on its website without editorial or peer review.

Abstract

Each year, 800,000 people experience a stroke in the United States, and many develop hemiparesis, a weakness occurring on one side of the body. Exercise is proven to be helpful in recovery from stroke. The goal of this project was to develop a human-powered device that can aid in recovery from a stroke, while also serving a recreational purpose. This project resulted in the creation of a tricycle, which stores the pedaling energy of the strong leg with a spring in order to assist the weak leg in pedaling. Testing with force plates demonstrated that the force required to pedal the weak side with the highest spring constant was 49% lower than the baseline with no spring. The tricycle was a good proof of concept and with further modifications could be a viable tricycle in the future.

Acknowledgements

The following people and organizations greatly assisted in the completion of this project, and we would like to thank them for their support:

Scott Guzman: Scott is a WPI alumnus. He provided us with feedback about the feasibility of many aspects of our design and provided us with advice about how to improve the design. In addition, Scott performed all of the welding for the build, including the seat extender, frame, and the spring sprocket support plate. Scott's welding was very helpful, as none of the group members had prior experience welding.

Burt Seger: Burt owns a small machine shop in Jefferson, MA. His machining work greatly expedited the manufacturing process. In just two brief visits, Burt was able to machine both the spring sprocket plate and the handlebar extenders to our desired specifications. In addition, Burt was very hospitable, allowing us to run some of his machines, and giving us advice to assist us in our future careers.

Worcester Earn-a-Bike: This organization allows volunteers to earn their own bike for free in exchange for performing work for the shop. The staff of Earn-a-Bike are very knowledgeable about bikes, and helped us install the brakes and sprockets to the tricycle. In addition, they sold us many of the components of our design for a reasonable price, including the BMX bike we used as part of the frame, and the cranksets we used to connect the spring sprocket mechanism.

Authorship

Abstract.....	EC
Introduction.....	EC
Literature Review.....	ALL
Strokes	JE
Goals for Rehabilitation.....	JG
Benefits of Recreational Therapy	JE, EC
Existing Therapies and Devices.....	JE, JP
Mechanics Involved in Cycling	EC
Mechanisms	EC, JP, JG
Goal Statement.....	JE
Design Specifications.....	JE, EC
Power Adjustability	JE, EC
Ergonomics	JE, EC
Cost	JE, EC
Manufacturability.....	JE, EC
Safety	JE, EC
Range of Motion	JE, EC
User Requirements.....	JE, EC
Stability.....	JE, EC
Preliminary Design Concepts.....	ALL
Design 1: Piston	EC
Design 2: Motor	EC
Design 3: Planetary Gear	JG
Design 4: Continuously Variable Transmission (CVT).....	JP
Design 5: Push Pedal	JG, JE
Design 6: Spring Resistance	JG, JE
Analysis of Initial Design Concepts.....	ALL
Power Mechanisms	JE
Remaining Tricycle Components.....	JE
Tipping Analysis.....	JP
Selection of Best Concepts	JE
Power Mechanism.....	JE
Remaining Design Components	JE
Selection of Final Design.....	ALL
Propulsive Force Calculations	JG
Performance Analysis	JG
Input Force Comparisons.....	JG, JE
Mechanism Bounding Conditions.....	EC, JP
Size and Complexity Analysis	EC
Decision Matrix	JE
Final Design.....	JG

Frame Selection and Modification	JG
Spring Mechanism and Support Structure	JG
Spring	JG
Design Analysis	JG, JE
Design Structural Analysis	JG
Spring Bracket Analysis	JG
Seat Extender Analysis	JG, JE
Manufacturing	EC, JP
Machined Parts	EC
Welding	EC, JP
Additional Modifications	EC
Assembly	EC
Testing	JG, JE, EC
Safety and Functionality Testing	EC
Qualitative Testing	JE
Quantitative Testing	JG
Results	JG, JE
Qualitative Results	JE
Quantitative Results	JG
Analysis of Results	JG, JE
Analysis of Qualitative Results	JE
Analysis of Quantitative Results	JG
Conclusion	ALL
Recommendations	EC, JP
Appendix A: Tricycle Safety Standards	EC, JE
Appendix B: Remaining Component Pictures	JE
Appendix C: Tipping Analysis	JP
Position and Weight of the Center of Gravity	JP
Appendix D: Additional Design Considerations for Selection of Best Concepts	JE
Appendix E: Propulsive Force Calculations	JG, JE
Appendix F: Additional Design Considerations for Selection of Final Design	JE

Table of Contents

Abstract.....	i
Acknowledgements.....	ii
Introduction.....	1
Literature Review.....	2
Strokes	2
Goals for Rehabilitation.....	3
Benefits of Recreational Therapy	4
Existing Therapies and Devices.....	5
Mechanics Involved in Cycling	9
Mechanisms	13
Goal Statement.....	19
Design Specifications.....	20
Power Adjustability	20
Ergonomics	21
Cost	21
Manufacturability.....	21
Safety	22
Range of Motion	22
User Requirements.....	23
Stability.....	24
Preliminary Design Concepts.....	25
Design 1: Piston	25
Design 2: Motor	26
Design 3: Planetary Gear	27
Design 4: Continuously Variable Transmission (CVT).....	31
Design 5: Push Pedal	32
Design 6: Spring Resistance	34
Analysis of Initial Design Concepts.....	36
Power Mechanisms	36
Remaining Tricycle Components.....	38
Tipping Analysis.....	42
Selection of Best Concepts	44
Power Mechanism.....	44
Remaining Design Components	51
Selection of Final Design.....	60
Propulsive Force Calculations	60
Performance Analysis	62
Input Force Comparisons.....	70
Mechanism Bounding Conditions.....	72
Size and Complexity Analysis	75
Decision Matrix	76

Final Design.....	77
Frame Selection and Modification.....	77
Spring Mechanism and Support Structure	79
Spring.....	80
Design Analysis	82
Design Structural Analysis	82
Spring Bracket Analysis	92
Seat Extender Analysis	96
Manufacturing.....	103
Machined Parts.....	103
Welding.....	105
Assembly	108
Testing	114
Safety and Functionality Testing	114
Qualitative Testing.....	114
Quantitative Testing.....	115
Results.....	119
Qualitative Results.....	119
Quantitative Results.....	120
Analysis of Results	123
Analysis of Qualitative Results.....	123
Analysis of Quantitative Results.....	124
Conclusion	130
Recommendations.....	132
Works Cited	138
Appendix A: Tricycle Safety Standards.....	142
Appendix B: Remaining Component Pictures	150
Appendix C: Tipping Analysis	160
Position and Weight of the Center of Gravity.....	161
Appendix D: Additional Design Considerations for Selection of Best Concepts.....	175
Appendix E: Propulsive Force Calculations	181
Appendix F: Additional Design Considerations for Selection of Final Design.....	182
Appendix G: Spring Bracket Analysis.....	184
Appendix H: Seat Extender Buckling Analysis Calculations	189
Appendix I: Qualitative Testing Procedures	192
Appendix J: Quantitative Testing Procedure	198
Appendix K: Updated Subject Testing Procedure	201
Appendix L: Subject Testing Results.....	207

List of Figures

Figure 1: CAD Model of the Pool Walker (Aqua Creek Products, 2015)	5
Figure 2: Isokinetic Exercise Machine (htherapy, 2015)	6
Figure 3: Tilt Table (triwg, 2015)	7
Figure 4: Limb Load Monitor (ASME, 2015)	7
Figure 5: Anti-gravity Treadmill (Alterg, 2015)	8
Figure 6: Split Belt Treadmill (Woodway, 2015)	9
Figure 7: Recumbent Tricycle (tyrx.com)	11
Figure 8: Centrifugal and Tangential Forces during Pedaling (Fonda, 2010)	12
Figure 9: Torque Converter Cross-Section (How Stuff Works, 2015)	15
Figure 10: Pulley Driven CVT (Pratte, 2014)	16
Figure 11: Toroidal CVT, 1:1 Ratio (Harris, 2015)	16
Figure 12: Toroidal CVT, High Ratio (Harris, 2015)	17
Figure 13: Differential (Nice, 2000)	18
Figure 14: Piston Design Concept	25
Figure 15: Motor Design	26
Figure 16: Motor Design Force Curves	27
Figure 17: Planetary Gear Design	28
Figure 18: Torque Splitter	29
Figure 19: Reducer	29
Figure 20: Torque Splitter Side View	30
Figure 21: Toroidal CVT Design	32
Figure 22: Push Pedal Design Sketch, A: Side View of Four Bar Mechanism; B: Front View	33
Figure 23: 3D Model of Push Pedal Mechanism	34
Figure 24: Spring Resistance Mechanism Sketch (angles measured from horizontal)	35
Figure 25: 3D Model of the Spring Resistance Mechanism	35
Figure 26: Plot of Rollover Velocity while Turning on an Inclined Surface	43
Figure 27: Powered Wheel Free Body Diagram	61
Figure 28: Piston Input Torque Required Versus Position in Pedaling Cycle for Spring Constants 100 N/m to 1900 N/m	63
Figure 29: Spring Resistance and Push Pedal Input Torque Required Versus Position in Pedaling Cycle for Spring Constants 200 N/m to 2000 N/m	64
Figure 30: Piston Design	65
Figure 31: Crank Slider Mechanism Definition (Norton 1999)	66
Figure 32: Slider Displacement vs Crank Rotation	67
Figure 33: Slider Crank Applied Piston Force (METU, nd.)	68
Figure 34: Diagram of Slider Crank Mechanism (METU, nd.)	68
Figure 35: Pedal Crank Torque versus Angle ($k = 100:2000$ N/m)	69
Figure 36: Piston Design Pedal Forces	71
Figure 37: Spring Resistance Design Pedal Forces	71
Figure 38: Boundary Box for the Spring Resistance Mechanism	73
Figure 39: Boundary Box for the Piston Mechanism	74
Figure 40: Boundary Box for the Spring Resistance Mechanism	75
Figure 41: MOBO Triton Pro (Mobo Triton Pro Ultimate Ergonomic Cruiser, 2015)	77
Figure 42: Custom Front End	78
Figure 43: Chain Profile	80

Figure 44: Spring Performance Curves	81
Figure 45: Support Structure	83
Figure 46: Typical Coupler Plate Connection Stack-Up	83
Figure 47: Secondary Sprocket Section w/ Applied External Spring Load	85
Figure 48: Geometry Analyzed using FEM	86
Figure 49: FEM Boundary Conditions	87
Figure 50: FEM Mesh	88
Figure 51: Von-Mises Fringe Plot, Bottom View	89
Figure 52: Von-Mises Fringe Plot, B1 Interface (Section A-A)	90
Figure 53: Minimum Factor of Safety at B2 Section	90
Figure 54: Spring to Sprocket Interface	91
Figure 55: Cantilevered Beam FBD (Beam Deflection Formulae)	91
Figure 56: Spring Bracket Location	93
Figure 57: Simplified Geometry and Spring Bracket Free Body Diagram	94
Figure 58: Free Body Diagram of Spring Bracket from Points A to B	95
Figure 59: Free Body Diagram of Spring Bracket from Points B to C	95
Figure 60: Axis of Orientation for Analysis of Seat Extender	97
Figure 61: Free Body Diagram of the Seat Extender Plate	98
Figure 62: MathCAD to Solve for Forces Acting on the Bolts	99
Figure 63: Area Over Which the Shear Stress Acts	99
Figure 64: MathCAD to determine the Shear Stresses Acting on the Bolt	100
Figure 65: Simplified Free Body Diagram Showing Eccentric Buckling of the Seat Extender	101
Figure 66: Plate with Tie Rod Ends	104
Figure 67: Outside Profile of Handlebar Extender	105
Figure 68: Frame with Welding Fixture	106
Figure 69: Welding of Plate to Channels	107
Figure 70: Fully Installed Seat Extender	109
Figure 71: Chain and Tie Rod Alignment	110
Figure 72: Bracket Installed into Plate Assembly	110
Figure 73: Spring Connected to Frame and Sprocket	112
Figure 74. Spring Attached to Sprocket	112
Figure 75: Force Sensor showing Load Cell Array	115
Figure 76: Force Sensor Applied Pressures	116
Figure 77: Load Cell Used (Load Sensor – 50kg)	116
Figure 78: Load Cell Internal Wiring	117
Figure 79: Load Sensor Wiring Diagram	117
Figure 80: Pedal Force Control, No Spring	120
Figure 81: Strong Leg Pedal Forces with three different springs	121
Figure 82: Weak Leg Pedal Forces with three different springs	121
Figure 83: Peaks and Valleys of Pedal Forces	125
Figure 84: Recumbent Pedaling Cycle	126
Figure 85: Upright Relative Pedal Force (Allen, Blasius & Puttre, Pp. 73)	127
Figure 86: Pedal Force Calculations Updated for Manufactured Tricycle	129
Figure 87: Attachment of spring to sprocket, detailing limited number of attachment points	134
Figure 88: National Instruments X-Series DAQ Box (National Instruments, 2016)	136
Figure 89: Illustration of a Bicycle and its Part	143
Figure 90: Diagram Demonstrating Area on a Bicycle where there can be no Protrusions	144

<i>Figure 91: Three Wheel, Single in Rear (Bicycleman, 2015)</i>	150
<i>Figure 92: Three Wheel, Single in Front (Target, 2015)</i>	150
<i>Figure 93: Four Wheels (Quadracycle, 2015)</i>	151
<i>Figure 94: Road Tire (Performance Bicycle, 2015)</i>	151
<i>Figure 95: Multi-Use Bike Tire (maxxis.com)</i>	152
<i>Figure 96: Mountain Tire (Old Glory MTB, 2015)</i>	152
<i>Figure 97: Upright Seat, No Back (Rideouttech, 2015)</i>	153
<i>Figure 98: Upright Seat with Added Back (Morgancycle, 2015)</i>	153
<i>Figure 99: Once Piece Molded Seat with Back (Hostel Shoppe, 2015)</i>	154
<i>Figure 100: Handle Bars (Kite, Bike, Surf, Rambling, 2015)</i>	154
<i>Figure 101: Tiller (Hell Bent Cycles, 2015)</i>	155
<i>Figure 102: Platform Pedal (The Mountain Bike Encyclopedia, 2015)</i>	156
<i>Figure 103: Pedal Toe Clips (Amazon, 2015)</i>	156
<i>Figure 104: Clipless Bike Pedals (Art of Triathlon, 2015)</i>	157
<i>Figure 105: Upright Design (Bike Forums, 2015)</i>	157
<i>Figure 106: Recumbent Design (Rehabmart, 2015)</i>	158
<i>Figure 107: Rim Brake (Bike-Riding-Guide, 2015)</i>	158
<i>Figure 108: Drum Brakes (Chester Cycling, 2015) (chestercycling.wordpress.com)</i>	159
<i>Figure 109: Drum Brakes (Singletracks, 2015)</i>	159
<i>Figure 110: Drivetrain of a four-wheeled vehicle</i>	160
<i>Figure 111: Bicycle Model of a Delta (left) and a Tadpole (right) Tricycle</i>	161
<i>Figure 112: Free Body Diagram of the Tricycle (Side View)</i>	163
<i>Figure 113: Minimum Deceleration during Braking based on Wheelbase Length</i>	164
<i>Figure 114: Change of contact area of tricycle by change of surface's incline.</i>	165
<i>Figure 115: Diagram for Tipping Analysis</i>	165
<i>Figure 116: Angle ϕ_2 based on Wheelbase Length</i>	166
<i>Figure 117: Free Body Diagram of a Delta Tricycle (Huston & Johnson, 1982)</i>	168
<i>Figure 118: Plot of Rollover Velocity when Turning</i>	170
<i>Figure 119: Free Body Diagram of a Delta Tricycle on an Incline (Huston & Johnson, 1982)</i>	171
<i>Figure 120: Maximum Incline Angle until Rollover, based on Wheelbase Length</i>	172
<i>Figure 121: Free Body Diagram of Tricycle Turning on an Inclined Surface (Huston & Johnson, 1982)</i>	173
<i>Figure 122: Test Path Along the Quadrangle (Google, 2016)</i>	192
<i>Figure 123: Test Course Diagram</i>	198
<i>Figure 124: Test Path along the Quadrangle (Google, 2016)</i>	201

List of Tables

<i>Table 1: Muscle Activation during Cycling (Fonda, 2010)</i>	10
<i>Table 2: Gear Definitions for Planetary Mechanism</i>	30
<i>Table 3: Power Mechanism Comparison Chart</i>	36
<i>Table 4: Wheel layout Comparison Chart</i>	39
<i>Table 5: Tire Comparison Chart</i>	39
<i>Table 6: Seat Comparison Chart</i>	40
<i>Table 7: Steering Comparison Chart</i>	40
<i>Table 8: Pedal Comparison Chart</i>	41
<i>Table 9: Frame Comparison Chart</i>	41
<i>Table 10: Brake Comparison Chart</i>	42
<i>Table 11: Mechanism Pairwise Comparison Chart Average</i>	46
<i>Table 12: Final Rank-Order of Design Goals for Mechanism</i>	46
<i>Table 13: Relative Weighting Factors for Mechanism</i>	47
<i>Table 14: Numerical Weighting Factor for Mechanism Design Goals</i>	47
<i>Table 15: Ranking Criteria for Power Mechanism</i>	48
<i>Table 16: Mechanism Component Decision Matrix Average</i>	51
<i>Table 17: Constant Components Summary</i>	52
<i>Table 18: Combination 1 Morphological Chart</i>	52
<i>Table 19: Combination 2 Morphological Chart</i>	53
<i>Table 20: Combination 3 Morphological Chart</i>	53
<i>Table 21: Combination 4 Morphological Chart</i>	53
<i>Table 22: Combination 5 Morphological Chart</i>	53
<i>Table 23: Combination 6 Morphological Chart</i>	53
<i>Table 24: Tricycle Component Pairwise Comparison Chart Average</i>	55
<i>Table 25: Final Rank-Order of Design Goals for Tricycle Components</i>	55
<i>Table 26: Relative Weighting Factors for Tricycle Components</i>	56
<i>Table 27: Numerical Weighting Factor for Tricycle Component Design Goals</i>	56
<i>Table 28: Ranking Criteria for Tricycle Components</i>	57
<i>Table 29: Tricycle Component Decision Matrix Average</i>	59
<i>Table 30: Final Initial Design Combinations</i>	59
<i>Table 31: Pedal Force Scaling Factors (Passive Assistance Pedaling Device MQP, 2014)</i>	70
<i>Table 32: Average Decision Matrix for Final Mechanism Design</i>	76
<i>Table 33: Spring Data</i>	80
<i>Table 34: Material Properties</i>	88
<i>Table 35: Connecting Bolt Properties</i>	92
<i>Table 36: Spring Bracket Dimensions</i>	93
<i>Table 37: Material Properties (AL 6061-T6)</i>	94
<i>Table 38: Summary of Factors of Safety in Seat Extender</i>	102
<i>Table 39: Subject Testing Results for Each Question on Survey</i>	119
<i>Table 40: Average Survey Scores from 6 Test Subjects</i>	123
<i>Table 41: Pedal Force Deviation from Control, All Spring Constants</i>	127
<i>Table 42: Eric’s Mechanism Pairwise Comparison Chart</i>	175
<i>Table 43: Jaime’s Mechanism Pairwise Comparison Chart</i>	175
<i>Table 44: Nick’s Mechanism Pairwise Comparison Chart</i>	175
<i>Table 45: Henry’s Mechanism Pairwise Comparison Chart</i>	176

<i>Table 46: Eric’s Power Mechanism Decision Matrix.....</i>	<i>176</i>
<i>Table 47: Jaime’s Power Mechanism Decision Matrix.....</i>	<i>176</i>
<i>Table 48: Nick’s Power Mechanism Decision Matrix.....</i>	<i>177</i>
<i>Table 49: Henry’s Mechanism Decision Matrix.....</i>	<i>177</i>
<i>Table 50: Eric’s Tricycle Component Pairwise Comparison Chart.....</i>	<i>177</i>
<i>Table 51: Jaime’s Component Pairwise Comparison Chart.....</i>	<i>178</i>
<i>Table 52: Nick’s Component Pairwise Comparison Chart.....</i>	<i>178</i>
<i>Table 53: Henry’s Component Pairwise Comparison Chart.....</i>	<i>178</i>
<i>Table 54: Nick’s Tricycle Component Decision Matrix.....</i>	<i>179</i>
<i>Table 55: Henry’s Tricycle Component Decision Matrix.....</i>	<i>179</i>
<i>Table 56: Jaime’s Tricycle Component Decision Matrix.....</i>	<i>180</i>
<i>Table 57: Eric’s Component Decision Matrix.....</i>	<i>180</i>
<i>Table 58: Henry’s Decision Matrix for Final Mechanism Design.....</i>	<i>182</i>
<i>Table 59: Nick’s Decision Matrix for Final Mechanism Design.....</i>	<i>182</i>
<i>Table 60: Jaime’s Decision Matrix for Final Mechanism Design.....</i>	<i>183</i>
<i>Table 61: Eric’s Decision Matrix for Final Mechanism Design.....</i>	<i>183</i>
<i>Table 62: Subject's Comments to Subject Testing Questions.....</i>	<i>207</i>

Introduction

Stroke is the 5th leading cause of death in the United States, with more than 800,000 strokes occurring each year. Of those 800,000 strokes, approximately 130,000 result in death, leaving behind 670,000 living stroke patients (CDC, 2015). Roughly 40% of stroke patients experience moderate to severe impairments that require special care (National Stroke Association, 2015). Among these impairments is hemiparesis, which is an isolated weakness occurring on one side of the body. Hemiparesis can make it extremely difficult for the patient to perform normal tasks, such as movement. In addition to physical impairments, many stroke patients experience emotional effects such as anxiety and depression.

An effective way to treat the physical effects of strokes is to undergo physical therapy. However, many patients only attend therapy 2-3 times per week (National Stroke Association, 2015). Therefore, patients need other forms of exercise in their daily lives to help improve their mobility (American Heart Association, 2014). Exercise has also been shown to help reduce the emotional effects of stroke, such as depression (Harvard, 2009). One form of exercise, which can be used to help treat hemiparesis is cycling. In addition to helping treat the effect of stroke, cycling can also help stroke patients regain a sense of independence and normalcy in their lives.

An extensive search of existing recreational products for stroke patients revealed that there are a limited number of products for that purpose on the market. A previous MQP group developed a recreational tricycle for stroke patients, which used a compound gear train with a separate gear ratio for each leg. Although their tricycle allowed the two legs to pedal with different forces, it did so by allowing the pedals to rotate at different angular velocities, which makes even pedaling challenging. Therefore, our design focused on alternative methods to vary the required force from each leg while keeping an even cadence between pedals.

Literature Review

In order to create a device that can serve a recreational purpose for a stroke patient, it is important to understand how strokes affect people, including through hemiparesis (isolated weakness in one side of the body). It is also important to research common methods of rehabilitation for hemiparesis, and how those devices can be related to a recreational device.

Strokes

Prevalence

Stroke, a disease that affects the arteries, occurs when a blood vessel that carries oxygen-enriched blood to the brain is either blocked or bursts. When the blood cannot reach its destination, oxygen does not reach this part of the brain, which leads to death of brain cells (American Stroke Association, 2015).

Stroke is the 5th leading cause of death in the United States, killing around 130,000 Americans each year (CDC, 2015). With more than 800,000 strokes occurring each year, an American dies from a stroke every four minutes. Nearly a quarter of strokes occur to people who have previously had a stroke. Ischemic strokes, which take place when blood flow to the brain is stopped, account for 87% of all strokes (CDC, 2015). Although stroke risk does increase with age, 34% of people hospitalized for strokes are under the age of 65. Of all stroke patients, 10% recover almost completely, 25% recover with minor impairments, 40% have moderate to severe impairments that require special care, 10% require care in a long-term facility or nursing home, and 10% die shortly after the stroke (National Stroke Association, 2015).

Physical Impacts of Strokes

Stroke is the leading cause of long-term disability in the United States (Mozaffarian, 2015). Effects of a right hemisphere stroke include partial or full paralysis on the left side of the body, difficulty recognizing familiar objects and understanding their use, short term memory loss, mood swings and poor judgment, and inability to judge distances. Effects of a left hemisphere stroke include partial or total

paralysis of the right side, difficulty communicating, difficulty learning and retaining information, and trouble communicating (Public Health Agency of Canada, 2011). Including the cost of medications, health services, and missed work, strokes cost the United States approximately \$34 billion each year (CDC, 2015).

Mental and Emotional Effects of Strokes

Very often, people who experience a stroke experience devastating mental and emotional effects. Stroke survivors can develop depression and anxiety. Most often, the best treatment for these issues is therapy and medication (National Stroke Association, 2015). However, there is growing evidence that exercise can also play a role in the treatment of anxiety and depression (Anxiety and Depression Association of America, 2015).

Goals for Rehabilitation

When a person experiences a stroke, they can lose the ability to perform basic functions that are usually taken for granted. Common impairments include loss of muscle strength, motor control, and balance, which can inhibit leg use and walking. Stroke rehabilitation helps stroke survivors re-learn skills that were lost due to brain damage. A common skill lost is the ability to coordinate leg movements. While stroke rehabilitation cannot “cure” the effects of a stroke, its benefits can allow stroke survivors to move on with a sense of “normality.” Stroke rehabilitation can begin as soon as a patient becomes stable, which may be as soon as 24 to 48 hours after the initial attack. Typical stroke rehabilitation programs include four elements: physical therapy, occupational therapy, speech therapy, and recreational therapy. Physical therapy aims to recover basic motor skills such as walking and maintaining balance, whereas occupational therapy specifically focuses on learning everyday tasks such as eating and dressing. Strokes can cause difficulty with skills such as speaking or swallowing, and speech therapy is designed to help recover some of these skills. Finally, recreational therapy is essential in re-introducing social and leisure activities into one’s life.

Benefits of Recreational Therapy

By conducting common leisure activities which they enjoyed before their stroke, patients will not only be able to rehabilitate their weaker limbs, but also be able to keep themselves mentally and emotionally healthy.

Physical

Typical stroke patients only go to formal physical therapy 2-3 times a week, making recreational activity key to successful rehabilitation. Recreational activities can include stretching, walking, yoga, paddle sports, and interactive computer games (National Stroke Association, 2015). Stretching, walking, and yoga help strengthen the body and keep it flexible. Paddle sports work on hand-eye coordination and motor function, while interactive computer games encourage increased focus. These activities can help improve quality of life, mobility, and improve the patient's ability to carry out activities of daily living (American Heart Association, 2015). In a 6-month study of a home exercise program, stroke patients who exercised at least 3 times a week showed significant reduction in cholesterol and resting heart rate, which help to reduce the risk of a second stroke (Gordon et al., 2004).

Anxiety and Depression

Exercise has been shown to be an effective therapy for anxiety and depression. A study published in the Archives of Internal Medicine compared people who took medication, people who exercised, and people who did both, and found that 60-70 percent of people in all 3 groups no longer had depression after 16 weeks of treatment. This study suggests that exercise can be just as effective as antidepressants at treating depression. Another study found that a 60-minute walk 3 times per week could reduce mild to moderate depression symptoms (Harvard, 2009). Since exercise has been shown to alleviate depression and anxiety, and strokes often cause these disorders, we can conclude that recreational activities can be beneficial to the mental and emotional health in stroke patients.

Existing Therapies and Devices

Therapies

Various types of therapeutic devices have been created to facilitate recreational pastimes for the patients. Some of these activities include aquatic therapy and yoga, all of which help the patient not only strengthen the function of their limbs and regain their balance, but to have social interaction with a group while doing so (Pande, 2012).

Recreational Devices

Various recreational devices have been made in order to help stroke patients be able to return to their favorite leisure activities once again. If a patient's leisure activity is swimming or relaxing in the pool, a pool walker (*Figure 1*) can be used to walk around the shallow part of the pool. Similar to a common walker, but made mostly out of PVC piping, this device is lightweight enough for the user to easily move the walker through the water.

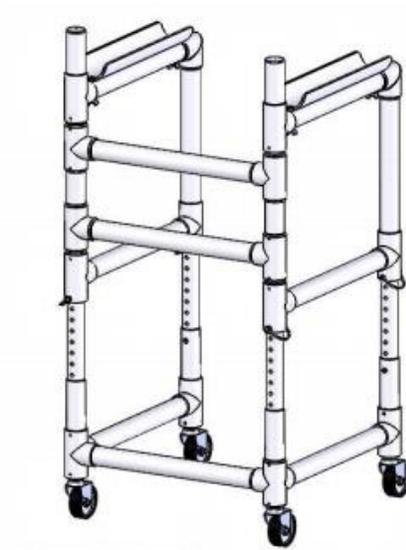


Figure 1: CAD Model of the Pool Walker (Aqua Creek Products, 2015)

Therapeutic Devices

In stroke rehabilitation, patients use a variety of devices including isokinetic exercise machines, tilt tables, limb load monitors, and anti-gravity treadmills. Isokinetic exercise machines are designed to target individual muscle groups by using uniform resistance that is adjustable to each user's abilities. To use the isokinetic exercise machine (*Figure 2*), the patient sits in the chair, and their leg is firmly attached to the lever of the machine. The machine then resists the patient's motion when they both bend and straighten their leg, working on strengthening both of these motions. This device is useful because it can be adjusted so that the patient still maintains full range of motion and proper form, while maximizing the amount of strengthening.



Figure 2: Isokinetic Exercise Machine (htherapy, 2015)

The tilt table (*Figure 3*) allows patients to learn to stand through progressive weight addition. The user is attached to a board, and as the patient goes from horizontal to vertical, more weight is supported by their feet as they stand. This type of therapy is useful because the patient relearns to stand without the

potential for injury that comes if they attempt to stand up but cannot support their own weight. This device is also useful because the patient can start with very little weight and increase to full body weight in whatever increments are necessary.



Figure 3: Tilt Table (triwg, 2015)

A limb load monitor can be used in combination with the tilt table or other devices to ensure that the patient does not exceed the amount of force they can support. The patient steps on the limb load monitor (*Figure 4*) to measure the amount of force being applied. The device can also be used to determine the maximum amount of weight the patient can currently support, so that weight can be progressively increased as the patient gets stronger.

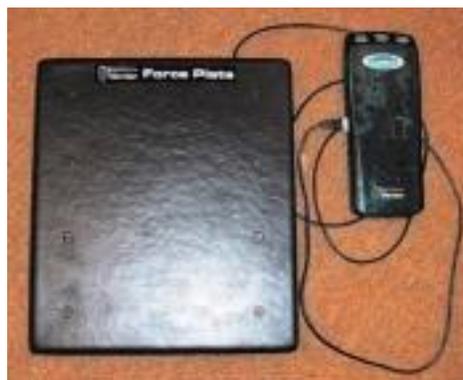


Figure 4: Limb Load Monitor (ASME, 2015)

The anti-gravity treadmill (*Figure 5*) allows users to “reduce gravity’s impact” (AlterG, 2015) by selecting 20-100% of their body weight. With the reduced body weight, patients can relearn proper walking mechanics and strengthen lower body muscles. The reduced weight allows patients to more easily move their lower limbs through a maximum range of motion while reducing the pain of walking. The level of safety also increases because the patient can easily adjust the amount of weight they are supporting so they do not exceed their abilities. The treadmill also works to increase the patient’s confidence in their ability to walk.



Figure 5: Anti-gravity Treadmill (Alterg, 2015)

Split belt treadmills (*Figure 6*) are often used in stroke rehabilitation. The split belt design allows for independent, variable speed control for each leg. The control for each leg helps stroke patients to recover a normal gait. The speed of the affected leg can be slowed down so that the patient can focus on proper form on that leg. Repetitive split belt treadmill usage has been shown to reduce post stroke step length asymmetry (Reisman, 2013).



Figure 6: Split Belt Treadmill (Woodway, 2015)

Mechanics Involved in Cycling

One important aspect of this project is the mechanics involved in cycling. This topic is very broad, and includes aspects such as biomechanics, muscle activation, position (upright or recumbent), mechanical efficiency, and the effects of pedaling rate, seat height, and the movement of the back leg upon the rider. Biomechanics covers the joint excursions during cycling. This topic, along with the muscle activation sequence and the position, helps provide an understanding of how the user must interact with a bicycle in order to cycle successfully. The latter four topics help provide an understanding of the basic forces governing the pedaling cycle, which will assist in the creation, testing, and realization of the design concepts which are discussed later in this report.

Biomechanics of Cycling

In order to fully understand the benefits of cycling, the biomechanics of cycling, which includes the activation sequence of the muscles as well as the transmission of power, must be studied. Much of the research for this project focused on cyclical pedaling, which has many advantages for rehabilitation. During cycling, the forces on the leg muscles are not significantly influenced by the weight of the rider. Therefore, the rider who cannot overcome their weight is able to successfully exercise and regain their

strength. In addition, cycling allows a therapist to change the geometry of the pedaling cycle in order to selectively strengthen specific muscles (Fonda, 2010).

Muscle Activation during Cycling

The motion of cycling requires a very complex sequence of muscle activation. Muscle activation is typically defined in relation to the position of the foot within the pedaling cycle. The 0 and 360-degree positions are defined as the pedal being completely vertical and above the axis of rotation. The 180-degree position is defined as the pedal being vertical below the axis of rotation. Table 1 illustrates the muscles activated during the pedaling sequence.

Table 1: Muscle Activation during Cycling (Fonda, 2010)

Muscle	Crank Position (Degrees)	Peak Activation Position (Degrees)
Gluteus Maximus (GMax)	340-130	80
Vastus Lateralis (VL) & Vastus Medialis (VM)	300-130	30
Rectus Femoris (RF)	200-110	20
Soleus (SOL)	340-270	90
Gastrocnemius Medialis (GM) & Gastrocnemius Lateralis (GL)	350-270	110
Tibialis Anterior (TA)	0-360	280
Semimembranosus (SM) & Semitendinosus (ST)	10-230	100
Biceps Femoris (BF)	350-230	110

Comparison of Upright and Recumbent Cycling

In order to create a wide variety of design concepts, many different configurations must be considered. Besides upright cycling, one common form of cycling is recumbent cycling, in which the rider sits in a reclined position to pedal. The muscle activation during recumbent cycling was therefore investigated in order to ensure that it does not change the mechanics of cycling when compared to upright cycling.

In upright cycling, the crank and seat are aligned close to vertical, whereas in recumbent cycling, they are aligned close to horizontal. Recumbent cycling is an excellent tool for rehabilitation, and has many advantages over upright cycling. One advantage of recumbent cycles, *Figure 7*, is that they have backrests on the seats, which can help provide support for the upper body. In addition, they are lower to the ground, which makes it easier for people with mobility impairments to access the bike (Lopes, 2014). However, for recumbent cycling to be a viable alternative to upright cycling, it must not significantly change the mechanical patterns of cycling.



Figure 7: Recumbent Tricycle (tyrx.com)

In a study published in the International Journal of Sports Physical Therapy, researchers measured muscle activity in the legs of 10 participants while they pedaled at a set cadence of 80 rpm and

a workload of 100 watts using both upright and recumbent cycles. The results showed no significant difference in the muscle activity between the two types of pedaling (Lopes, 2014).

It can be concluded that recumbent cycling could in fact be a viable design for a final design. This finding allows for flexibility in selecting the most appropriate design to meet the design goals.

Mechanical Efficiency

The mechanical efficiency of pedaling is highest when the force is tangent to the path of the pedal (Fonda, 2010). *Figure 8* illustrates both tangent and centrifugal pedaling force components. A cyclist will only transmit the entirety of their power tangent to the pedal's path when the crank is at 90 degrees (Pruitt, 2014). Studies have shown that the highest centrifugal force (most inefficient) occurs between 120 and 195 degrees off top dead center of the pedaling cycle. In addition, expert cyclists have been shown to be 11% more mechanically efficient than amateurs while only doing 9% more work. This finding shows that the expert cyclists are better at applying tangential force during the drive phase of the cycle (Fonda, 2010).

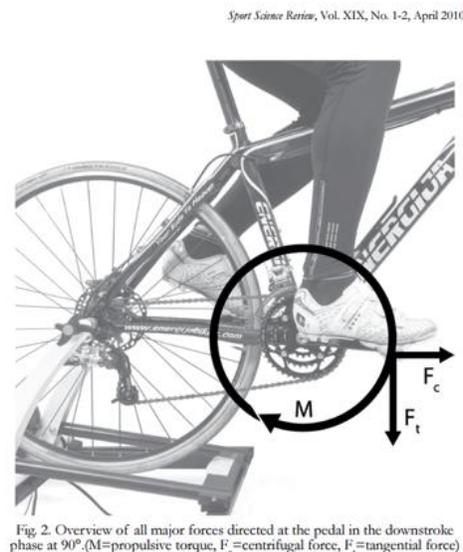


Figure 8: Centrifugal and Tangential Forces during Pedaling (Fonda, 2010)

Effects of Seat Height

Saddle height is defined as the distance from the top of the seat to the pedal when the pedal is in the lowest position (Fonda, 2010). Adjusting the height of the seat changes the angles of the joints and affects efficiency. One study found that a saddle height which is 109% of inseam length is most powerful, while 107% is most energy efficient (Woznia-Timmer, 1991). However, there is no single most optimal position for all riders at all times. Another study found the optimal height to be closer to 103% of inseam length. A seat position that is too low is associated with knee pain (Fonda, 2010).

Effect of the Back Leg on the Pedaling Cycle

Many people have long believed that pulling up the back leg during the recovery phase of pedaling can help increase efficiency. If this fact is true, then elite cyclists should show some upward force with the back leg during recovery. However, many studies have shown that even elite cyclists do not demonstrate very much upward force (Wozniak-Timmer, 1991). A human in the act of pedaling must use the front foot to overcome the weight of the back leg, which resists the motion of the pedal, thus explaining why the force on the front pedal doubles in magnitude from the back pedal. The finding that the back leg does not pull up is very significant for our project. When deciding on the mechanical advantage we give the hemi- paretic leg, we must take into account the fact that the hemi-paretic leg will have to provide the power for the healthy leg to recover. Depending on the severity of the hemiparesis, the patient might need significant help to provide this recovery.

Mechanisms

The previous section of this report described the various parameters that govern the pedaling motion in cycling. Although this research will make it easier to understand the mechanics of cycling, the aforementioned information does not fully set the foundation for the creation of a successful device. The users of the device will have a lateral discrepancy in strength, which will make the normal pedaling mechanics difficult, if not impossible for the users. Additional mechanisms must be added to the device in

order to modify it and differentiate it from a normal tricycle. These mechanisms will be used to provide a mechanical advantage to the weak leg, thus allowing the user to successfully propel the device. Therefore, this section will investigate many mechanisms, including torque converters, continuously variable transmissions (CVTs), differentials, and flywheels, which can be used to create a device which achieves the desired functionality.

Torque Converters

A torque converter (*Figure 9*) is a type of mechanical device that transfers torque via hydraulic coupling. Most commonly, they are seen on automatic transmissions in automobiles, as a way of eliminating a mechanical clutch. Torque is transferred from a power source to an output shaft by spinning hydraulic fluid from the “pump” to the “turbine”. The advantage to torque converters compared to a conventional clutch is the ability for the output shaft to remain stationary without mechanically decoupling from the power source. This could be especially useful in developing a power transmission with multiple inputs requiring different amounts of force, as the hydraulic coupling of a torque converter would not require both input sources to be mechanically tied together. However, in order to obtain efficient torque transfer, a function of fluid viscosity and angular velocity of the input shaft, the device must be moving at high speeds, such as in a car.

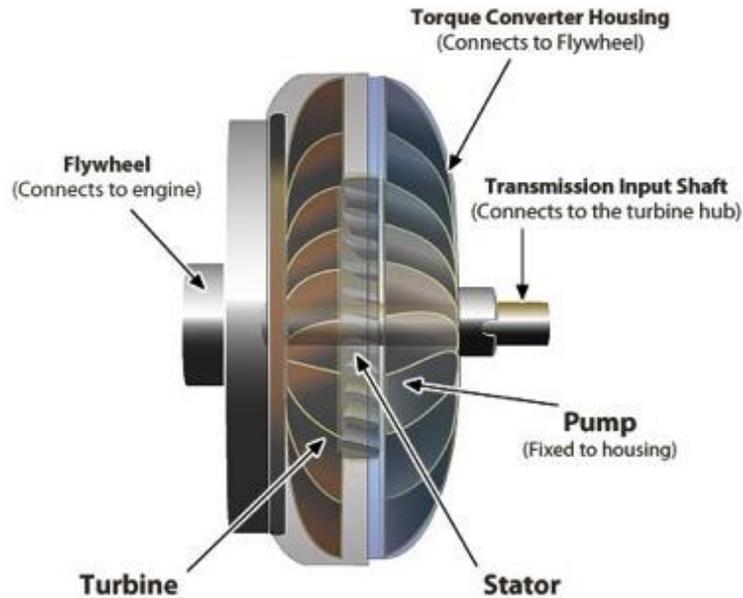


Figure 9: Torque Converter Cross-Section (*How Stuff Works, 2015*)

Continuously Variable Transmission

The most common type of continuously variable transmission (CVT) uses a pulley system, which has an infinite number of gear ratios. No discrete shifts are needed, unlike traditional gears. CVTs consist of 3 main parts:

- Metal or rubber belt
- Driven Gear
- Driving Gear

CVTs usually also require microprocessors and sensors to make shifting possible. A basic CVT, such as the one shown in Figure 10, contains 2 cones that are driven by a belt with a v-shaped cross-section.

The pulleys must change the pitch radius relative to each other in order to keep the belt in tension. In order to change the pitch radius, each pair of cones must change their spacing, and the two pairs of cones must move closer or further apart. Metal belts are superior to rubber belts because they do not wear out as easily, can withstand more torque, and are quieter. Another type of CVT is known as a toroidal CVT, appears in Figure 11. This type of CVT uses 2 cone-shaped discs that connect to the engine and drive

shaft. Two rollers perpendicular to the axis change gear ratios by tilting up and down. An example of this tilting motion is shown in Figure 12 (Harris, 2015).



Figure 10: Pulley Driven CVT (Pratte, 2014)

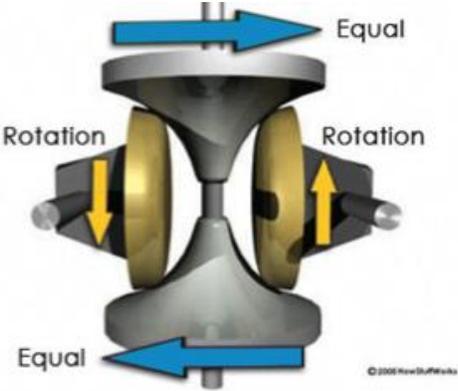


Figure 11: Toroidal CVT, 1:1 Ratio (Harris, 2015)

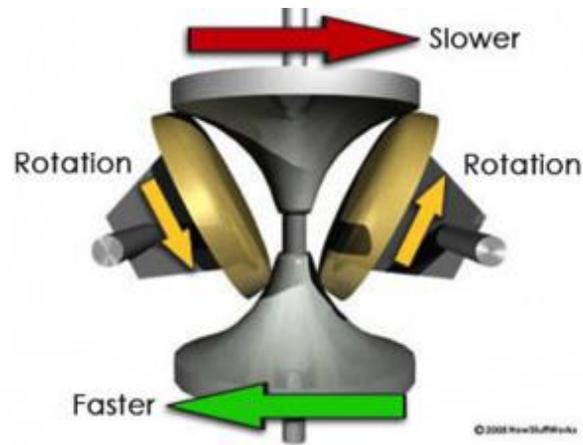


Figure 12: Toroidal CVT, High Ratio (Harris, 2015)

Differentials

A differential is a mechanism that allows two wheels on the same shaft to rotate at different speeds, which allows for smooth turning. When a car turns, the inside back wheel rotates more slowly than the outside back wheel because it has to cover less distance in the same amount of time. By allowing the wheels to rotate at different speeds, the differential eliminates the need for one tire to slip in order to make the turn (Nice, 2000). Differentials use a planetary gear system, as shown in Figure 13. The input pinion drives the ring gear, which is coaxial with one of the sun gears. The two sun gears connect through the two planet gears. When both shafts rotate at the same speed, the planet gears do not rotate with respect to the sun gears, locking the two sun gears into the same rotational speed. When the two output shafts turn at different speeds, the planet gears rotate with respect to the ring gear, allowing the two sun gears to turn at different speeds (Pearlman, 1999). A regular differential will always transmit the same amount of torque to each wheel. If one wheel slips, such as on ice, the wheel will just keep spinning. Because of this problem, many cars have limited slip differentials to allow more torque to be transmitted to the wheel that has more traction when the other is slipping (Nice, 2000).

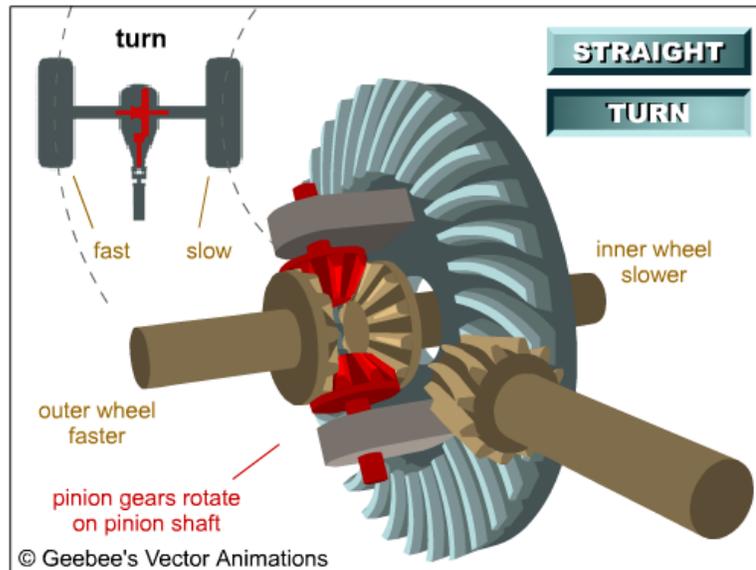


Figure 13: Differential (Nice, 2000)

Flywheels

Flywheels store kinetic energy, which can be produced with electricity, an engine (such as in a car), or pedaling. A previous MQP group proposed the use of a flywheel as a component in one of their designs (Allen et al., 2014). The flywheel keeps spinning due to inertia. The amount of energy stored by a flywheel is a function of the rotational speed squared. Higher speeds are necessary to store more energy, and thus maximum speed is needed for highest energy storage. Flywheels have many advantages including high resistance to wear, good energy density, maintenance of good mechanical properties, even after many cycles, and very quick response times (Flywheels, 2015).

An engineering student has made a flywheel bicycle that utilizes a CVT. When the bike slows down, the rider shifts to maximize the flywheel to bike speed ratio. To speed up, the rider must minimize this ratio. The maker claims that flywheel increases acceleration and provides a 10% energy savings. However, the flywheel weighs about 15 lbs. (Coxworth, 2011). The previous MQP group cited not adding a lot of weight to their design as part of their specifications, so the weight of the flywheel suggests that this design would be unsuitable to this project (Allen et al., 2014).

Goal Statement

Stroke is a leading cause of death in the United States. Many people who experience strokes have hemiparesis, or weakness in one side of the body. The goal of this project is to develop a human-powered device that can be used by people experiencing hemiparesis to aid in recovery from a stroke. The device should allow the user to slowly build up strength by offering varying levels of pedaling assistance to the weak leg. This recreational product should provide a sense of freedom to its user and encourage exercise to aid in rehabilitation.

Design Specifications

The design specifications are divided into 9 categories: power adjustability, ergonomics, cost, manufacturability, safety, range of motion, user requirements, ease of control, and stability.

Power Adjustability

1. The device must be propelled by different power inputs from each leg.
 - Stroke patients that experience hemiparesis are weaker in one leg than the other. This weakness would make pedaling a standard bike very difficult if each leg was required to output the same amount of force. Having different power inputs for each leg allows the patient to pedal using less force with the weaker leg while using the stronger leg to help power the device.
2. The required power input must be adjustable independently of each leg.
 - If the power input is independent of each leg, soon after the stroke, the patient can set the weaker side to only require a small amount of force. As the leg becomes stronger, the amount of force given to the weaker leg can increase so that the amount of force it takes to pedal becomes more similar to that of the stronger leg.
3. The device must be powered by human input.
 - The purpose of the device is to be a recreational device that also provides therapeutic benefits. The device must be primarily powered by the movement of the legs of the user to encourage physical activity and provide satisfaction for the rider knowing that they are capable of powering the device.
4. The power input from each leg should be with an even cadence.
 - The previous group's design allowed the two pedals to have separate angular velocities. This pedaling pattern was unfamiliar to many of their test subjects. Although some people were able to use the device successfully, many people were unable to adapt to the

pedaling motion (Allen et al., 2014). Therefore, it would be preferable if the next device allowed users to pedal with an even cadence.

Ergonomics

Each of the seat dimensional requirements is based on standard wheelchair dimensions. We decided to use wheelchairs as our reference because it is a position that will be most familiar to a stroke patient. Additionally, if both their wheelchair and the seat in the device are at approximately the same height, it will be much easier for the user to transfer to the device from a wheelchair.

5. Seat height should be ± 4 inches from the standard wheelchair seat height of 20 inches.
6. Seat backrest height should be ± 4 inches from the standard wheelchair backrest height of 36 inches off ground.
7. Seat width should be ± 2 inches from the standard wheelchair width of 19.5 inches.

Cost

8. The device should be able to be constructed for less than the budget of \$800.
 - The budget allowed for MQP groups is \$200 per team member. This MQP team contains 4 members, so the allowable budget is \$800.

Manufacturability

9. The device should be able to be manufactured by the team using primarily parts ordered off the shelf.
 - Due to the many other project groups, as well as the limited resources of the WPI machine shop, it will be difficult to machine parts. In addition, creating custom parts requires a lot of time. Therefore, parts should be ordered already made unless they are unique to the device and must be created from scratch.

Safety

10. The device must conform to the Consumer Products Safety Commission standards for bicycles (Code of Federal Regulations Title 16, Chapter II, Subchapter C, and Part 1512).

- The requirements specify that the tricycle will have no sharp edges, no loose fasteners, and have no protrusions in the user's personal space, among other requirements. The full requirements can be found in Appendix A.

11. The device must allow the user to freely pedal without colliding with any part of the device.

Range of Motion

In the following 3 cases (12-14), the user may not be able to produce these ranges of motion due to hemiparesis. In fact, the joint angles the user is capable of producing will most likely be much smaller than the values given. However, a trained physical therapist may adjust the geometrical configuration of the device in order to accommodate users with different degrees of flexibility. Therefore, the device will be able to accommodate users without full mobility. Since the device will be able to accommodate users with up to and including full mobility, the users will be able to use the device throughout every stage of their recovery. The users will be able to use the device up to, and including the point at which they regain full mobility. If the user regains full mobility, they can still use the device to rebuild their strength.

12. The device must allow the user to move through a range of motion from their knee of up to 37-111 degrees.

- According to the *Journal of Orthopedic & Sports Physical Therapy*, the typical range of motion in the knee during cycling is 37-111 degrees (Wozniak-Timmer, 1991).

13. The device must allow the user to move through a range of motion from their hips over 28 degrees.

- The *Journal of Orthopedic & Sports Physical Therapy* states that a minimum of 28 degrees of flexion is required to ride a bicycle. The flexion can be as high as 90 degrees (Wozniak-Timmer, 1991).

14. The device must allow the user to move through a range of motion from their ankle of up to 53-103 degrees.

- The *Journal of Orthopedic & Sports Physical Therapy* states that the ankle motion required to ride a bicycle is 53-103 degrees, where the neutral position is 90 degrees (Wozniak-Timmer, 1991). Other medical literature defines the neutral position as 0 degrees, which would make the range -37 to 13 degrees (Perry, 2015).

User Requirements

15. The user must be between 57” – 75” tall.

- For women in the United States, the 5th percentile of height is approximately 57”. For men in the United States, the 95th percentile of height is approximately 75” (CDC, 2012). Since men are taller than women on average, a device which can accommodate users between 57” and 75” should benefit the vast majority of potential users.

16. The user must weigh less than 250 pounds.

- For men in the United States, the 95th percentile of weight is 279 pounds, while for women it is much lower (CDC, 2012). In addition, many wheelchair distributors sell wheelchairs at a standard weight capacity of 250-300 pounds (PHC, 2015). Since users of the device could possibly require the use of a wheelchair, the device should benefit as many wheelchair users as possible.

17. User must be able to propel him or herself up a 4.8 degree grade using the device.

- The Americans with Disabilities Act (ADA) requires that a wheelchair ramp will not have a rise to run ratio of less than 1:12, which corresponds to an angle of 4.8 degrees

from the horizontal (ADA, 2010). Since users of the device could possibly require the use of a wheelchair, they should be able to traverse this slope easily.

18. The user must be able to support his or her own weight without assistance.

- The force required to pedal a bicycle is difficult to determine due to the multitude of factors affecting the pedaling. There are no existing data on the average force to pedal a bicycle, but it is reasonable to assume that it will not exceed the weight of the user due to the mechanical advantage of the gear system.

Stability

19. The device must be able to traverse pavement, grass, hard-packed dirt and dried mud.

- In order to operate the device in diverse terrain, it must be able to transition into softer surfaces and not get stuck.

Preliminary Design Concepts

In order to select the best overall design for the tricycle, the team generated multiple design concepts for the power mechanism. The generated designs include a variety of different types of mechanisms including a piston, a motor, planetary gears, a CVT (continuously variable transmission), a push pedal device, and a spring resistance design. Each of the initial designs creates the potential for different pedaling inputs from each leg.

Design 1: Piston

The piston design (Figure 14) uses a spring-loaded piston to artificially resist the strong leg. The driving sprocket has a linkage attached to it. As the strong leg reaches 0 degrees of the pedaling cycle, the piston begins advancing into the cylinder, compressing the spring. Once the strong leg reaches 180 degrees of the pedaling cycle, the piston will reach its lowest vertical position and thus fully compress the spring. As the strong leg enters the recovery phase, and the weak leg begins the drive phase, the spring will decompress, thus assisting the effort of the weak leg.

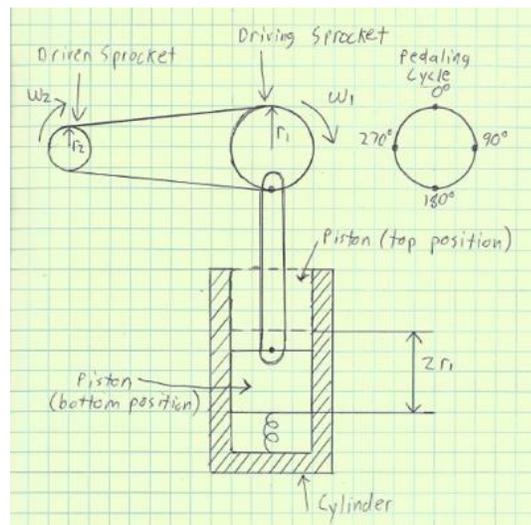


Figure 14: Piston Design Concept

Design 2: Motor

The motor design (Figure 15) uses a motor to assist the pedaling motion of the weak leg. The device will contain a processor and two strain gages. The strain gages will allow the processor to measure the torque applied by each leg throughout each leg's drive phase. The processor will store the torque data from the strong leg for each cycle. The processor will then detect the torque applied by the weak leg on a 1-millisecond delay. The motor will then apply a torque equal to the difference between the strong and weak leg torques for each equivalent position of the weak leg. If the strong leg applies 100 N-m of torque at the 15-degree position, and then the weak leg applies 75 N-m of torque at 15 degrees, then the motor will apply 25 N-m of torque to make up for the difference in torques. Figure 16 shows the difference in applied torque between the legs throughout the pedaling cycle. The motor will supply the difference in pedaling torques to the drive train. This design would also make it very easy to switch the advantage between the left and right legs.

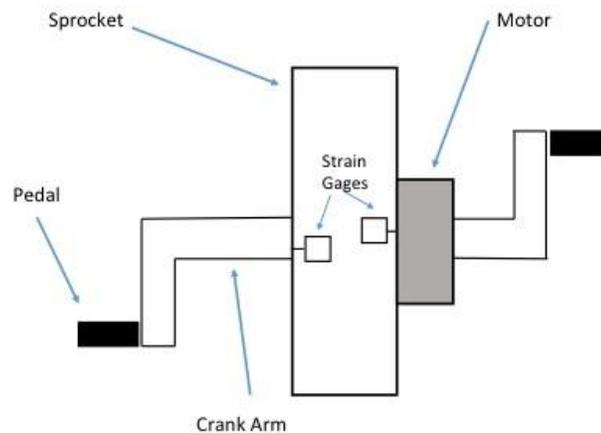


Figure 15: Motor Design

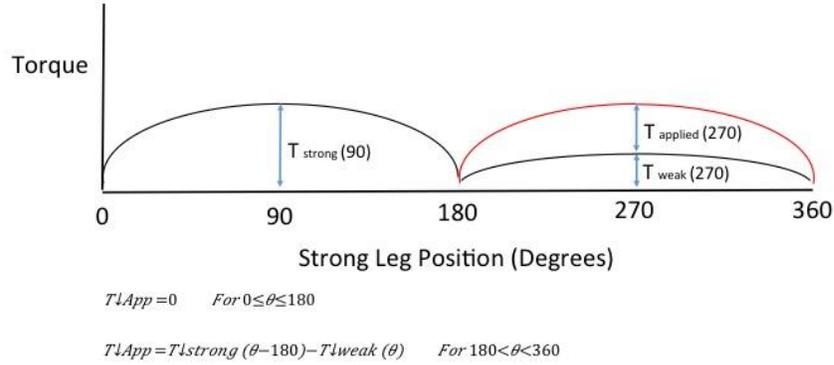


Figure 16: Motor Design Force Curves

Design 3: Planetary Gear

The planetary gear design (Figure 17) consists of a gear transmission with two major components, the torque splitter (Figure 18) and the reducer (Figure 19). Input torques are taken from the right and left side of the torque splitter (Figure 20) with values τ_{left} and τ_{right} and angular velocities ω_{left} and ω_{right} . Once combined, the output torque is transferred through an outer ring gear, which serves as the input for the reducer. The reducer is a single stage gear train in which the angular velocity from the torque splitter is reduced while raising the output torque. Within the torque splitter, two sets of internal pinions rotate around Sun 1 and Sun 2. Sun 1 (red) is connected to the left pedal and acts as a torque input for the system. Sun 2 is fixed, allowing the ring gear to rotate concentric to it. The ring gear has both internal (not shown) and external teeth, allowing it to couple with the reducer.

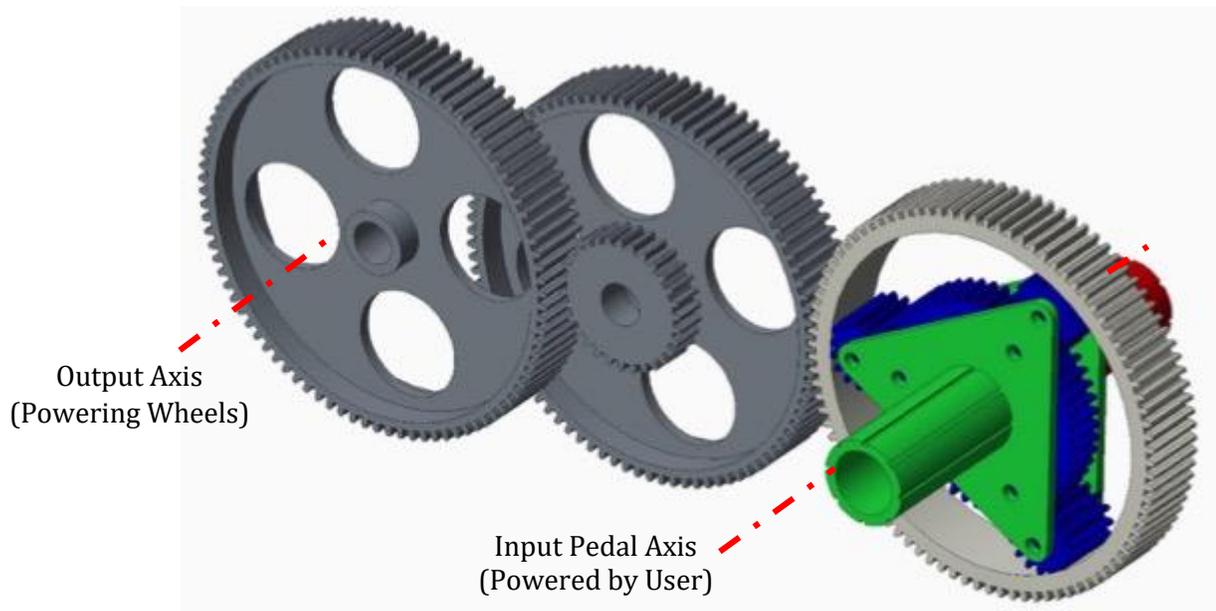


Figure 17: Planetary Gear Design

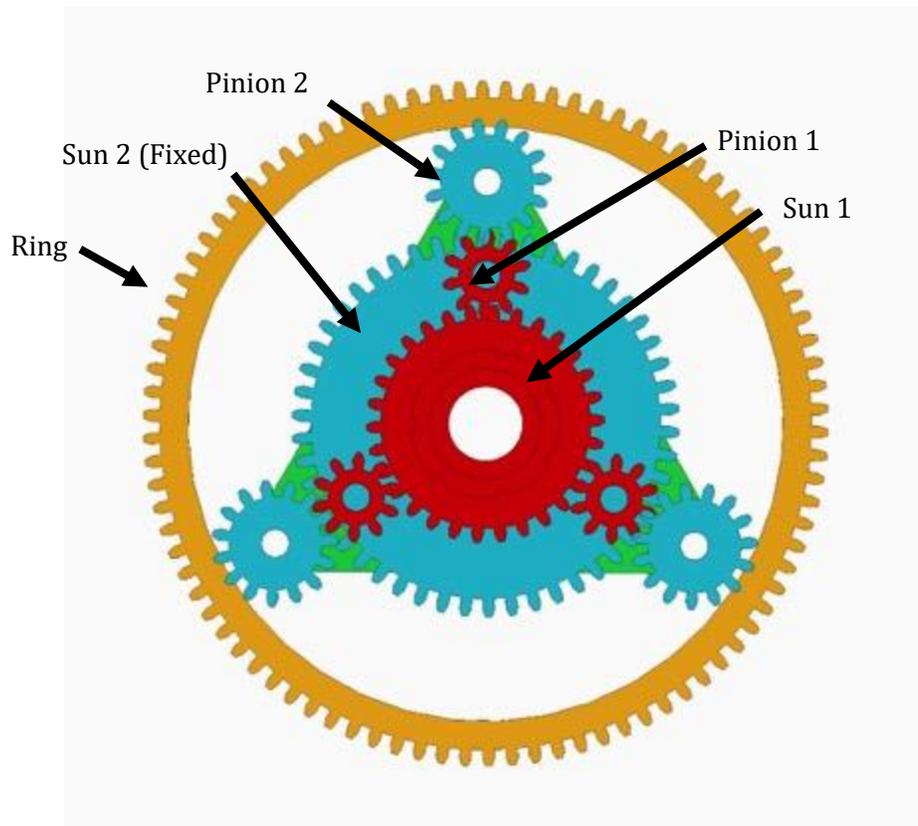


Figure 18: Torque Splitter

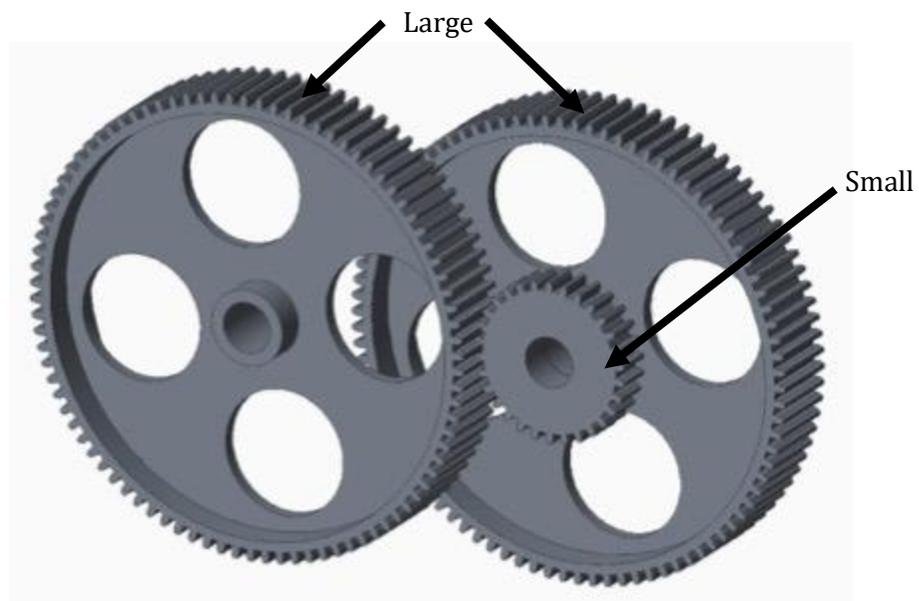


Figure 19: Reducer

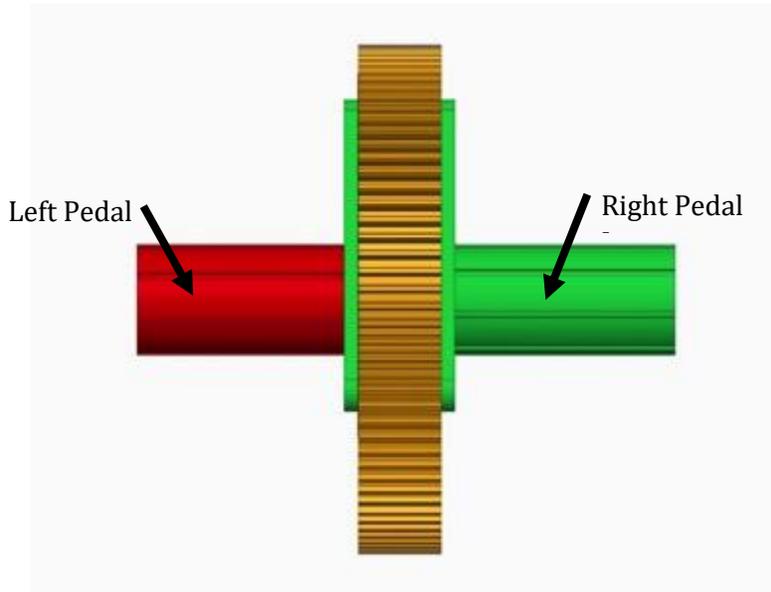


Figure 20: Torque Splitter Side View

The gear definitions for this proof of concept can be found in Table 2.

Table 2: Gear Definitions for Planetary Mechanism

Gear	Diametric Pitch	Number of Teeth	Pitch Diameter	Variable
Sun 1	20	30	1.5	D1
Sun 2	20	50	2.5	D3
Pinion 1	20	10	0.5	D2
Pinion 2	20	15	0.75	D4
Ring	20	80	4	D5
Large	20	90	4.5	D6
Small	20	30	1.5	D7

The torque values at gear connections inside the torque splitter are expressed as:

$$\begin{aligned} \tau_4 &:= \tau_5 \cdot \left(\frac{D_5}{D_4} \right) & \tau_2 &:= \tau_4 \cdot \left(\frac{D_4}{D_2} \right) \\ \tau_{L1} &:= \tau_4 \cdot \left(\frac{D_4}{D_3} \right) & \tau_{R1} &:= \tau_2 \cdot \left(\frac{D_2}{D_1} \right) \end{aligned}$$

Where τ_{R1} and τ_{R2} are the input torques for the right and left side, prior to the application of the “Reducer”. The “Reducer” ratio is expressed as:

$$\tau_6 := \frac{D7}{D6}$$

Therefore, the final input torques are given as:

$$\tau_{L2} := \tau_{L1} \cdot \tau_6 \quad \tau_{R2} := \tau_{R1} \cdot \tau_6$$

Which yields system gear ratios of:

$$RL = 0.533 \quad RR = 0.889$$

This means that the input torque applied by each leg will be less than the final, combined output torque of the system. Furthermore, this design allows for one side of the system to require significantly less input torque than the other, ideal for patients experiencing hemiparesis. It should be noted that the pedals will rotate at different angular velocities.

Design 4: Continuously Variable Transmission (CVT)

The CVT design (Figure 21) uses a wheel (shown in red) and two spindle cones to change the torque input of each leg to achieve the same torque output. As the wheel moves from one side of the cones to the other, the ratio between the input and output cone contact diameters changes, thus changing the torque ratio.

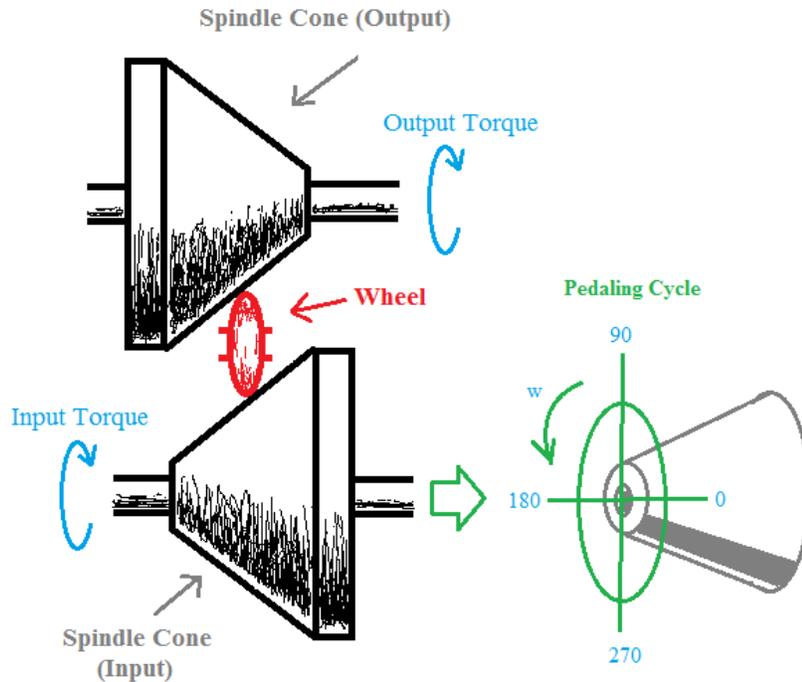


Figure 21: Toroidal CVT Design

Just before the strong leg begins to apply torque (before reaching 0 degrees on the pedaling cycle), the wheel will shift left between the cones. This shift will make the output torque smaller than the input torque. Once the strong leg begins to apply torque, it will need to maintain a large amount of torque to achieve a certain output torque. When the strong leg reaches its point of recovery (180 degrees of the pedaling position cycle) and the weak leg is about to turn the input spindle, the wheel will shift to the right. This shift will allow the weak leg to apply the same output torque as strong leg, but with a smaller input torque required.

Design 5: Push Pedal

The push pedal design is shown in Figure 22. The wheels are connected by the metal axle. The bars attached to the pedals (1) are also connected to the frame. As the bars move back and forth due to the pushing of the pedals, the metal axle rotates in a circular motion, which rotates the wheel. As the left pedal is pushed, the axle (2) rotates 180 degrees, and then when the right pedal is pushed, the axle rotates

the remaining 180 degrees. To make one side easier to press, a torsion spring (Figure 23) was added at the pivot for link 2 (Figure 22). As the left pedal is pushed, link 2 is forced to rock forward, thus stretching the spring and resisting that pedal. Then, as the right pedal is pressed, link 2 rocks back while the torsion spring releases its energy. This energy release is partly captured to assist the leg in pushing the right pedal forward. Additionally, due to the linear motion rather than rotational motion, this mechanism requires less range of motion for the user.

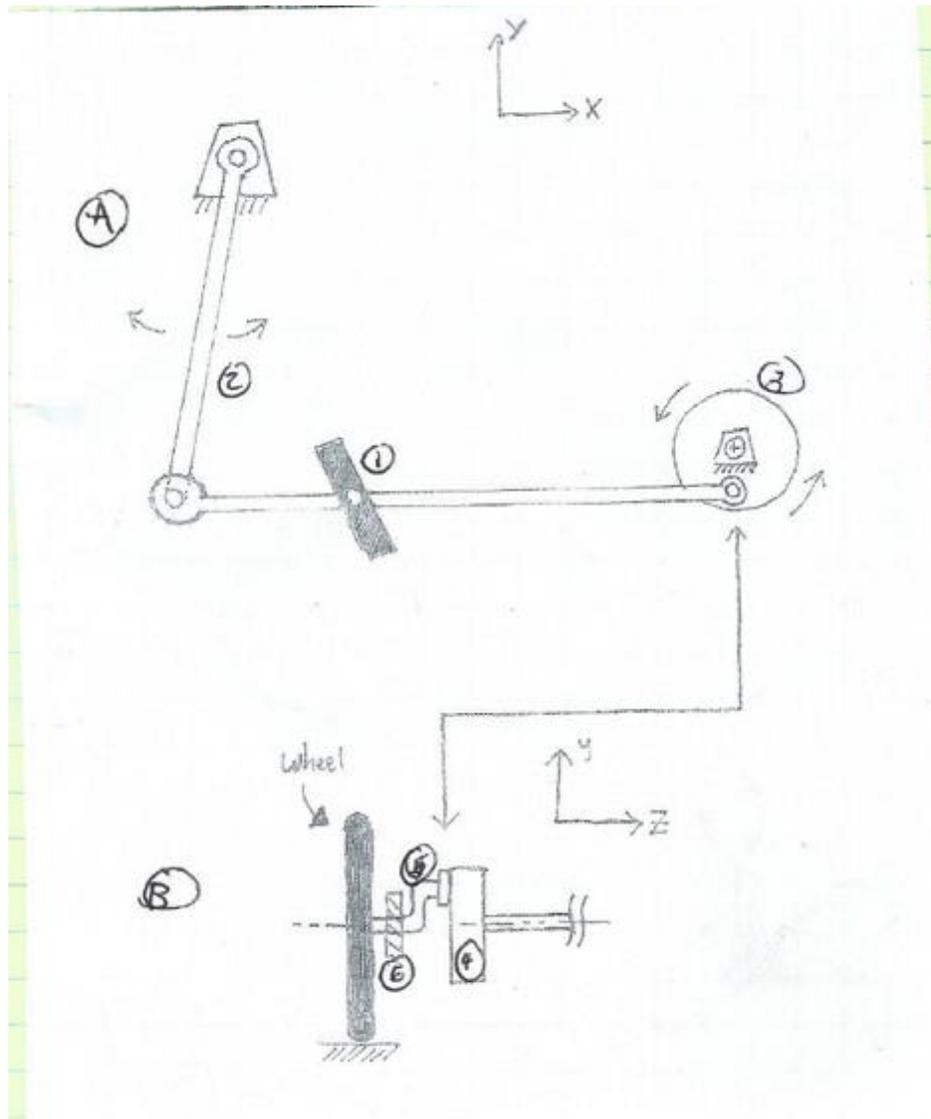


Figure 22: Push Pedal Design Sketch, A: Side View of Four Bar Mechanism; B: Front View

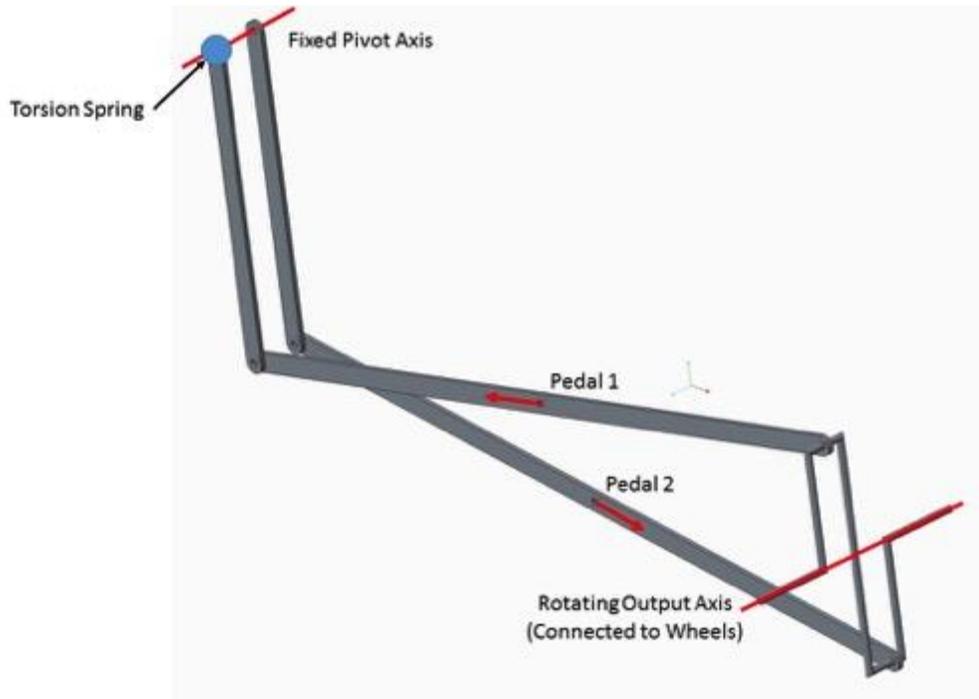


Figure 23: 3D Model of Push Pedal Mechanism

Design 6: Spring Resistance

In the spring resistance design (Figure 24) the pedals are attached to a gear (3). This is meshed with a gear of the same size (4). Gear (4) is attached to a spring (2) that is attached to a stationary point on the frame. As the reference pedal (1) rotates to 0 degrees off the horizontal (B), the spring stretches and resists the pedal rotation. At 270 degrees the spring is fully extended. As the pedal returns to 90 degrees, recoils, making 270 – 90 degrees aided by spring retraction. Figure 25 gives an overview of this mechanism in 3 dimensions.

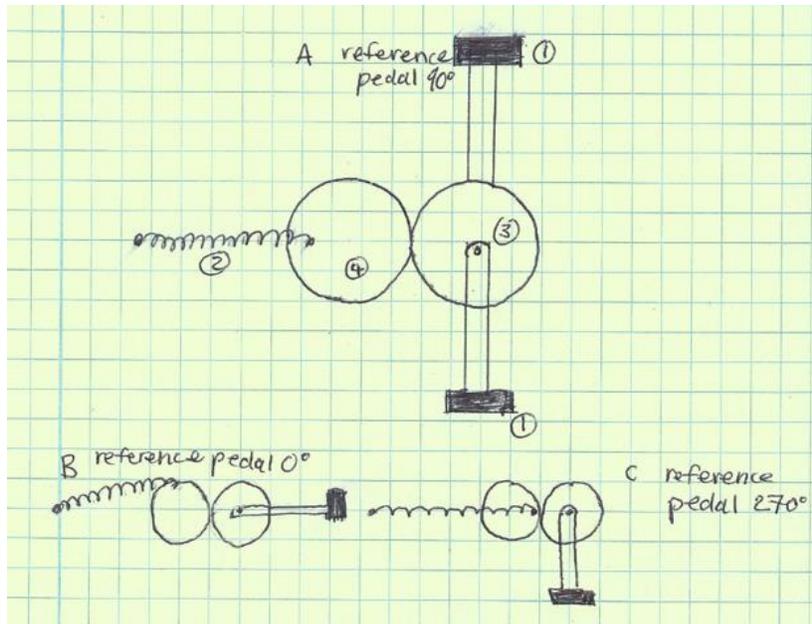


Figure 24: Spring Resistance Mechanism Sketch (angles measured from horizontal)

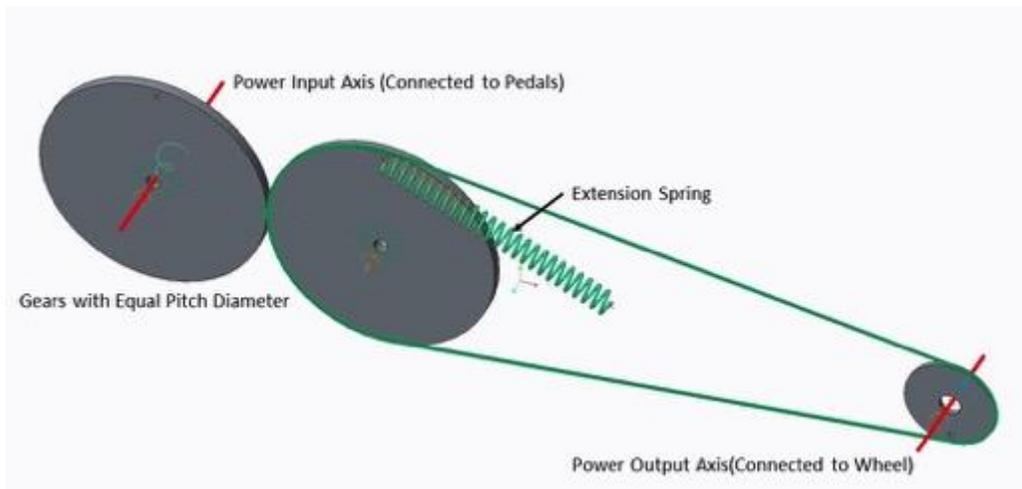


Figure 25: 3D Model of the Spring Resistance Mechanism

Analysis of Initial Design Concepts

Prior to selecting the top designs, the advantages and disadvantages of the initial design concepts were analyzed to get a better understanding of how well each aspect of the design would work for our overall design. The information obtained from this analysis will be used during the decision making process in the following chapter.

Power Mechanisms

For the power mechanism initial design concepts, in addition to the advantages and disadvantages for each design, fixed and variable parameters were also examined to determine the feasibility of each design (Table 3).

Table 3: Power Mechanism Comparison Chart

<i>Design</i>	<i>Fixed Parameters</i>	<i>Variable Parameters</i>	<i>Advantages</i>	<i>Disadvantages</i>
Piston	<ul style="list-style-type: none"> • Rotational speed between legs • Mechanical advantage between legs 	<ul style="list-style-type: none"> • Pedaling rate • Power input 	<ul style="list-style-type: none"> • Easy to fabricate • Can be used to modify existing device • Allows strong leg to create stored energy, which assists the weak leg 	<ul style="list-style-type: none"> • High wear • Cannot change advantage between legs • Cannot change sides for different users

<i>Design</i>	<i>Fixed Parameters</i>	<i>Variable Parameters</i>	<i>Advantages</i>	<i>Disadvantages</i>
Motor Design	Rotational speed between pedals	<ul style="list-style-type: none"> • Pedaling rate • Power input from strong leg • Power output from motor • Mechanical advantage between legs Which side has mechanical advantage	<ul style="list-style-type: none"> • Allows for different mechanical advantages between legs • Can switch to assist either left or right leg Allows weak leg to rehabilitate at a natural pace	<ul style="list-style-type: none"> • Would require batteries, thus increasing weight and limiting operation time • Would require modifications if installed into existing device
Planetary Gear Design	<ul style="list-style-type: none"> • Torque input for each leg (as is), could be redesigned with more ratios. 	<ul style="list-style-type: none"> • “Pedal” Orientation • Torque input between legs. 	<ul style="list-style-type: none"> • Allows for different mechanical advantages between legs. • Can be adapted to switch assist to either side. • Forces weak leg to pedal • Could be integrated into a standard bicycle chain system. 	<ul style="list-style-type: none"> • May require specialized gears. • Requires custom frame to support device. • Complex
Variable Pulley Mechanism (CVT)	<ul style="list-style-type: none"> • Torque input for each leg. 	<ul style="list-style-type: none"> • “Pedal” Orientation • Torque input between legs. 	<ul style="list-style-type: none"> • Continuously variable torque ratios. • Potential to be lightweight. 	<ul style="list-style-type: none"> • Complex • Difficult to manufacture • Potential for slippage of wheel with spindle cones.

<i>Design</i>	<i>Fixed Parameters</i>	<i>Variable Parameters</i>	<i>Advantages</i>	<i>Disadvantages</i>
Push Pedal	<ul style="list-style-type: none"> • Even cadence 	<ul style="list-style-type: none"> • Force acting between each “Pedal” 	<ul style="list-style-type: none"> • Less range of motion required for pushing instead of rotating. • Even cadence • Switch assist between legs. 	<ul style="list-style-type: none"> • Not continuously variable.
Spring Resistance Design	<ul style="list-style-type: none"> • Even cadence • 	<ul style="list-style-type: none"> • Force acting between each “Pedal” • Torque input between each leg. • Variable torque. 	<ul style="list-style-type: none"> • Even cadence • Independently adjustable torque for each leg. • Simple design • Switch assist between legs. 	<ul style="list-style-type: none"> • Not continuously variable.

Remaining Tricycle Components

Although the power transmission mechanisms are an important aspect of the design, the design will not be successful unless these mechanisms can be seamlessly integrated into the overall tricycle configuration. The configuration consists of many aspects, including the wheel layout, tires, seat, pedals, steering mechanism, and brakes. Finding the ideal combination of components, as well as the ideal mechanism to work with these components, allowed the team to generate the best possible design.

Portions of the device will be made using commercially available parts. To ensure the best design, several options must be considered for each aspect of the design. Comparisons of potential commercially available options can be found in Table 4 – Table 10. Pictures of each available option are in Appendix B.

Table 4: Wheel layout Comparison Chart

Wheel layout		
	Advantages	Disadvantages
Three Wheel, Single in Rear	<ul style="list-style-type: none"> • Better controlled braking (2 wheels contacting ground to brake in front) • More even weight distribution 	<ul style="list-style-type: none"> • More difficult to steer with 2 wheels rather than one
Three Wheel, Single in Front	<ul style="list-style-type: none"> • Simple, direct steering 	<ul style="list-style-type: none"> • Poor weight distribution • Less contact area on the front of the vehicle for braking
Four Wheels	<ul style="list-style-type: none"> • Increased stability 	<ul style="list-style-type: none"> • Increased weight and size

Table 5: Tire Comparison Chart

Tire		
	Advantages	Disadvantages
Road Tires	<ul style="list-style-type: none"> • Light weight 	<ul style="list-style-type: none"> • Decreased comfort over bumps • Reduced Stability
Multi-Use Tires	<ul style="list-style-type: none"> • Increased comfort of bumps • Improved stability 	<ul style="list-style-type: none"> • Medium weight
Mountain Tires	<ul style="list-style-type: none"> • Maximum comfort over bumps • Maximum stability 	<ul style="list-style-type: none"> • Heavy weight

Table 6: Seat Comparison Chart

Seat		
	Advantages	Disadvantages
Upright Seat, No Back	<ul style="list-style-type: none"> • Light weight • Readily available 	<ul style="list-style-type: none"> • Uncomfortable • Requires balance to remain seated • Little support for legs
Upright Seat with Added Back	<ul style="list-style-type: none"> • Provides support for back • Back and seat individually adjustable 	<ul style="list-style-type: none"> • Multi-piece design requires more moving parts • Little support for legs
One-Piece Molded Seat with Back	<ul style="list-style-type: none"> • Simple one piece design • Provides more support for legs 	<ul style="list-style-type: none"> • Minimally adjustable

Table 7: Steering Comparison Chart

Steering		
	Advantages	Disadvantages
Handle Bars	<ul style="list-style-type: none"> • Intuitive design • Integrated braking and steering 	<ul style="list-style-type: none"> • Requires force to physically turn wheels • Must use both arms equally
Tiller	<ul style="list-style-type: none"> • Allows for use with only one arm • Requires less force to turn 	<ul style="list-style-type: none"> • Less intuitive design requires time for the user to learn

Table 8: Pedal Comparison Chart

Pedals		
	Advantages	Disadvantages
Platform Pedals	<ul style="list-style-type: none"> • Large area evenly distributes force • No need to attach and reattach when getting on and off the device 	<ul style="list-style-type: none"> • Does not allow user to power the pedal stroke when pulling up with their foot
Pedal Toe Clips	<ul style="list-style-type: none"> • Allows user to power the pedal stroke when pulling up with their foot • Does not require special shoes 	<ul style="list-style-type: none"> • Have to attach and reattach to the pedals when getting on and off the bike
Clipless Bike Pedals (shoes clip into metal or plastic clip on pedal)	<ul style="list-style-type: none"> • Firmly attached pedal to user's feet for a very natural feel • Allows user to power the pedal stroke when pulling up with their foot 	<ul style="list-style-type: none"> • Requires special shoes • Clipping in and out of the pedal can be difficult and requires practice

Table 9: Frame Comparison Chart

Frame		
	Advantages	Disadvantages
Upright	<ul style="list-style-type: none"> • Ready available frames • 	<ul style="list-style-type: none"> • High sitting height may make it difficult for the user to get onto the seat • Requires balance to remain upright
Recumbent	<ul style="list-style-type: none"> • Height is more similar to a chair, so it makes it easier for users to sit on the seat • Activates the same muscles as upright bicycling despite a more comfortable position 	<ul style="list-style-type: none"> • Fewer frames available

Table 10: Brake Comparison Chart

Brakes	Advantages	Disadvantages
Rim	<ul style="list-style-type: none"> • Can be used on any frame • Lightweight • Inexpensive 	<ul style="list-style-type: none"> • Perform poorly when wet • Require replacement of pads
Drum	<ul style="list-style-type: none"> • Consistent braking regardless of condition (wet or dry) • Require less maintenance 	<ul style="list-style-type: none"> • Heavy • Complicated design • Weaker braking
Disc	<ul style="list-style-type: none"> • Compatible with rear and front suspensions • Strong braking • Consistent braking regardless of condition 	<ul style="list-style-type: none"> • Heavy • Expensive

Tipping Analysis

Another vital design aspect for the tricycle is its stability. The tipping analysis makes it possible to determine the conditions that will lead to the tricycle rolling over when making a turn or riding on an inclined plane. It is very important to determine these conditions, as a propensity to tip will make the design unsafe for the rider. This analysis determines what slopes and what turning speeds the tricycle can traverse without tipping over, which will be compared to the desired characteristics of the design configurations in order to determine their feasibility.

If the velocity of the tricycle, at a certain turning radius and wheel-span length, goes above the curve, tipping will occur. By taking into account the maximum angle of incline for static turnover on hills (17°), the rollover velocity curve dramatically changes based on the wheel-span length. For this case, the curve with the lowest rollover velocity values at certain turning radii, in Figure 26, will be considered. To ensure stability while turning on an inclined surface (one no larger than 17°), the rollover velocity curve for the shortest possible wheel-span length ($L= 117.2$ cm) must be used. The full calculations for this graph can be found in Appendix C.

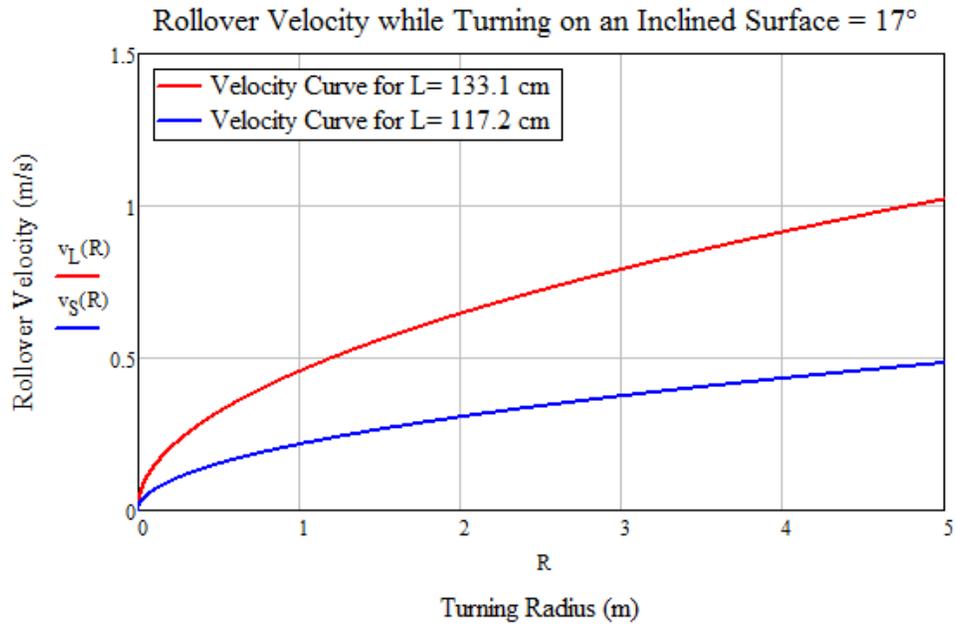


Figure 26: Plot of Rollover Velocity while Turning on an Inclined Surface

Selection of Best Concepts

Once all of the aspects of the design were accounted for, each design was analyzed. The team used various techniques to determine the feasibility of each design. The team first generated pairwise comparison charts for both the mechanism and the configuration. These charts allowed the team to determine the ranking order of the design criteria. From the ranking order, the team was able to determine the weight of each design aspect for the decision matrix. The group then generated a ranking rubric for each design criterion. The score given to each aspect of each mechanism and configuration was multiplied by the weighting factor in order to create full decision matrices. From these selections, the top four designs were determined. These four designs were further analyzed in order to select the final design.

When selecting a final design, the mechanism for the power train and the other components of the design were analyzed separately. This analysis method works because any power train can be used with any combination of the other components of the design.

Power Mechanism

To select the best power mechanism, each design was evaluated using a decision matrix. After completion of the decision matrix, the best designs were carried forward for further analysis prior to selection of a final design. The power mechanism initial designs that are evaluated in the following sections are the piston, motor, planetary gear, push pedal, spring resistance, and CVT.

Design Goals

The first step in the decision making process was to create design goals. The design goals describe components of the power mechanisms that should be included to have an optimal design.

Power Adjustability: The primary goal for creating this device is the power adjustability between each pedal, including the choice of the assistive pedal, and the torque ratios that can be achieved between each pedal.

Ergonomics: The mechanism should allow the user to pedal with an even cadence, no aspect of the mechanism should interfere with the pedaling motion, and the mechanism should be adjustable for comfortable pedaling based on different rider heights and weights.

Conform to User Requirements: The mechanisms must not prevent users that fit the user requirements from being able to use the device by making the force to steer or pedal too large.

Ease of Control: The input rotational velocity should be constant throughout the entire pedaling cycle and the mechanism should allow the rider to "coast" when they stop pedaling.

Safety: The mechanism must not create a safety issue for the user.

Manufacturability: The mechanism must not be so complicated in design that it cannot be manufactured in a standard machine shop and with off the shelf components.

Cost: The mechanism components must not be expensive so that the overall cost of the device remains affordable.

Pairwise Comparison Chart

Once the design goals were created, pairwise comparison charts were carried out to determine the relative importance of each design goal. In the pairwise comparison charts, at the cell intersecting a design goal in a row and a design goal in a column, if the design goal in the row is more important than

the design goal in the column, a one is placed in the cell. If the item in the row is less important than the item in the column, a 0 is put in the cell, and if they are equally important, a 0.5 is put in the cell. The values in the cells are summed across the row, and the total at the end of the row represents the number for the design goal in that row. The larger the total for a design goal, the more important that design goal is for the power mechanism. Each member of the team completed a pairwise comparison chart individually (Appendix D) and then the results were averaged to determine a final pairwise comparison chart (Table 11).

Table 11: Mechanism Pairwise Comparison Chart Average

Mechanism	Ergonomics	Safety	Conform to User Rqmts	Power Adjustability	Ease of Control	Manufacturability	Cost	Total
Ergonomics	-	0.375	0.125	0	0.75	1	0.5	2.75
Safety	0.625	-	0.5	0.5	0.625	0.75	0.75	3.75
Conform to User Rqmts	0.875	0.5	-	0.625	0.625	0.375	0.5	3.5
Power Adjustability	1	0.5	0.375	-	0.875	1	1	4.75
Ease of Control	0.25	0.375	0.375	0.125	-	0.375	0.75	2.25
Manufacturability	0	0.25	0.625	0	0.625	-	0.5	2
Cost	0.5	0.25	0.5	0	0.25	0.5	-	2

Rank Ordering

Based on the values in Table 11, the design goals were rank ordered based on the total values for each criterion (Table 12).

Table 12: Final Rank-Order of Design Goals for Mechanism

	Final Rank Order
1	Power Adjustability
2	Safety
3	Conform to User Req
4	Ergonomics
5	Ease of Control
6 (Tie)	Manufacturability
6 (Tie)	Cost

Weighting Factors

Next, weighting factors were assigned to the design goals. A range for ranking factors was established based on whether the design goal was critical, important, or encouraged (Table 13). Based on the ranges, each design goal was awarded a numerical weighting factor (Table 14).

Table 13: Relative Weighting Factors for Mechanism

Critical	31-40
Important	11-30
Encouraged	6-10

Table 14: Numerical Weighting Factor for Mechanism Design Goals

Critical	Power Adjustability	35
Important	Safety	18
	Conform to User Requirements	16
	Ergonomics	11
Encouraged	Ease of Control	10
	Cost	5
	Manufacturability	5

Power adjustability is the most important factor, and therefore accounts for around a third of the total weight. Safety, conform to user requirements, and ergonomics are important design goals, with safety being weighted the highest. Finally, ease of control, cost, and manufacturability are encouraged design goals.

Ranking Criteria

After creating weighting factors for the design goals, ranking criteria were created to evaluate how well each mechanism design meets the design goals (Table 15). In the ranking criteria, each design

goal is split into excellent (5), good (4), satisfactory (3), mediocre (2), and unacceptable (1). For each design goal, the necessary criteria are listed for that design goal to achieve an excellent, good, satisfactory, mediocre, or unacceptable ranking.

Table 15: Ranking Criteria for Power Mechanism

	Excellent (5)	Good (4)	Satisfactory (3)	Mediocre (2)	Unacceptable (1)
Ergonomics	The mechanism allows the user to pedal with an even cadence between the two pedals, and no component interferes with the user during a normal pedaling cycle, and the device can be adjusted to achieve a comfortable pedaling position.	The mechanism allows the user to pedal with an even cadence between the two pedals, but the device cannot be adjusted to achieve a comfortable pedaling position. No component interferes with the user during a normal pedaling cycle.	The mechanism does not allow the user to pedal with an even cadence between the two pedals, but the device can be adjusted to achieve a comfortable pedaling position. No component interferes with the user during a normal pedaling cycle.	The mechanism does not allow the user to pedal with an even cadence between the two pedals, and the device cannot be adjusted to achieve a comfortable pedaling position. No component interferes with the user during a normal pedaling cycle.	The mechanism does not allow the user to pedal with an even cadence between the two pedals, and the device cannot be adjusted to achieve a comfortable pedaling position. Mechanism components may interfere with the user during a normal pedaling cycle.

	Excellent (5)	Good (4)	Satisfactory (3)	Mediocre (2)	Unacceptable (1)
Safety	Meets the Consumer Product Safety Commission standards on bicycle safety. Code of Federal Regulations (CFR) in Title 16, Part 1512.				Does not meet the Consumer Product Safety Commission standards on bicycle safety. Code of Federal Regulations (CFR) in Title 16, Part 1512.
Conform to User Rqmts	The mechanism does not use stored mechanical energy to assist the weak leg. The mechanism can be driven using solely human power.	The mechanism does not add additional force to the strong leg unless the additional force is stored as energy, and released to the weak leg. The device can be driven using solely human power.	The mechanism adds additional force to the strong leg without storing the energy to release to the weak leg. The device can be driven using solely human power.	The mechanism does not add additional force to the strong leg, but assists the weak leg using stored electrical energy.	The mechanism adds additional force to the strong leg and assists the weak leg using stored electrical energy.

Power Adjustability	Both pedals can be more assistive, and any torque ratio within a specified range can be achieved.	Either pedal can be more assistive, limited torque ratios can be achieved	Either pedal can be more assistive, fixed torque ratio	Only one pedal can be assistive, fixed torque ratio	Neither pedal can be assistive, fixed torque ratio
	Excellent (5)	Good (4)	Satisfactory (3)	Mediocre (2)	Unacceptable (1)
Ease of Control	The input torque shape profile is the same for each pedal, although they have different magnitudes. The device can "coast" when the user stops pedaling.		The input torque shape profile is similar for each pedal, although they have different magnitudes. The device can "coast" when the user stops pedaling.		The input torque shape profile for each pedal is dissimilar. The device cannot "coast" when the user stops pedaling.
Manufacturability	All major components can be purchased "Commercially Off the Shelf" and require minimal modifications.	More than half the major components can be ordered off the shelf, manufactured parts are simple and can be machined at the WPI shop	Some of the major components can be ordered off the shelf and parts of simple to moderate complexity can be machined at the WPI shop.	Some of the major components can be ordered off the shelf and manufactured parts are complex and may require outside machining.	None of the major components can be ordered off the shelf and are very complicated to manufacture.
Cost	The mechanism costs \$0-64 USD.	The mechanism costs \$65-128 USD.	The mechanism costs \$129-192 USD.	The mechanism costs \$193-256 USD.	The mechanism costs more than \$256 USD.

Decision Matrices

Finally, using the weighting factors and the ranking criteria, each member of the group individually created a decision matrix (Appendix D), and then the values were averaged to create a final decision matrix (Table 16). The design was assigned a numerical value 1-5 for each design goal based on the ranking criteria, multiplied by the weighting factor, and finally the values for each design goal were summed to get a total for each power mechanism.

Table 16: Mechanism Component Decision Matrix Average

Final Version	Criteria							
Mechanisms	Safety	Cost	Ergonomics	Ease of Control	Manufacturability	Conform to User Requirements	Power Adjustability	
Weighting Factors	18	5	11	10	5	16	35	Total
Piston	5	3	5	3	3	4	4	398
Motor	1	2	5	5	4	2	5	343
Planetary	5	3	3	5	2	5	3	391
Push Pedal	5	4	5	4	4	4	4	419
Spring Resistance	5	4	5	4	4	4	4	414
CVT	5	1	3	5	1	5	5	437

Based on the decision matrix average, the highest design was the CVT. However, because this design contains very complex and customized parts, it received a 1 (unacceptable) in cost, so the design was eliminated. Upon further examination of the bicycle safety codes, a bicycle with a motor would not pass the standards of the code, so the ranking for safety of the motor design was shifted to a 1. The motor was then eliminated because it received a 1 (unacceptable) in safety. After eliminating these two designs, the highest three designs are the piston, the push pedal, and spring resistance designs, which will be paired with the highest designs in the remaining components section to follow.

Remaining Design Components

To analyze the components of the design, morphological charts of the possible component combinations were created. Prior to creating the morphological charts, several components were pre-selected independent of the other components. The components that remain constant throughout each design combination are frame, pedals, wheels, and seat. We began by selecting the recumbent frame with a one-piece molded seat design. We chose these components because they are far more feasible for use

with recovering stroke patients. The recumbent frame allows patients to sit in a more comfortable, well-supported position, at a height that is easy to climb onto. In addition, as previously shown in our background chapter, these positive factors do not change the muscle activation required to pedal. With the selection of a recumbent design, platform pedals were also chosen because clips are not used in recumbent cycling. Finally, multi-use wheels were chosen as a compromise between the lightweight design of road tires and the stability of mountain tires. The patients are not trying to achieve a maximum speed; so adding some additional weight to the tires does not negatively affect the user. The patients are also not navigating harsh terrain, so the additional stability from the mountain tires does not prove useful for this specific application. The constant components are summarized in Table 17.

Table 17: Constant Components Summary

Frame	Pedals	Wheels	Seat
Upright	Platform	Road Tires	Upright seat-no back
Recumbent	Pedal toe clips	Multi-Use Tires	upright seat with added back
	Clipless bike pedals	Mountain Tires	one-piece molded seat with back

The components that were analyzed in different combinations were drive-train, brakes, and steering. The rim brake design was eliminated from every design because the brakes do not function well when wet. Due to the single wheel in the front, the three wheel single in front design could be paired with either handlebars or a tiller for steering and either drum or disc brakes. The three wheel single in the rear and four wheel designs were limited to the tiller steering and disc brakes because both handlebar steering and drum brakes are only suited to rear-drive train designs. Each morphological chart is shown in Table 18-Table 23.

Table 18: Combination 1 Morphological Chart

Combination 1 (Rear, Tiller, Disc)		
<i>Drivetrain</i>	<i>Brakes</i>	<i>Steering</i>
3 Wheel Single in Rear	Rim	Handle bars
3 Wheel single in front	Drum	Tiller

4 wheels	Disc	
----------	------	--

Table 19: Combination 2 Morphological Chart

Combination 2 (Front, Handle Bars, Drum)		
<i>Drivetrain</i>	<i>Brakes</i>	<i>Steering</i>
3 Wheel Single in Rear	Rim	Handle bars
3 Wheel single in front	Drum	Tiller
4 wheels	Disc	

Table 20: Combination 3 Morphological Chart

Combination 3 (Front, Handle Bar, Disc)		
<i>Drivetrain</i>	<i>Brakes</i>	<i>Steering</i>
3 Wheel Single in Rear	Rim	Handle bars
3 Wheel single in front	Drum	Tiller
4 wheels	Disc	

Table 21: Combination 4 Morphological Chart

Combination 4 (Front, Tiller, Drum)		
<i>Drivetrain</i>	<i>Brakes</i>	<i>Steering</i>
3 Wheel Single in Rear	Rim	Handle bars
3 Wheel single in front	Drum	Tiller
4 wheels	Disc	

Table 22: Combination 5 Morphological Chart

Combination 5 (Front, Tiller, Disc)		
<i>Drivetrain</i>	<i>Brakes</i>	<i>Steering</i>
3 Wheel Single in Rear	Rim	Handle bars
3 Wheel single in front	Drum	Tiller
4 wheels	Disc	

Table 23: Combination 6 Morphological Chart

Combination 6 (Four, Tiller, Disc)		
---	--	--

<i>Drivetrain</i>	<i>Brakes</i>	<i>Steering</i>
3 Wheel Single in Rear	Rim	Handle bars
3 Wheel single in front	Drum	Tiller
4 wheels	Disc	

Design Goals

Similar to the decision making process for the power mechanism, for the remaining tricycle components, first, design goals were created.

Ergonomics: To encourage the use of the device, it must be comfortable to sit on. The device should have a backrest, the seat width and height should fall within the standard set in the design specifications, and the device should allow for use by patients within the height and weight limits set in the design specifications.

Safety: To ensure the safety of the user, the device must have functioning and easy to control brakes and steering.

Conform to User Requirements: The device must be adjustable to fit any person within the height and weight ranges set in the user requirements.

Ease of Control: The device should allow the user to steer and brake with one hand.

Stability: To ensure safety, the device must balance on its own, and require minimal balance from the patient while they are riding. The device must also fit the standards set in the tipping analysis.

Cost: The more economical the device is, the more people who will be able to afford it.

Manufacturability: A majority of the components should be available to buy off the shelf.

Pairwise Comparison Chart

To establish the relative importance of the design goals, the group individually filled out pairwise comparison charts of the design goals (Appendix D), and averaged these values to get a final pairwise comparison chart (Table 24).

Table 24: Tricycle Component Pairwise Comparison Chart Average

Mechanism	Ergonomics	Safety	Conform to User Rqmts	Stability	Ease of Control	Manufacturability	Cost	Total
Ergonomics	-	0.38	0.38	0.13	0.63	0.88	1.00	3.38
Safety	0.63	-	0.88	0.50	0.63	1.00	1.00	4.63
Conform to User Rqmts	0.63	0.13	-	0.38	0.63	0.88	0.75	3.38
Stability	0.88	0.50	0.63	-	0.50	0.88	0.88	4.25
Ease of Control	0.38	0.38	0.38	0.50	-	1.00	1.00	3.63
Manufacturability	0.13	0.00	0.13	0.13	0.00	-	0.38	0.75
Cost	0.00	0.00	0.25	0.13	0.00	0.63	-	1.00

Rank Ordering

From Table 24 the design goals were rank ordered (Table 25).

Table 25: Final Rank-Order of Design Goals for Tricycle Components

	Final Rank Order
1	Safety
2	Stability
3	Ease of Control
4 (Tie)	Ergonomics
4 (Tie)	Conform to User Req.
6	Cost
7	Manufacturability

Weighting Factors

Next, weighting factors were assigned to the design goals. Again, a range for ranking factors was established based on whether the design goal was critical, important, or encouraged (Table 26). Based on the ranges, each design goal was awarded a numerical weighting factor (Table 27).

Table 26: Relative Weighting Factors for Tricycle Components

Critical	17-20
Important	11-16
Encouraged	0-10

Table 27: Numerical Weighting Factor for Tricycle Component Design Goals

Critical	Safety	20
	Stability	18
Important	Ease of Control	16
	Conform to User Requirements	14
	Ergonomics	14
Encouraged	Cost	10
	Manufacturability	8

Safety and stability are the most important factors, and therefore account for the greatest weight. Ease of control, conform to user requirements, and ergonomics are important design goals, with ease of control being weighted the highest. Finally, cost and manufacturability are encouraged design goals.

Ranking Criteria

Ranking criteria were also created for the tricycle components (Table 28). Similarly, each design goal is split into excellent (5), good (4), satisfactory (3), mediocre (2), and unacceptable (1). For each design goal, the necessary criteria are listed for that design goal to achieve an excellent, good, satisfactory, mediocre, or unacceptable.

Table 28: Ranking Criteria for Tricycle Components

	Excellent (5)	Good (4)	Satisfactory (3)	Mediocre (2)	Unacceptable (1)
Ergonomics	Device configuration includes a backrest. The seat height and width fall within the stated requirements. Frame allows for a pedaling range of motion within those defined in the user requirements.	The seat height and width fall within the stated requirements. Frame allows for a pedaling range of motion within those defined in the user requirements.	The seat height or width may fall within the stated requirements. Frame allows for a pedaling range of motion within those defined in the user requirements.	The seat height and width do not fall within the stated requirements. Frame allows for a pedaling range of motion within those defined in the user requirements.	The seat does not fall within the stated requirements. Frame does not allow for a pedaling range of motion within those defined in the user requirements.
Safety	Meets the Consumer Product Safety Commission standards on bicycle safety. Code of Federal Regulations (CFR) in Title 16, Part 1512.				Does not meet the Consumer Product Safety Commission standards on bicycle safety. Code of Federal Regulations (CFR) in Title 16, Part 1512.
Conform to User Rqmts	Fully adjustable to accommodate any user height and weight beyond the given user requirements.		Fully adjustable to accommodate any user height and weight up to the given user requirements.		Does not accommodate user height and weight up to the user requirements.

	Excellent (5)	Good (4)	Satisfactory (3)	Mediocre (2)	Unacceptable (1)
Stability	The device is dynamically stable above the assumed maximum tipping angle of 27 degrees. Additionally, the device remains stable while cornering fast turns.	The device is dynamically stable up to the assumed maximum tipping angle of 27 degrees. Additionally, the device remains stable while cornering fast turns.	The device is dynamically stable up to the assumed maximum tipping angle of 27 degrees; however, the device may tip while cornering too fast.	The device may tip while cornering fast turns or well below the assumed maximum tipping angle.	The device is inherently unstable.
Ease of Control	The device allows the user to both steer and brake with one hand.	The device allows the user to either steer or brake with one hand.	The device requires the user to use two hands to steer.	The device requires two hands to steer or brake.	Device cannot be steered, the brakes cannot be applied.
Manufacturability	All major components can be purchased "Commercial Off the Shelf" parts with minimal modifications.	More than half the major components can be ordered off the shelf, manufactured parts are simple and can be machined at the WPI shop	Some of the major components can be ordered off the shelf and parts of simple to moderate complexity can be machined at the WPI shop.	Some of the major components can be ordered off the shelf and manufactured parts are complex and may require outside machining.	None of the major components can be ordered off the shelf and are very complicated to manufacture.
Cost	The tricycle costs between \$0-136 USD	The tricycle costs between \$137-280 USD	The tricycle costs between \$281-368 USD	The tricycle costs between \$369-544 USD	The tricycle costs more than \$544 USD

Decision Matrices

Next, using the weighting factors and the ranking criteria, each member of the group individually created a decision matrix (Appendix D), and then the values were averaged to create a final decision matrix (Table 29).

Table 29: Tricycle Component Decision Matrix Average

Final Version	Criteria							
Mechanisms	Safety	Cost	Ergonomics	Ease of Control	Manufacturability	Conform to User Requirements	Stability	
Weighting Factors	20	10	14	16	8	14	18	Total
1 (Rear, Tiller, Disc)	5	3	3	5	3	5	3	389
2 (Front, Handle Bars, Drum)	5	4	3	3	4	4	4	380
3 (Front, Handle Bars, Disc)	5	4	3	3	4	5	4	407
4 (Front, Tiller, Drum)	5	4	3	4	3	4	4	394
5 (Front, Tiller, Disc)	5	3	3	5	3	5	4	418
6 (Four, Tiller, Disc)	5	2	3	3	3	5	5	398

Based on Table 29, the two best tricycle component combinations are single front wheel, handle bars, disc brakes; and single front wheel, tiller, and disc brakes. Using the information from Table 16 and Table 29, the final six full device combinations can be found in Table 30.

Table 30: Final Initial Design Combinations

	Front, Handle Bars, Disc	Front, Tiller, Disc
Push Pedal	1. (Spring Resistance, Front, Handle Bars, Disc)	2. (Spring Resistance, Front, Tiller, Disc)
Push Pedal	3. (Push Pedal, Front, Handle Bars, Disc)	4. (Push Pedal, Front, Tiller, Disc)
Spring Resistance	1. (Spring Resistance, Front, Handle Bars, Disc)	2. (Spring Resistance, Front, Tiller, Disc)

Selection of Final Design

After analyzing the tiller and handlebar designs in more detail, the group decided that the tiller steering is more suited to a tricycle for a stroke patient. The tiller allows for the user to steer effectively with one arm, as would be safer for a person affected by hemiparesis. The tiller design also can be more easily placed in the recumbent frame design without being uncomfortable or out of the reach of the user. Therefore, the front, tiller, disc brakes design from Table 30 will be paired with the best mechanism design.

In order to select the best design among the piston, push pedal, and spring resistance design, propulsive force calculations were carried out to analyze the force input required by the rider for each of the top three designs. An analysis on the size and complexity of each design was also carried out. With the information obtained from the detailed analysis of the top three designs, another decision-making process was completed to determine a final design.

Propulsive Force Calculations

In order to analyze the designs, the forces required by the user to propel the device forward must be calculated. With these forces, and an assumed gear ratio, the required input torque can be found for which the user must overcome. From this required input torque, the designs can be individually analyzed to determine the assistive potential of the device. The essential equations for this analysis are shown in this section of the report.

Assumptions

The wheels were given an assumed diameter of 0.54m. The cross-sectional area of the rider and the device perpendicular to the direction of travel was assumed to be 1.5m². The rolling friction coefficient between the tires and the road was assumed to be 0.004 while the drag coefficient of the device and rider moving through air was assumed to be 0.8 (Device moving through static wind, wind velocity = 10m/s). For the wind resistance, the air was assumed to have a density of 1.225 kg/m³. It was

further assumed that the rider would operate the device in the range of 0 m/s to 10 m/s. For all of the calculations, it was assumed that the rider would accelerate the device from rest to each speed in 5 seconds. The full derivation of this analysis can be found in Appendix E.

Force Calculations

Once the assumptions had been determined, the friction force, acceleration force, and wind forces were calculated (Figure 27).

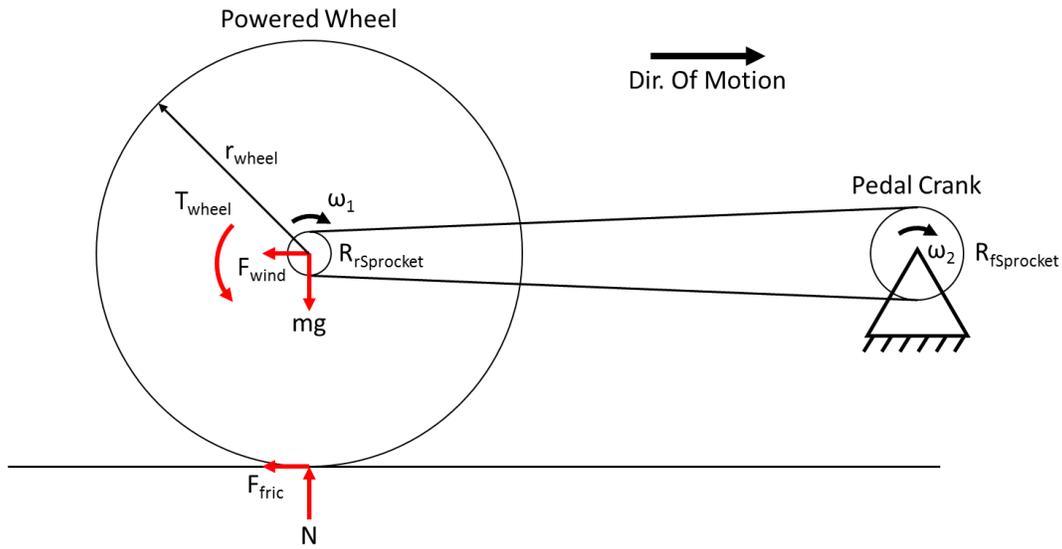


Figure 27: Powered Wheel Free Body Diagram

The frictional force is exerted horizontally on the wheels opposite to the direction of travel.

$$F_{fric} = \text{friction coefficient} * 9.81 \frac{m}{s^2} * (m_{rider} + m_{device})$$

The force of the wind was determined by the following equation:

$$F_{wind}(v) = \frac{1}{2} * \rho * v^2 * C_D$$

Where F_{wind} is the drag force due as a function of velocity, ρ is the density of air at STP, v is the rider's velocity, and C_D is the transverse cross sectional area of the rider and device.

Since the equation is a function of the velocity, the change in the wind force as the rider accelerates can be accounted for.

Torque Calculations

The torque at the wheels was calculated by using the total force and the radius of the wheel.

$$T_{wheel} = (F_{fric} + F_{wind}) * \frac{d_{wheel}}{2}$$

With the torque at the wheel determined, it was next necessary to relate the torque at the driven wheels to the torque at the crank. A standard gear ratio for a bicycle drivetrain is 53:39 (Wikstrom, 2014). The torque at the wheels was multiplied by this gear ratio to find the torque required at the crank, yielding a resistive torque of 30 N*m. This value was used in the mechanism analyses.

Angular Velocity Calculations

In order to analyze the mechanisms, the angular velocity was needed in addition to the torque. The angular velocity (ω_{wheel}) was calculated by dividing the linear velocity (v) of the device by the radius of the wheels (r_{wheel}). This calculation yielded the angular velocity in radians per second since it determined the number of full rotations of the wheel needed in order to cover a given distance every second.

$$\omega_{wheel} = \frac{2\pi v}{c_{wheel}}$$

Where v is the linear velocity of the device and c_{wheel} is the circumference of the driven wheel.

Multiplying this by the sprocket ratio of 52:39 yielded a pedal crank angular velocity of 18120 rad/sec at a device velocity of 10m/s.

Performance Analysis

For each of the three designs, the analysis was carried out to obtain a plot that demonstrates the input torque required versus the position in the pedaling cycle.

Spring Resistance and Pedal Car Design Analysis

The plots for the input torque versus pedal position for the piston and spring resistance and push pedal designs can be found in Figure 28 and Figure 29.

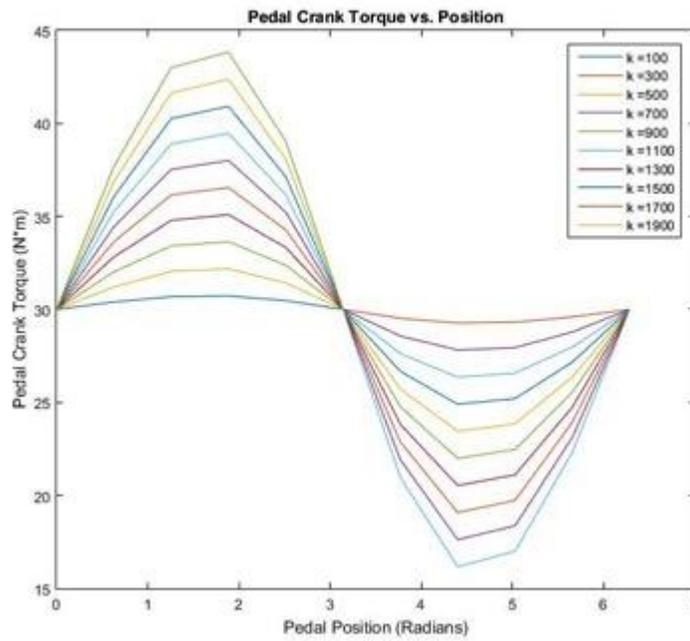


Figure 28: Piston Input Torque Required Versus Position in Pedaling Cycle for Spring Constants 100 N/m to 1900 N/m

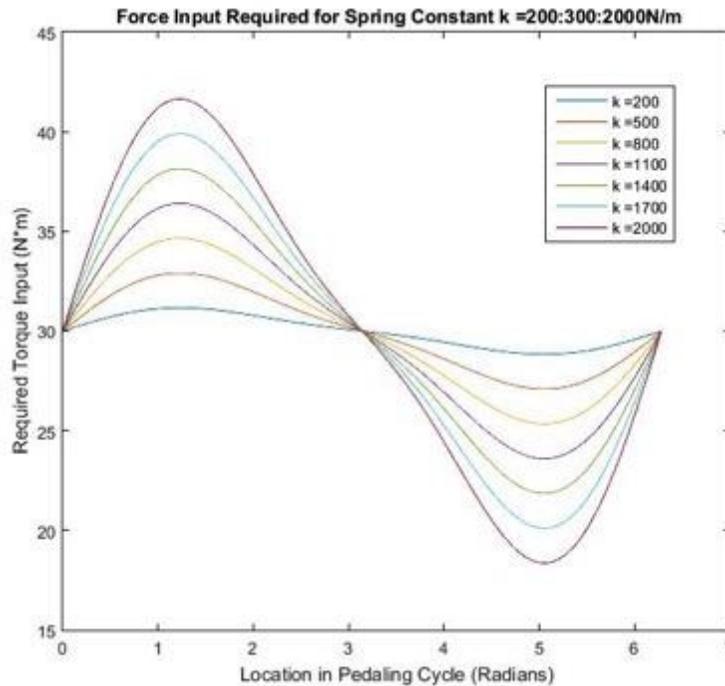


Figure 29: Spring Resistance and Push Pedal Input Torque Required Versus Position in Pedaling Cycle for Spring Constants 200 N/m to 2000 N/m

The spring acts the same on the spring resistance and the push pedal designs, so the analysis for these mechanisms is the same. Figure 28 and Figure 29 show the effect of the spring constants varying from 200-2000 N*m on the required input torque. In order provide a more accurate understanding of how spring stiffness effects level of assistance, a simulated torque resistance of 30 N*m (as calculated in Propulsive Force Calculations) was applied to the wheel axis in the opposite direction of travel. The plot also includes constant lines at -30, 0, and 30 N*m. When selecting a final design, a spring constant that keeps the magnitude of the curve between these values should be selected. The goal of the mechanism is to reduce the force required by the weak leg, not make the weak leg do no work at all. Once the curve passes -30 N*m, the weaker leg would be doing no work. When the curve is 0-30 N*m, the torque required is reduced, but the weak leg is still doing work.

Piston Design Analysis

The piston design (Figure 30) utilizes a simple crank-slider mechanism, in which the pedal crank is the driving link, to store and use potential energy within a spring. As the strong leg enters its power cycle during pedaling, it is also compressing a spring connected to the piston slider. This energy is then used as the weak leg enters its power cycle and extends the spring. This analysis aims to provide a baseline understanding of how this mechanism works with respect to assisting the weak leg. Additionally, it studies the effects of different spring constants on providing assistance.

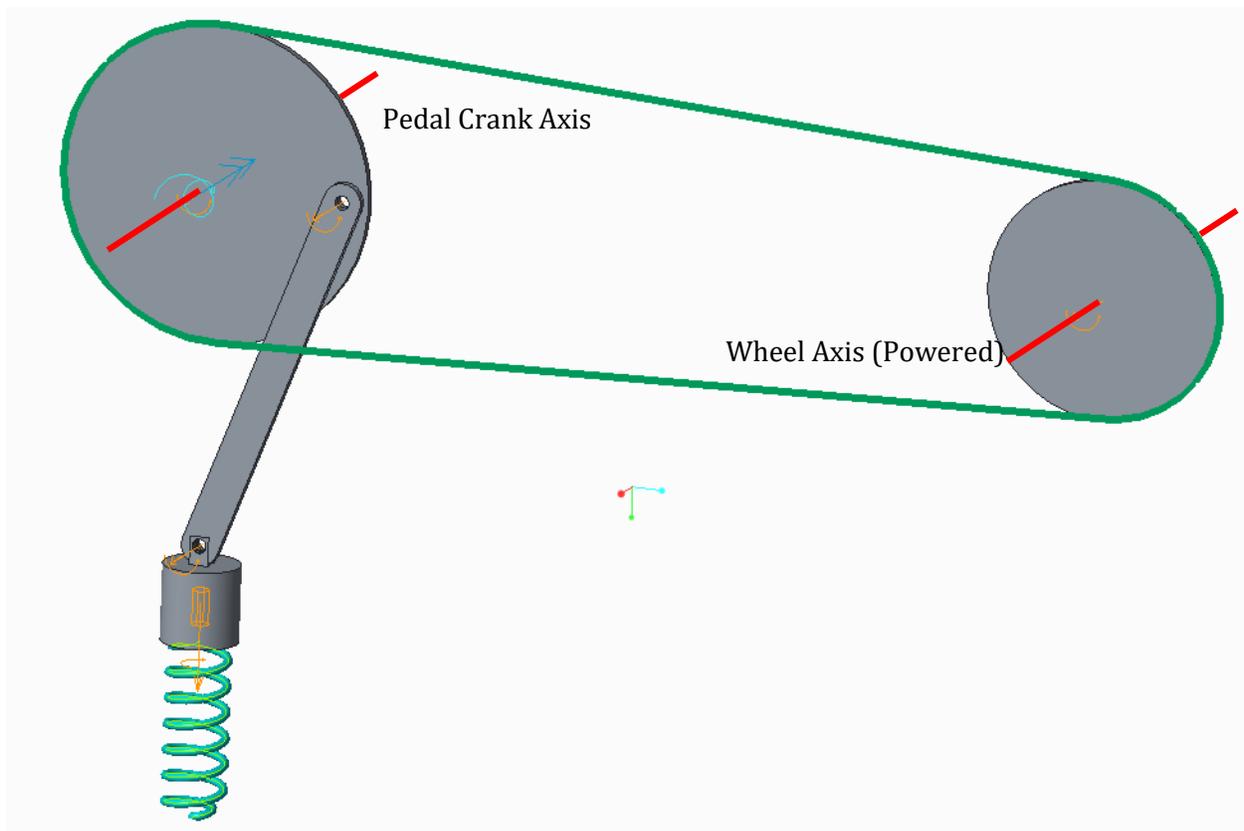


Figure 30: Piston Design

Assumptions

In order to provide a more accurate understanding of how spring stiffness effects level of assistance, a simulated torque resistance of $30 \text{ N}\cdot\text{m}$ (as calculated in Propulsive Force Calculations) was applied to the wheel axis in the opposite direction of travel. The size of each link was chosen to best

represent a four-bar linkage that satisfies the Grashof condition and is reasonably sized to fit within a standard bicycle frame (Figure 31): $a = 0.0181\text{m}$, $b = 0.127\text{m}$, and $c = 0\text{m}$.

Position Calculations

Figure 31 shows the definitions for calculations of the crank-slider mechanism. Solving for d yields the displacement with respect to a fixed point in space (O_2). This fixed point was treated as the stationary end of the spring. This then allowed for Hooke's law to be applied when calculating spring force.

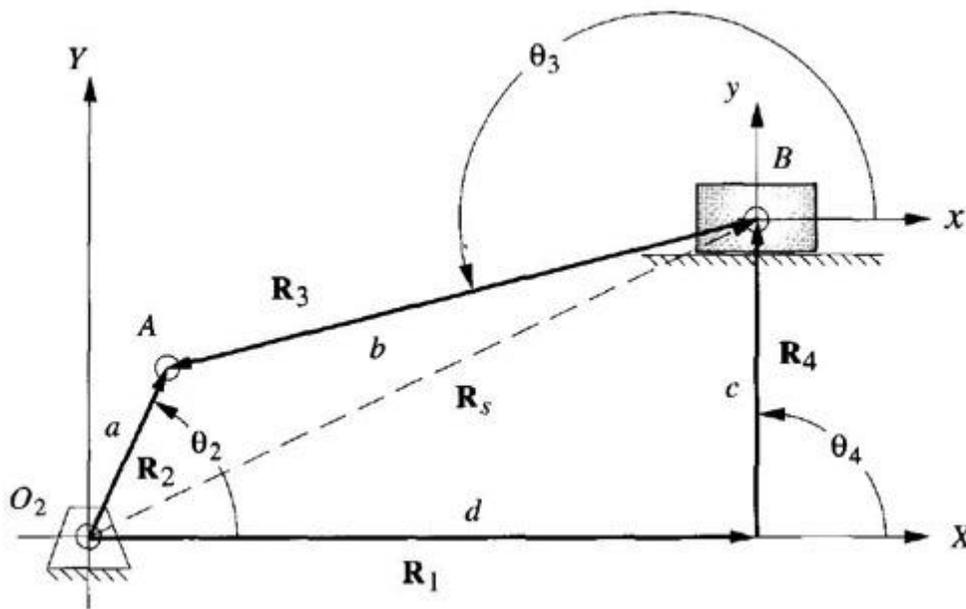


Figure 31: Crank Slider Mechanism Definition (Norton 1999)

All equations in this position analysis were taken as functions of the pedal crank rotation, θ_2 . θ_3 is expressed as,

$$\theta_3 = \arcsin\left(\frac{a * \sin(\theta_2) - c}{b}\right)$$

This yields the link length d as a function of θ_2 and θ_3 ,

$$d = a * \cos(\theta_2) - b * \cos(\theta_3)$$

The distance (d) of the slider with respect to the crank axis of rotation is shown in Figure 32.

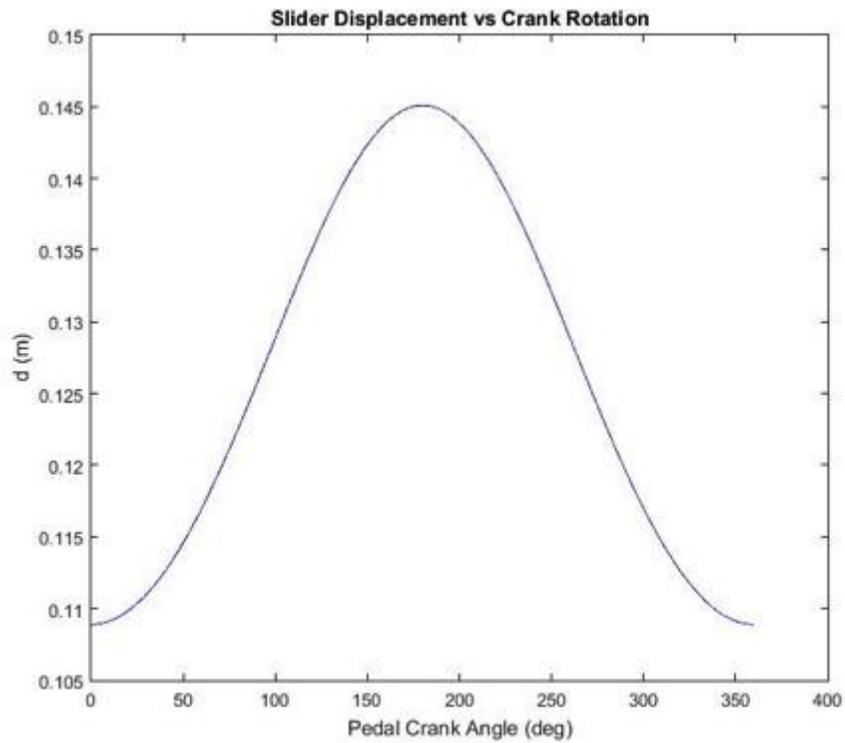


Figure 32: Slider Displacement vs Crank Rotation

Force Calculations

The force on the spring can be expressed using the independent variable, k , and the dependent variable, d , as derived in the position analysis using Hooke's law:

$$F_{spring} = kd$$

The free body diagram of the slider-crank mechanism is shown in Figure 33 and Figure 34.

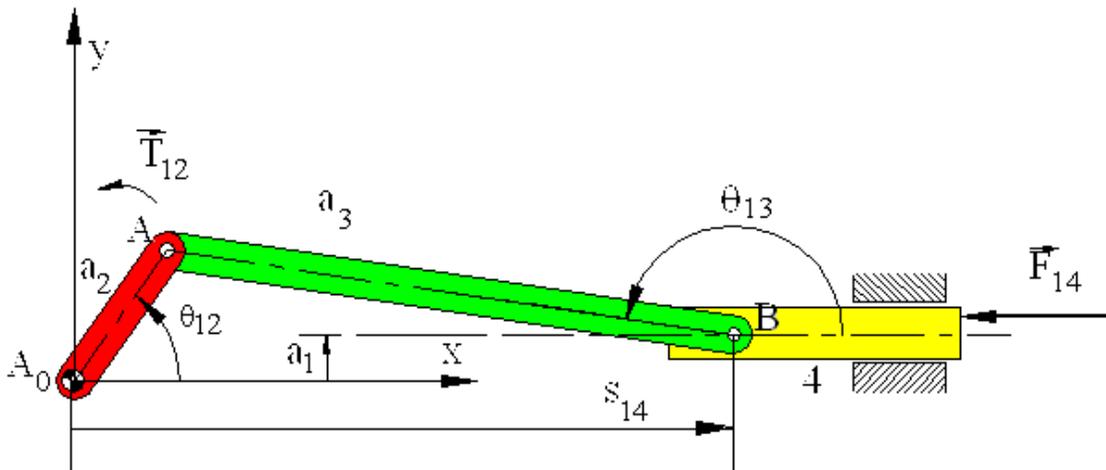


Figure 33: Slider Crank Applied Piston Force (METU, nd.)

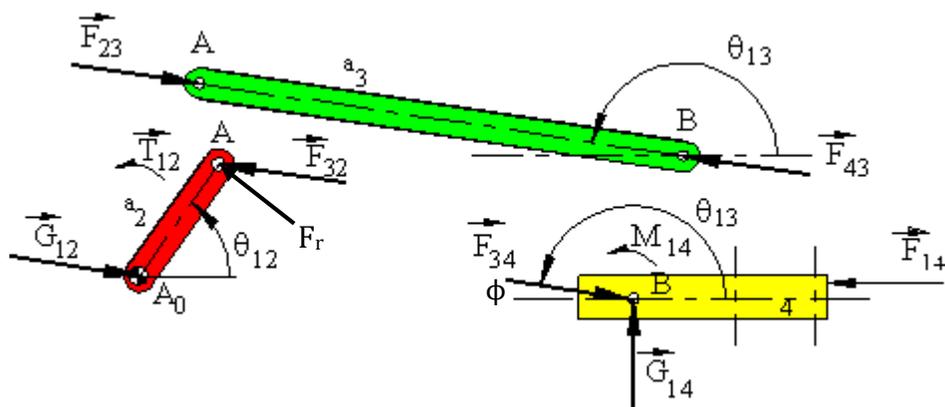


Figure 34: Diagram of Slider Crank Mechanism (METU, nd.)

Where the angle between F_{34} and the horizontal axis is defined as φ ,

$$F_{14} = F_{spring}$$

$$-\varphi = 180 - \theta_3$$

Thus the force acting on the two force member, link AB can be defined as,

$$F_{43} = F_{14} * \cos(\varphi)$$

$$F_{23} = -F_{43}$$

The free body diagram at point A is described in Figure 34, where F_r is orthogonal to link OA.

Where,

$$\psi = 90 - \theta_2 - \varphi$$

Thus, the radial force acting on the pedal crank can be expressed as,

$$F_r = F_{32} * \cos(\psi)$$

Finally, the torque acting on the pedal crank is,

$$T_{12} = (F_r * a) + T_0$$

Where T_0 is the simulated resistance, which occurs from the device’s motion. A plot of experienced torque versus pedal crank is shown in Figure 35.

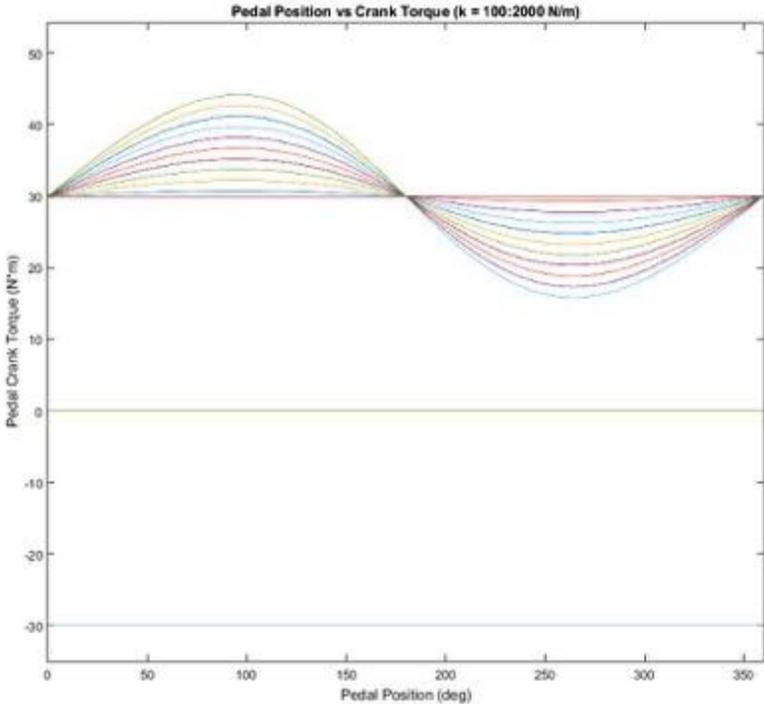


Figure 35: Pedal Crank Torque versus Angle ($k = 100:2000 \text{ N/m}$)

Any value above or below the “neutral” simulated torque is either assisting or resisting the strong and weak legs respectively. The assistive torque should come close to zero in order to provide maximum help to the weak leg; however, if this value drops below zero, the pedal will have the tendency to move the pedal without any input from the weak leg.

Input Force Comparisons

When selecting a final design, it is important to understand how the user must interact with each concept. For example, it can be seen that the spring designs store mechanical potential energy to assist the weak leg; however, the amount of force each leg must exert is not immediately clear. Without investigation, it cannot be known whether the spring stiffness required to achieve a certain level of assistance consequently forces the strong leg to exert more force than would be acceptable. Throughout the pedaling cycle, the normal force applied at the pedal is not constant, Table 31 shows the pedal force scaling factor (F_1) for eight discrete points in the cycle. For each of the spring designs, the required pedaling force was calculated by dividing the resistive torque by the pedal crank radius, and then multiplying this constant normal force by the corresponding scaling factor to its location in the pedaling cycle.

Table 31: Pedal Force Scaling Factors (Passive Assistance Pedaling Device MQP, 2014)

Crank Position (Radians)	Relative Force Scalar Magnitude of F_{applied}	Θ (degrees)	Relative Force Scalar of F_1	Percentage of Maximum Applied Force
0	1.5	135	1	10%
$\pi/4$	6	123	5	50%
$\pi/2$	11	66	10	100%
$(3\pi)/4$	10	45	7	70%
π	6	40	4	40%
$(5\pi)/4$	4	53	3	30%
$(3\pi)/2$	2.5	55	2	20%
$(7\pi)/4$	2	70	1.5	15%

By scaling the forces to reflect approximately what a rider would experience, curves could be generated to understand how each mechanism can be used to assist the weak leg during use. The force curves for the piston and spring resistance designs are shown in Figure 36 and Figure 37.

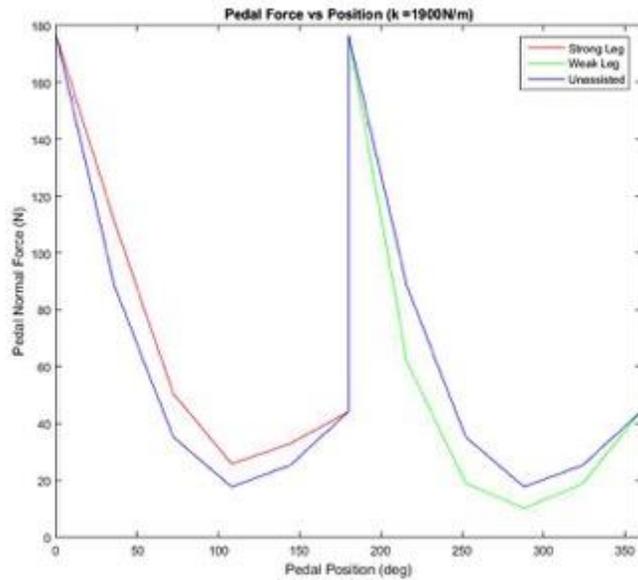


Figure 36: Piston Design Pedal Forces

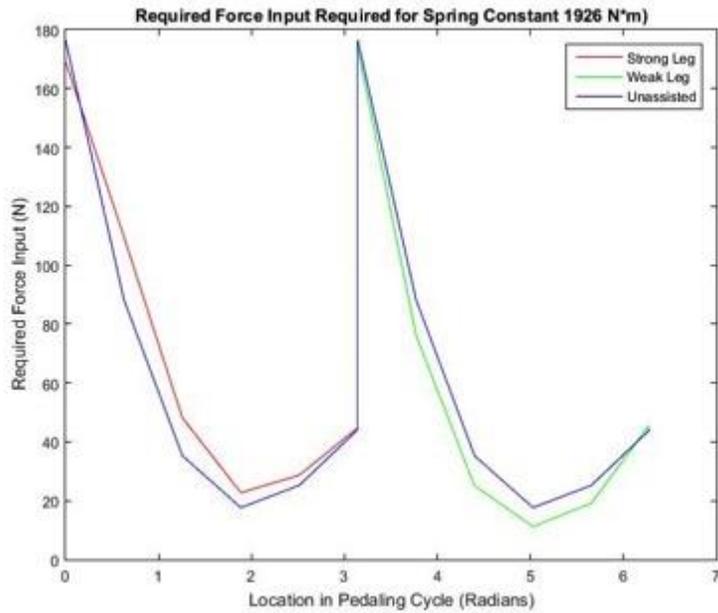


Figure 37: Spring Resistance Design Pedal Forces

The pedal forces and amount of assistance between the spring designs is comparable. With further design optimization better assistance levels can be achieved; however, the similarities between designs would remain. Therefore, a decision must be based on other factors such as design complexity and manufacturability.

Mechanism Bounding Conditions

The mechanism bounding conditions illustrate the volume through which parts of the mechanisms must operate. The larger each box is, the more likely it is that the mechanism will interfere with other parts being added to the device, such as the wheels or the steering mechanism. These boundaries may also affect the configuration of the device. For example, the push pedal mechanism uses long links, so it will limit the length of the device to a very specific dimension, thus affecting the adjustability for the riders.

Push Pedal Mechanism

Figure 38 shows the arrangement of the push pedal design. In the figure, the stationary link 1 measures 43 cm. The driving link 2 has a length of 9 cm. The rocker, link 4, has a length of 20 cm. Link 2 reaches its highest position at an angle of $\pi/2$ radians, and reaches its largest horizontal extension at an angle of π radians. Link 4 sweeps between the angles 3.89 and 4.81 radians from the horizontal. Positions 1 and 2 denote the largest vertical and horizontal positions of link 2, respectively. Positions 3 and 4 are the minimum and maximum angular displacements of link 4, respectively.

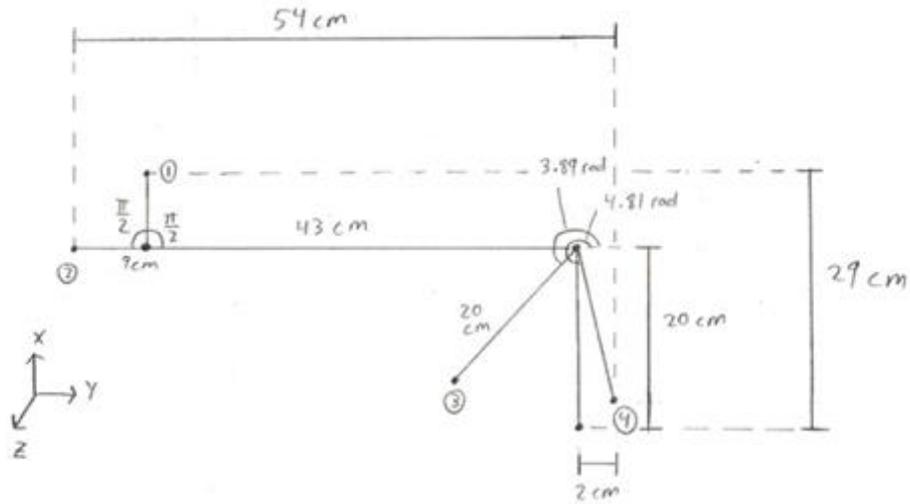


Figure 38: Boundary Box for the Spring Resistance Mechanism

For link 2, the maximum horizontal and vertical displacements are as follows:

$$y_{max} = 9 \text{ cm} * \sin \frac{\pi}{2} = 9 \text{ cm}$$

$$x_{max} = 9 \text{ cm} * \cos \pi = -9 \text{ cm}$$

For position 3 of link 4:

$$y = 20 \text{ cm} * \sin 3.89 = -14 \text{ cm}$$

$$x = 20 \text{ cm} * \cos 3.89 = -15 \text{ cm}$$

For position 4 of link 4:

$$y = 20 \text{ cm} * \sin 4.81 = 20 \text{ cm}$$

$$x = 20 \text{ cm} * \cos 4.81 = 2 \text{ cm}$$

For link 4, position 4 represents the largest horizontal displacement since the link sweeps past the pivot point. However, largest vertical displacement will occur when the link is at $3\pi/2$ radians. Therefore, the displacement will be 20 cm.

In the x direction, the sum of displacements is 54 cm. In the y direction, the sum of displacements is 29 cm. In the z direction, the mechanism extends 25 cm symmetrical about the x-y plane. Therefore, the boundary box for the push pedal design measures 54 cm x 29 cm x 25 cm.

Piston Mechanism

The piston mechanism is shown in Figure 39. For the piston mechanism, the x boundary is 21 cm, the y boundary is 54 cm, and the z boundary is 6 cm. Therefore, the boundary box for the piston design measures 21 cm x 54 cm x 6 cm.

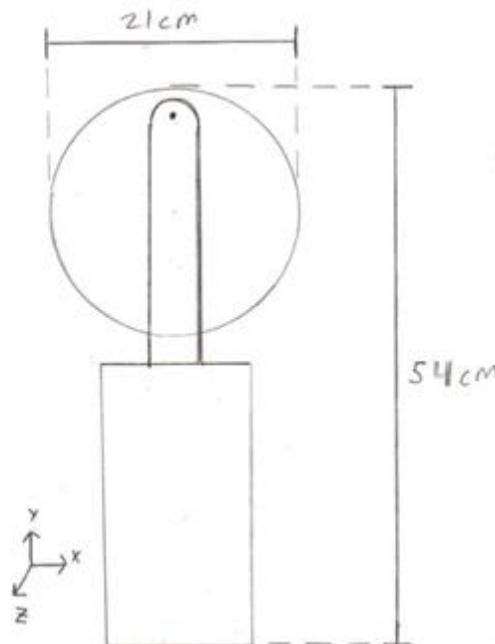


Figure 39: Boundary Box for the Piston Mechanism

Spring Resistance Mechanism

Figure 40 shows the front two sprockets of the spring resistance design. The rear sprocket is a normal rear sprocket of a bicycle drivetrain. Since that area of the design will not require any modification, it will not be included in the boundary analysis. The two sprockets have the same diameter. The x dimension will therefore be twice the diameter, 42 cm. The y dimension will be 21 cm. The z

dimension will be the thickness of the sprockets, which should be no larger than 2 cm. Therefore, the boundary box for the spring resistance will be 42 cm x 21 cm x 2 cm. It must be noted that this analysis does not account for the width of the spring.

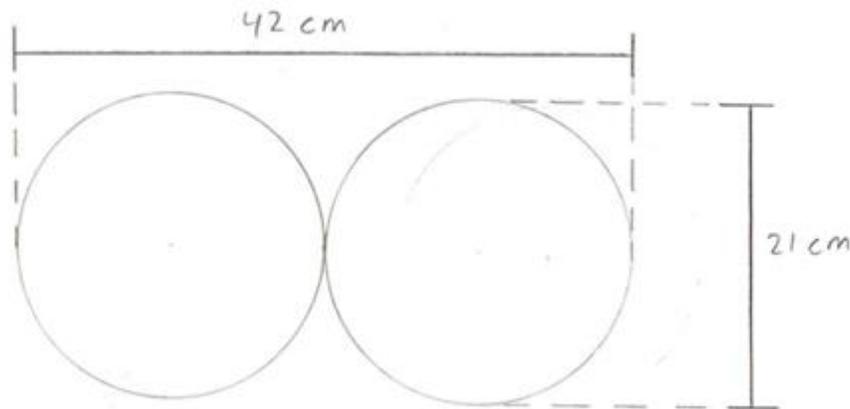


Figure 40: Boundary Box for the Spring Resistance Mechanism

Size and Complexity Analysis

One important consideration for the final design selection was the size of each mechanism. As described in the bounding conditions section, the piston and push pedal mechanisms both added significant volume to the device. The outer boundary of the piston mechanism measures 21 cm x 54 cm x 6 cm (6,804 cm³), while the boundary of the push pedal mechanism was 54 cm x 29 cm x 25 cm (39,150 cm³). In contrast, the spring resistance mechanism only reaches a boundary of 42 cm x 21 cm x 2 cm (1,764 cm³). Since the spring resistance mechanism has the smallest boundary, it will be the most compact and also the easiest mechanism to integrate into the device. The mechanism takes up the least amount of space, so it will be the least likely to interfere with the addition of parts such as the wheels and steering mechanisms. The spring resistance design will also require the least amount of modification to an existing device, thus making it easier to integrate into an existing device.

Another important consideration for the final design selection is the complexity of each mechanism. The push pedal design requires three links (one of which is irregularly shaped), a custom

sprocket, and a spring to be added to the standard drivetrain of a tricycle. The piston design requires a link, a piston, a cylinder, and a spring to be added to the standard drivetrain of a tricycle. In addition, these designs will require many of the parts to be machined, which will significantly increase manufacturing time. In contrast, the spring resistance design only requires the addition of a sprocket, a spring, and potentially an additional chain, all of which can be purchased and then modified. Thus, the spring resistance design will have the lowest potential of manufacturing error of the three mechanisms.

Decision Matrix

After the additional analysis, another decision matrix was used to determine the best design. The previously created ranking criteria for the mechanism were used, and each team member individually filled out the decision matrix (Appendix F) before an average was taken to determine the best design (Table 32).

Table 32: Average Decision Matrix for Final Mechanism Design

Mechanisms	Criteria							Total
	Safety	Cost	Ergonomics	Ease of Control	Manufacturability	Conform to User Requirements	Power Adjustability	
Weighting Factors	18	5	11	10	5	16	35	
Piston	5.00	2.75	4.00	3.75	3.00	3.25	4.00	390
Push Pedal	5.00	2.25	4.25	3.25	3.00	3.25	4.00	385
Spring Resistance	5.00	4.00	4.50	3.50	4.00	3.25	4.00	407

Based on the decision matrix, along with the analysis of the force required by the user, the team moved forward with the spring resistance design.

Final Design

After selecting the spring resistance design, it was paired with the single wheel in front, recumbent design, disc brakes, tiller, platform pedals, and multi-use tires to create a detailed design. A frame including the tricycle components was modified from an existing product. The unique spring resistance design was incorporated into the remaining components.

Frame Selection and Modification

When creating the final design, it was determined that using an existing product for the frame would allow for feasible manufacturing. The majority of recumbent tricycles cost between \$1500 and \$3000, which is not feasible for this project. Manufacturing the entire tricycle is also not feasible for this project due to time and machine space limitations. Therefore, a commercially available tricycle (Figure 41) was purchased to provide the rear portion of the frame and remaining components, combined with a custom front wheel mechanism (Figure 42). The custom front end will be discussed in more detail in the following section.



Figure 41: MOBO Triton Pro (Mobo Triton Pro Ultimate Ergonomic Cruiser, 2015)

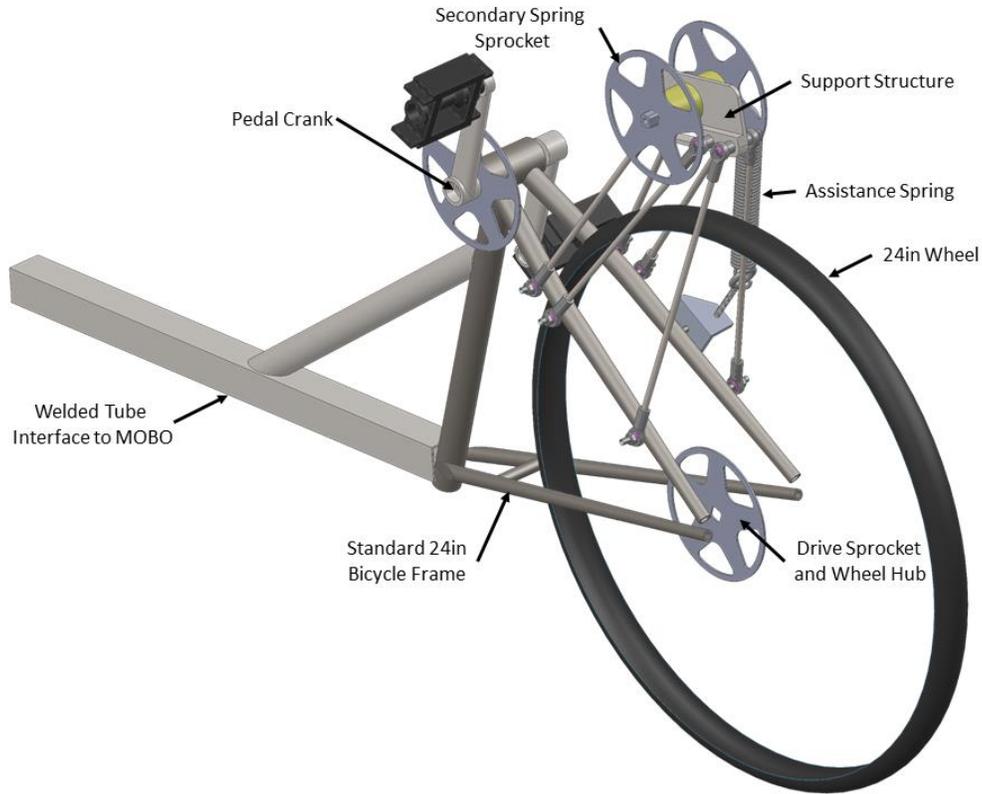


Figure 42: Custom Front End

The MOBO Triton tricycle contains many of the selected remaining design components, but also requires a few compromises. The MOBO has a single wheel in the front, recumbent design, platform pedals, and multi-use tires, all of which meet our previous selections. The main difference in the MOBO design and our selected design is the type of brakes. We selected disc brakes as the preferred type of brakes for our design, but the MOBO has rim brakes. The primary reason for selecting disc brakes for a tricycle is because of the large weight increase of a tricycle over a bicycle. However, due to the low to the ground and lightweight design of the MOBO, it does not have the increased weight of higher end tricycles. In addition, the MOBO already has the hardware and design necessary for the rim brakes, allowing for a simple and safe design.

The MOBO also has slightly different steering than the single tiller originally selected for the design. When examining different types of steering, handlebars and tiller were examined. The MOBO has

a unique type of steering that was not examined before choosing the best design. The double tiller has the same advantage that led to the selection of the single tiller: it can be operated with one hand. Therefore, using the double tiller of the MOBO design does not significantly alter our design considerations.

Spring Mechanism and Support Structure

The design is a hybrid design, which implements a combination of a commercially available tricycle and a custom front wheel mechanism. The stock front end that comes on the MOBO Triton pro couples to the rear end by means of a steel tube that fits inside a steel sleeve on the rear portion of the frame. The custom front mechanism uses a commercially available bicycle frame welded to a steel tube. The steel tube will connect to the rear end of the MOBO.

Using an existing bicycle frame allows for use of the existing structure which has the correct geometry to hold a standard 24-inch bicycle wheel, rear sprocket cassette, front and rear derailleur, and front crank set with pedals. With the bicycle frame inverted, the front crank set is positioned such that the user pedals recumbently with respect to the rest of the frame.

The spring resistance mechanism is driven by a secondary sprocket of equal radius with the lowest gear sprocket in the front crankset. The primary sprocket in the front crankset will be reserved as the driving sprocket to the front wheel (Figure 43).

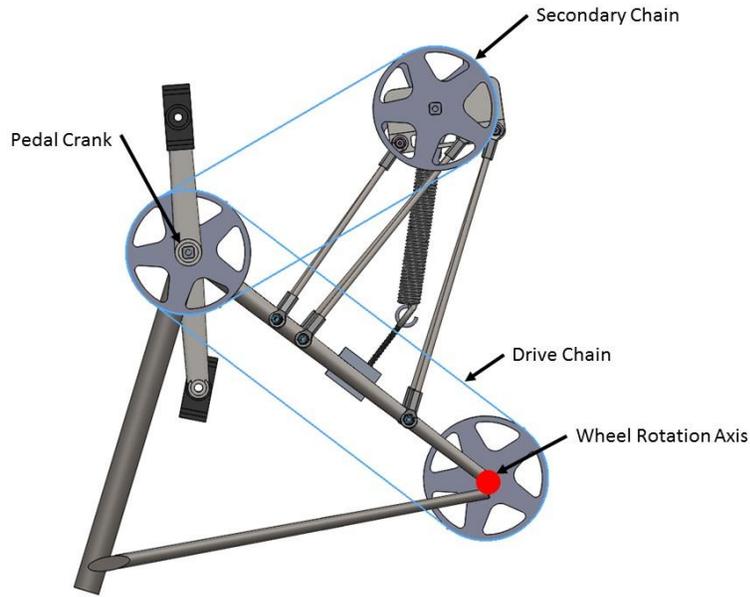


Figure 43: Chain Profile

Spring

The spring was chosen based on calculations from the preliminary design analysis, which showed a spring constant of ~ 2000 N/m as the most viable candidate (Figure 44). However, the design will be validated for significantly stiffer springs to allow for variance in testing. Geometric constraints and part availability was also a factor in the selection. Details on the nominal spring are shown in Table 33. However, a variety of springs will be selected for testing.

Table 33: Spring Data

Century Spring Corp	
Part Number	5597
Rate	111bf/in (1926N/m)
Free Length	7.71in (0.196m)

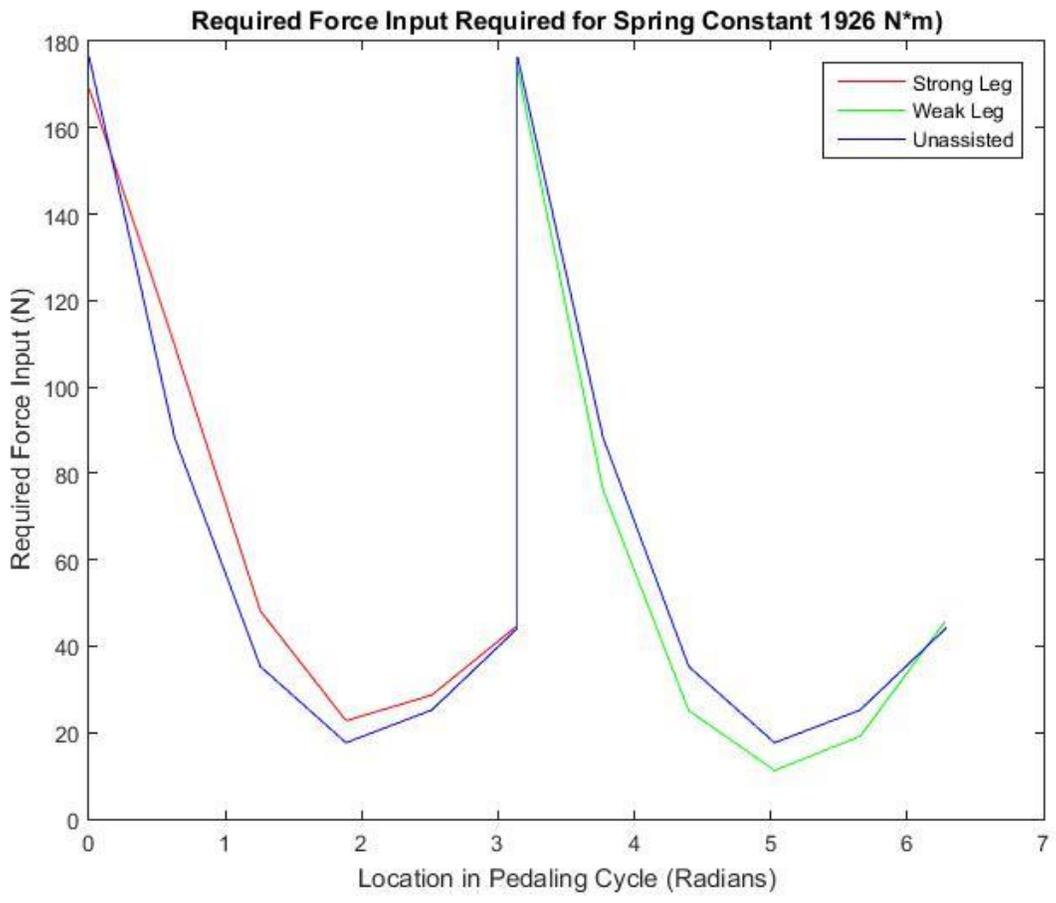


Figure 44: Spring Performance Curves

Design Analysis

To determine the feasibility of the detailed design, various analyses were completed on the components of the tricycle. Analyses were completed on the frame of the tricycle, including stress analysis, mobility analysis, and Finite Element Analysis. The analysis also included finding the factor of safety for the components of the tricycle, to ensure each component could withstand the applied forces. Finally, a stress and fatigue analysis of the bracket supporting the spring-assisted sprocket was completed.

Design Structural Analysis

As part of the design validation process, a detailed structural analysis was conducted on each critical component to ensure that it will survive normal use. The design was split into two parts: the support structure and the spring mechanism.

Support Structure

The support structure is defined as the connecting structure between the bicycle frame and the spring mechanism (Figure 45). It consists of six connecting rods and a coupler plate. The connecting rods attach at each end using swiveling tie-rod ends. Each tie-rod end has 3 rotational degrees of freedom, as well as axial adjustment, which gives the structure the flexibility to be attached on the frame even if the mounting points are imprecisely placed.

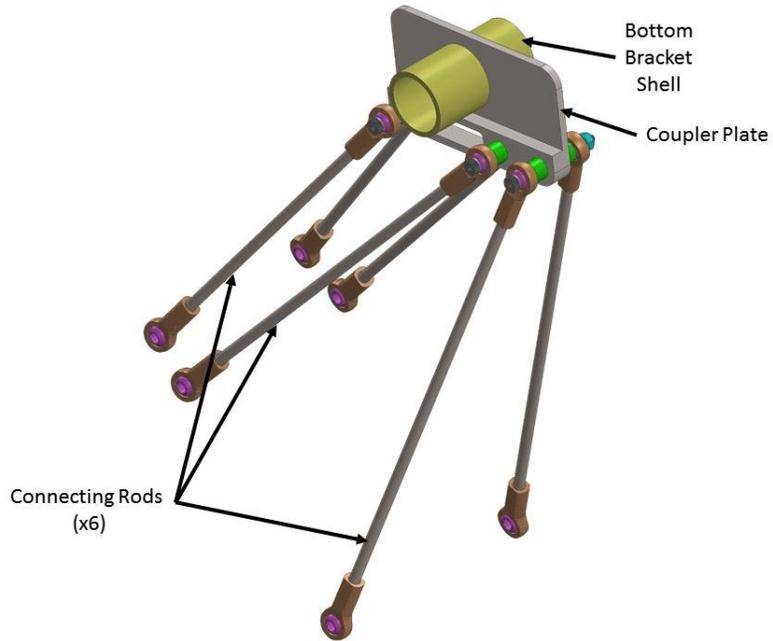


Figure 45: Support Structure

At each of the three connection points on the coupler plate a shoulder screw is used in conjunction with a flanged locknut in order to have less play in the structure. A full stack-up typical of all three connection points is shown in Figure 46.

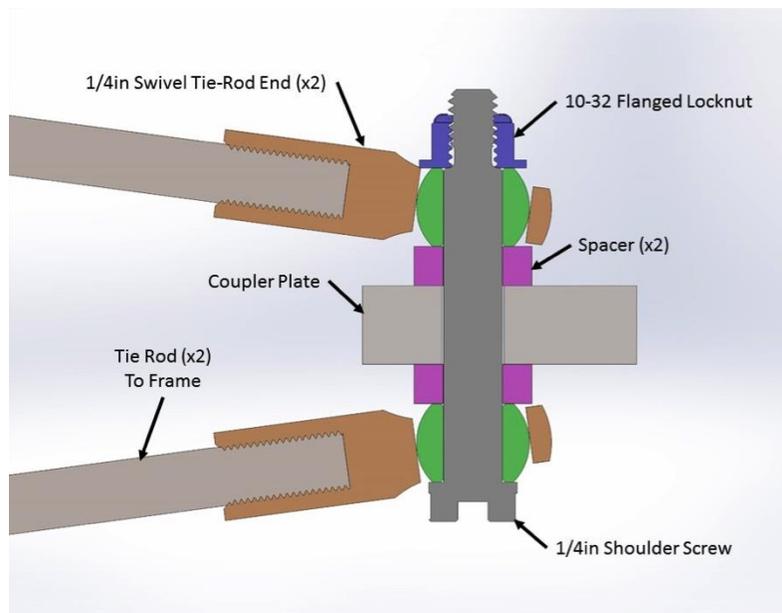


Figure 46: Typical Coupler Plate Connection Stack-Up

Mobility Analysis

The support structure is analogous to a linkage mechanism; however, to be considered a structure it must have 0 degrees of freedom. In three-dimensional space, the “linkage” has 2 grounded links (one on each chain-stay on the frame) and 6 other links, each with a two ball joints supporting 3 degrees of freedom. Finally the support plate itself is treated as a link, bringing the total count to 9 links with 2 being grounded. Using the Kutzbach Mobility equation:

$$M = 6(L - G) - 5J_1 - 4J_2 - 3J_3 - 2J_4 - J_5 = 6(9 - 2) - (3 * 12) = 6DOF$$

Although the mobility analysis shows the structure having 6 degrees of freedom, this system can still be treated as a structure instead of a mechanism because there is an idle DOF about the long axis of each tie rod. This rotation will not impact the rigidity of the structure but will still be reflected in the mobility equation.

Static Analysis Methodology

The support structure was analyzed statically in the condition where the forces generated by the pedals and spring are highest. This condition was determined to be when the spring is fully extended, where $T_{\text{effective}}$ is at its highest (Figure 47).

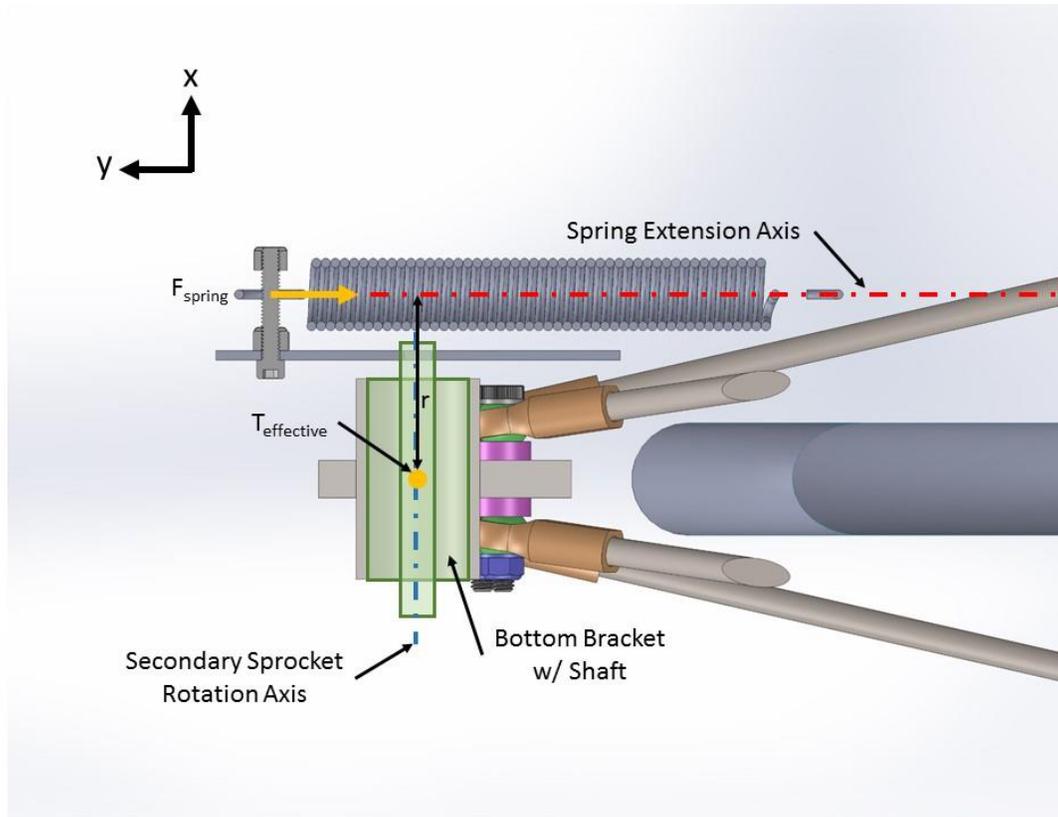


Figure 47: Secondary Sprocket Section w/ Applied External Spring Load

Using the chosen spring ($k = 1900\text{N/m}$), the max load F_{spring} was calculated to be $\sim 200\text{N}$ by applying Hooke's law and a deflection of 0.105m which was determined using the sprocket geometry:

$$F = -kx$$

However, the applied spring load in the forthcoming analyses was multiplied by a scalar of 5 to ensure structural integrity up to spring constants of 10000 N/m .

Finite Element Model

Due to the complex geometry presented in this analysis, Finite Element methods were used to validate the structural integrity of the design. The goal of this analysis is to determine the minimum static safety factor when a remote load of 1000N is applied to the support structure.

The coupler plate geometry was used to create a Finite Element Model (FEM) of the system (Figure 48). Bolts were reduced in complexity to reduce the element count. The entire system was left as an assembly to more accurately represent the behavior of the components together. Each part connection was chosen to most accurately represent the type of physical connection. These connections occur at points of contact between parts; components that are not supposed to move with respect to each other were deemed “welded.” For example, the Bottom Bracket Shell (Figure 45) is welded to the coupler plate, and therefore can be modeled as a rigidly bonded connection.

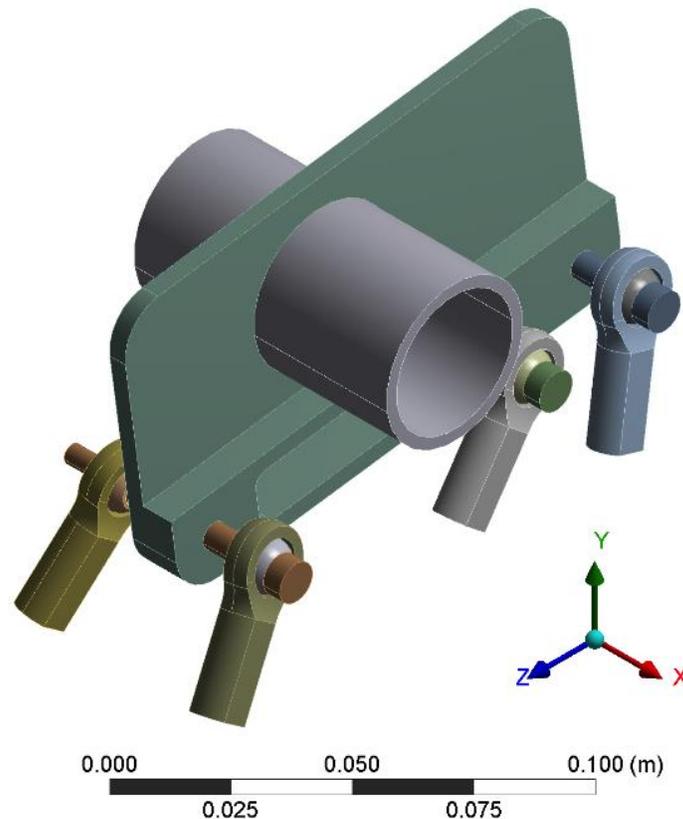


Figure 48: Geometry Analyzed using FEM

FEM Boundary Conditions

The next step in preparing the numerical solution was to apply boundary conditions, or supports and loads. Following the mobility analysis, each connecting rod was treated as a two-force member; therefore, each tie-rod end (A, B, C, D, E, and F as shown in Figure 49) was only fixed along its axis. This was done using “Cylindrical Supports,” which fixes displacement along an axis defined by a cylinder, in this case the allowed displacement is 0m. The external spring load was applied as a remote load acting on the interior surface of the bottom bracket shell (Figure 49). A remote load applied to a body simply takes a force located in space somewhere and finds the resultant forces and moments acting at the centroid of the body. In this case, the body is symmetrical and the centroid is located in the middle of the assembly. By applying the load vector remotely, it allowed for the spring force to be directly applied to the finite element model. Finally, Standard Earth Gravity was applied to factor in for the weight of the components.

A: Static Structural

Static Structural
Time: 1. s
3/27/2016 2:27 PM

- A** Cylindrical Support 0: 0. m
- B** Cylindrical Support 2: 0. m
- C** Cylindrical Support 3: 0. m
- D** Cylindrical Support 4: 0. m
- E** Cylindrical Support 5: 0. m
- F** Cylindrical Support 6: 0. m
- G** Acceleration: 9.8099 m/s²
- H** Remote Force: 1000. N

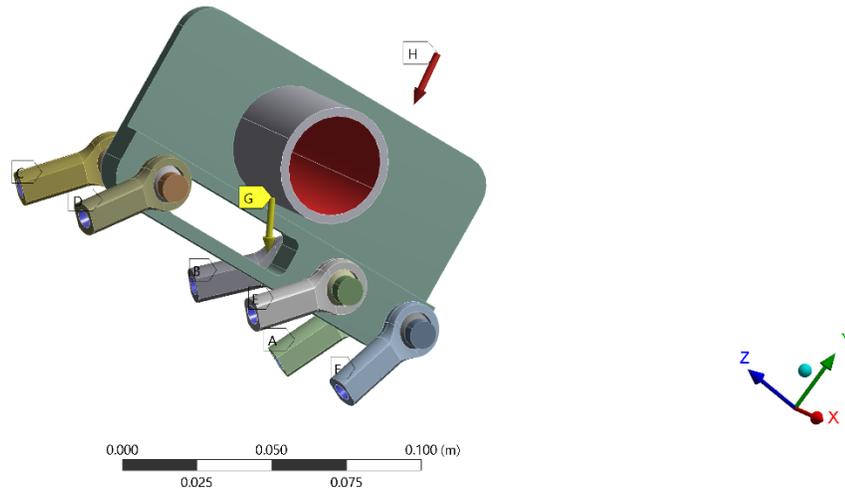


Figure 49: FEM Boundary Conditions

Materials

Two different materials were used in the FEM, Low Carbon Steel and Alloy Steel. All of the machined parts will be made out of AISI 1010, Cold Drawn Sheet, and the purchased fasteners are all made out of Alloy Steel (AISI 1340). Physical Properties are shown in Table 34.

Table 34: Material Properties

Material	AISI 1010, Cold Drawn	AISI 1340 Alloy Steel
Density	7.87 g/cm ³	7.87 g/cm ³
Young's Modulus	205 GPa	200 GPa
Poisson's Ratio	0.29	0.29
Tensile Yield Strength	305 MPa	565 MPa

Mesh

The model was meshed using Solid Tetrahedron Elements with automatic sizing per each component's surface details (Figure 50).

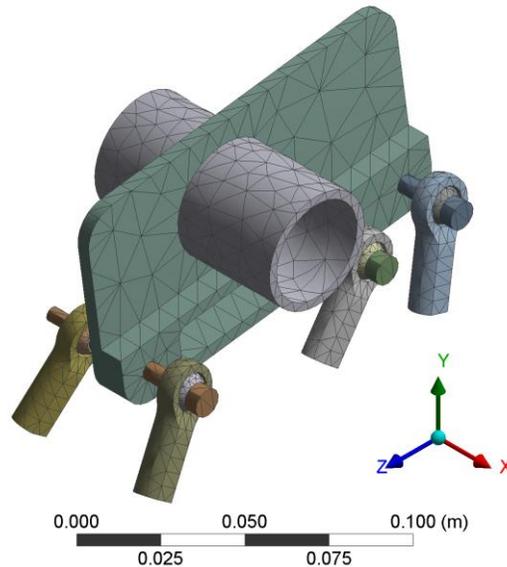


Figure 50: FEM Mesh

Results

After running a Static Structural Analysis using the ANSYS solver, stress, deformation and reactionary force data were computed. Intuitively, one would expect to see the highest stress at the bolts, as all of the load is transferred through the three shoulder screws. This is reflected in the Equivalent (von-Mises) Stress Fringe Plot (Figure 51 and Figure 52) where the peak stresses of 176MPa occur in the bolts where the bending moments are highest.

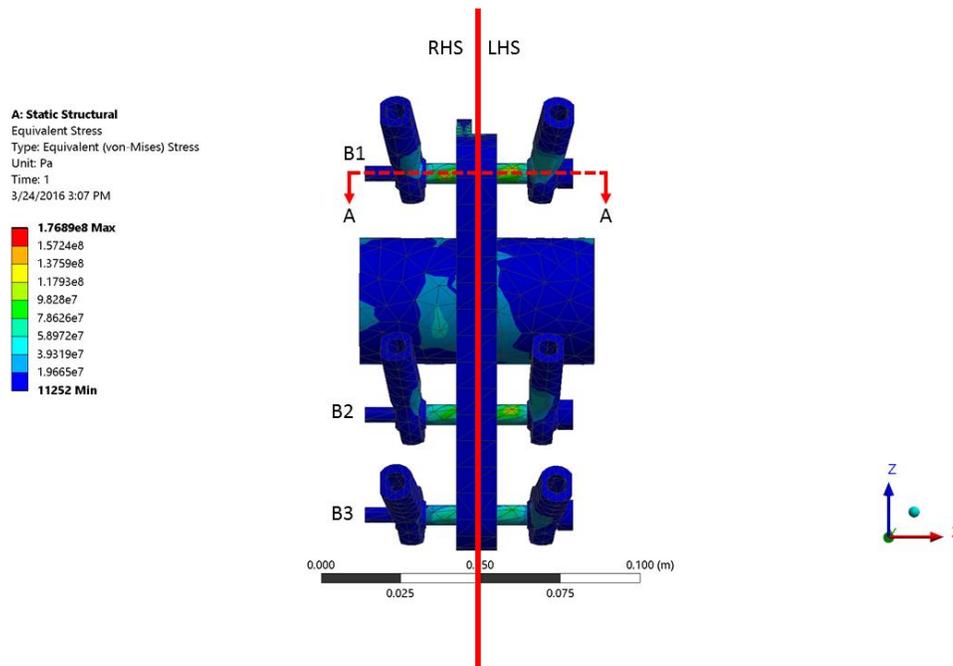


Figure 51: Von-Mises Fringe Plot, Bottom View

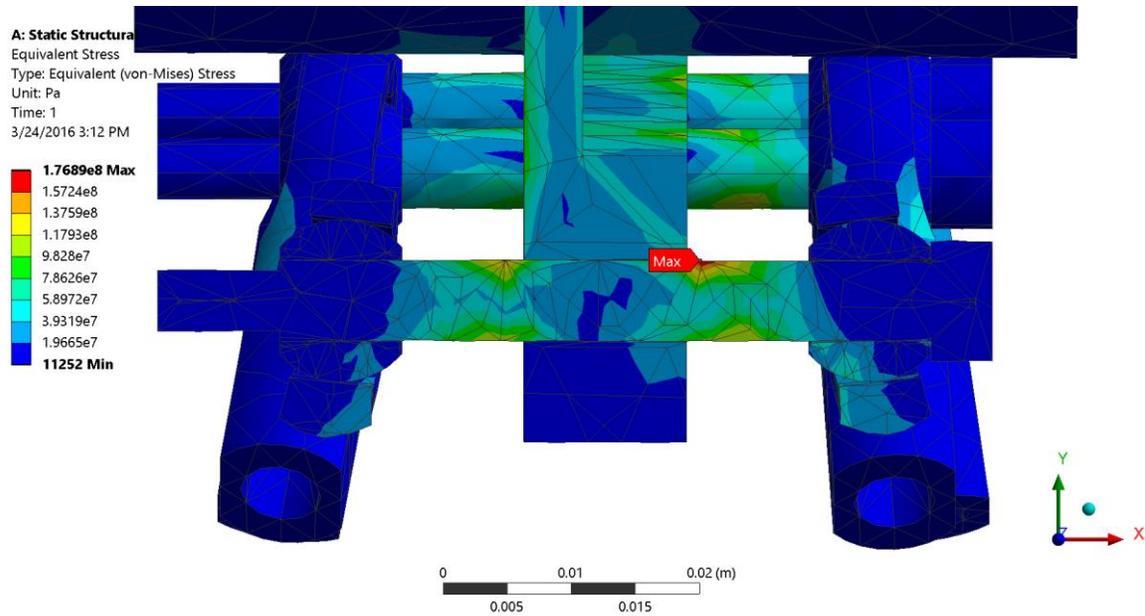


Figure 52: Von-Mises Fringe Plot, B1 Interface (Section A-A)

Factor of Safety

The minimum factor of safety on the support plate with a value of ~ 1.5 (Figure 53). It is also noteworthy that the applied load is already five times greater than the spring chosen for the final design, therefore making the true factor of safety much higher.

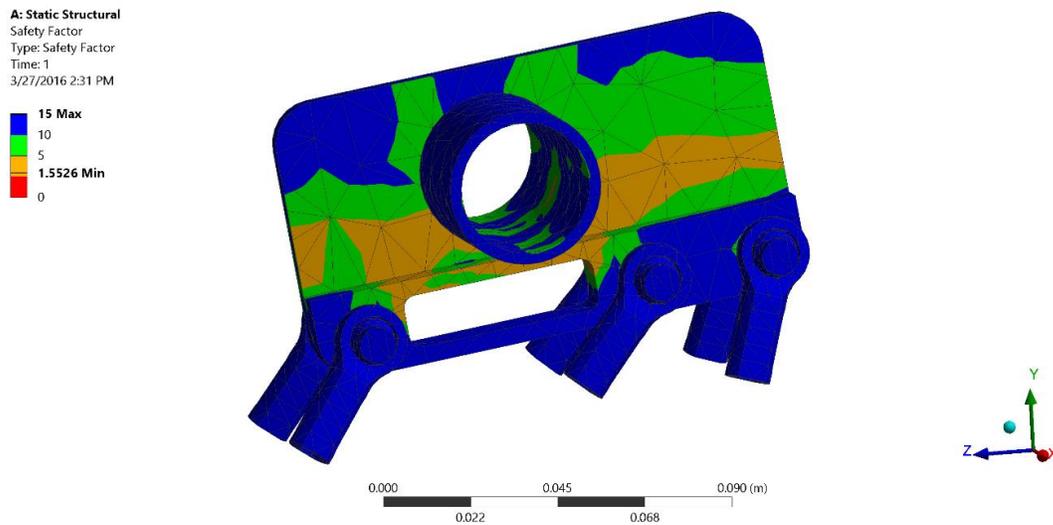


Figure 53: Minimum Factor of Safety at B2 Section

The bolt mechanical properties are described in Table 35.

Table 35: Connecting Bolt Properties

3/8-16 Socket Cap Screw	
Minor Diameter	0.007544m
Effective Length	0.01905m
Young's Modulus	200GPa
Yield Strength	565MPa

With an applied P of 1000N, the maximum stress occurred in bending with a value of 452MPa at $x = 0$. This yields a minimum Factor of Safety of 1.25 for springs rated up to 10000 N/m, which is 5 times stiffer than the spring expected to be used. Additionally, the maximum deflection of the screw occurred at $x = 0.01905\text{m}$ with a value of $\delta_{\max} = 7.2 \times 10^{-5}\text{m}$.

Spring Bracket Analysis

The spring bracket is mounted to the frame on the opposite side to the secondary chain sprocket in order to avoid interference between the spring and the chain (Figure 56). It provides a rigid anchor point for the stationary side of the extension spring providing assistance to the rider. The purpose of this analysis is to determine its safety factor against failing when a spring load of 1000N is applied.

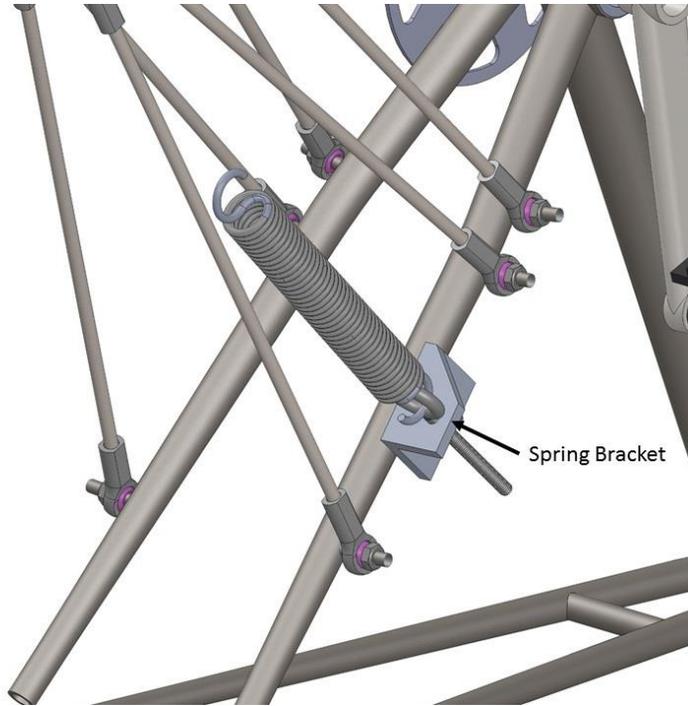


Figure 56: Spring Bracket Location

The geometry of the spring bracket was modified (Figure 57) in order to make stress calculations simpler. The new geometry is simply a right angle cross section with the dimensions as described in Table 36.

Table 36: Spring Bracket Dimensions

Dimension	Value (m)
L	0.0381
a	0.0191
t (thickness)	0.00635
w (width)	0.0762
d (Hole Diameter Typical)	0.00635

The material chosen for the spring bracket was Aluminum 6061-T6 for its high strength to weight ratio and machinability. The material properties used can be found in Table 37.

Table 37: Material Properties (AL 6061-T6)

Property	Value
Modulus of Elasticity (E)	71.7 GPa
Tensile Yield Strength (S_y)	276 MPa
Ultimate Tensile Strength (S_{ut})	310 MPa

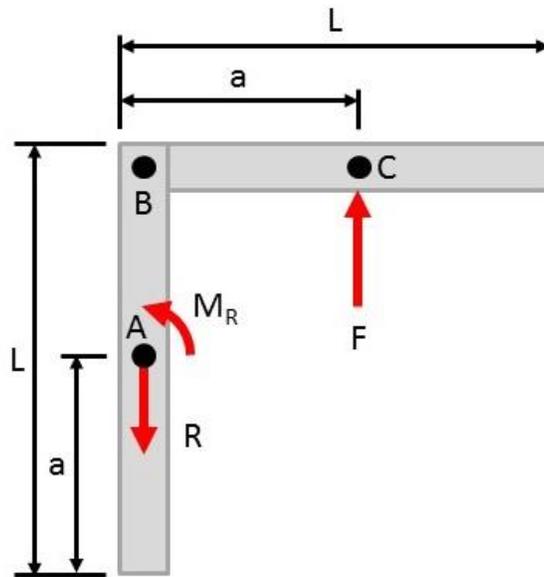


Figure 57: Simplified Geometry and Spring Bracket Free Body Diagram

This cross section was then split into two segments, the vertical component (Figure 58) and the horizontal component (Figure 59). Each was analyzed separately and individually checked for failure.

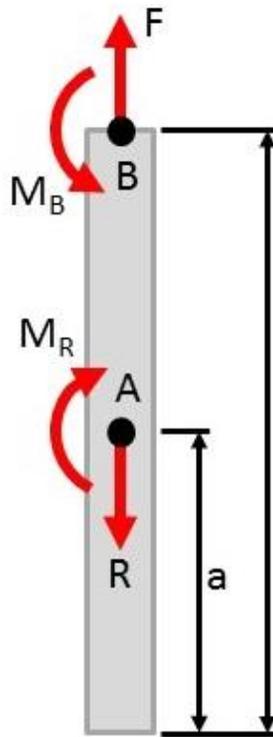


Figure 58: Free Body Diagram of Spring Bracket from Points A to B

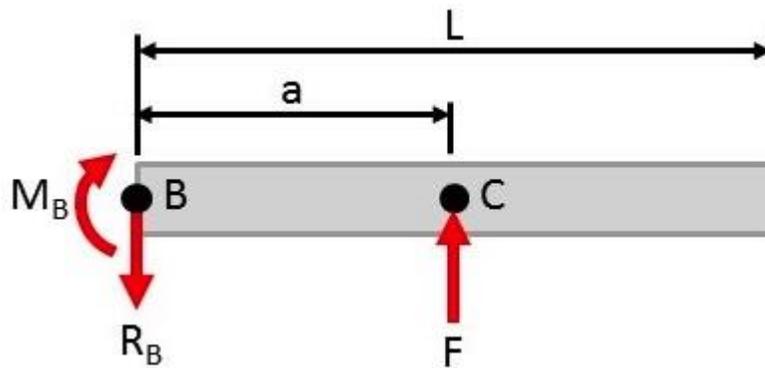


Figure 59: Free Body Diagram of Spring Bracket from Points B to C

First, reactions were calculated for segment BC based on the applied input force, the section was treated as a rigidly supported cantilevered beam. A fretting stress concentration factor of 2 was applied at point B to model the connection between AB and BC. Next, the input forces for section AB were applied as the reactions from BC. Section AB was treated as a beam and stress concentration factors due to bolt holes were calculated. Safety factors were calculated using the distortion-energy theory for ductile

materials, which is the ratio of material yield strength and the Von-Mises equivalent stress. The minimum safety factor was found to occur at the point of attachment to the bicycle frame, and had a value of 1.18 assuming a spring 5 times stiffer than what is expected to be used. The part was also checked for bearing stress at point A and had safety factor of 8.7. Based on these values, the part was deemed acceptable for use. A full derivation of the safety factors can be found in Appendix J.

Seat Extender Analysis

The purpose of this analysis is to determine if the force caused by the weight of the rider and the force caused by the rider pedaling will cause shearing in the bolts or plate or buckling in the plates. The weight of the rider was set to the maximum weight allowed by the design specifications: 250 pounds. The force caused by the pedaling was taken at the maximum value that occurs for the strong leg during the pedaling cycle, and found in the analysis of the spring: 180N. This maximum value occurs when using the spring with the highest spring constant. The axes used for the analysis are shown in Figure 60.

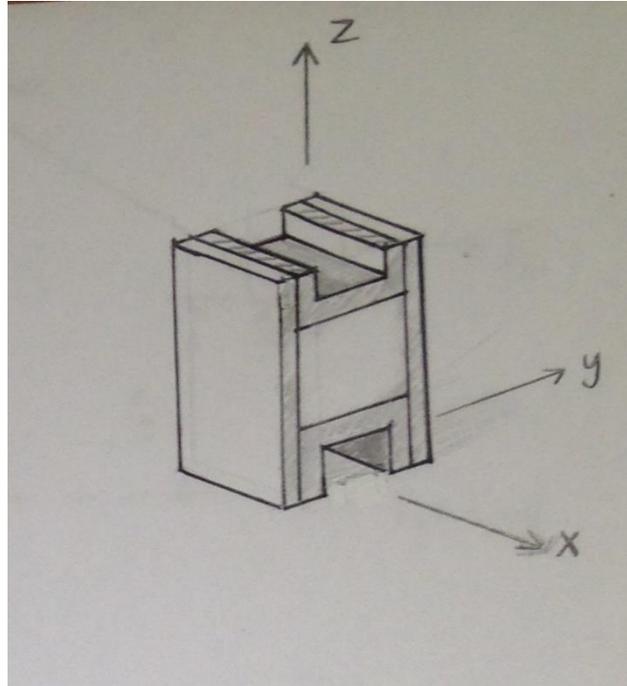


Figure 60: Axis of Orientation for Analysis of Seat Extender

Shearing in Bolts

The free body diagram of the plate is shown in Figure 61. The bolts are holding the seat extender to the frame that is held stationary. The weight of the rider, W_p , occurs in the center of the x-z plane of the extender. The force of the pedaling occurs on the pedal, which is at the same height as the hip.

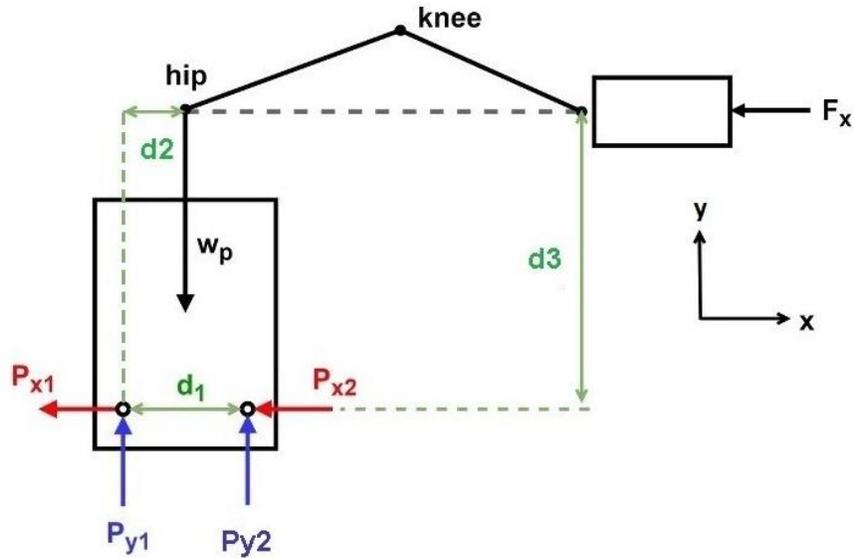


Figure 61: Free Body Diagram of the Seat Extender Plate

P_{x1} = support from bolt one in the x-direction

P_{y1} = support from bolt one in the y-direction

P_{x2} = support from bolt two in the x-direction

P_{y2} = support from bolt two in the y-direction

W_p = weight of the rider

F_x = pedaling force

d_1 = x distance between bolt one and bolt two

d_2 = x distance between bolt one and the location of the weight of the rider

d_3 = y distance between bolt one and the location of the pedaling force at maximum distance

MathCAD was used to solve for the forces acting on the bolts (Figure 62). Note that this is being treated as a planar system, meaning there are only 3 independent static equations. In order to calculate P_{x1} , P_{x2} , P_{y1} , and P_{y2} the deflection in the bolts must be calculated. However, for ease of calculations, it is assumed that the worst case scenario is present in which all of the force in the x direction is being supported entirely by one bolt.

$$d_1 := 4\text{in} = 0.102\text{m}$$

$$d_2 := 2\text{in} = 0.051\text{m}$$

$$d_3 := 8\text{in} = 0.203\text{m}$$

$$W_p := 1112\text{N}$$

$$F_x := 180\text{N}$$

$$\Sigma M_p := (P_{y2})(d_3) - (W)(d_2) - (F_x)(d_3) = 0$$

$$P_{y2} := \frac{(W_p \cdot d_2 + F_x \cdot d_3)}{d_1} = 916\text{N}$$

$$\Sigma F_y := P_{y1} + P_{y2} - W_p = 0$$

$$P_{y1} := W_p - P_{y2} = 196\text{N}$$

$$\Sigma F_x := F_x - P_{x1} - P_{x2} = 0$$

$$P_{x2} := F_x = 180\text{N}$$

$$P_2 := \sqrt{(P_{x2})^2 + (P_{y2})^2} = 934\text{N}$$

Figure 62: MathCAD to Solve for Forces Acting on the Bolts

The area over which the shear acts (Figure 63) is in the x-z plane.



Figure 63: Area Over Which the Shear Stress Acts

MathCAD was used to determine the shear stresses resulting from the forces acting on the bolts over the appropriate cross-sectional area (Figure 64).

$$D_{\text{bolt}} := .375 \text{ in} = 0.00953 \text{ m}$$

$$r_{\text{bolt}} := \frac{D_{\text{bolt}}}{2} = 0.00476 \text{ m}$$

$$A_{\text{bolt}} := \pi r_{\text{bolt}}^2$$

$$T_{\text{bolt}} := \frac{P_2}{A_{\text{bolt}}} = 13.1 \text{ MPa}$$

For Alloy Steel

$$\sigma_{\text{yieldalloy}} := 300 \text{ MPa}$$

$$T_{\text{yieldalloy}} := 1172 \text{ MPa}$$

$$FS_{\text{bolt}} := \frac{T_{\text{yieldalloy}}}{T_{\text{bolt}}} = 89$$

Figure 64: MathCAD to determine the Shear Stresses Acting on the Bolt

Buckling in the Plates

Safety factors due to buckling were determined using a model to find the eccentric buckling force. A free body diagram of the simplified geometry for the eccentrically loaded column is shown in Figure 65.

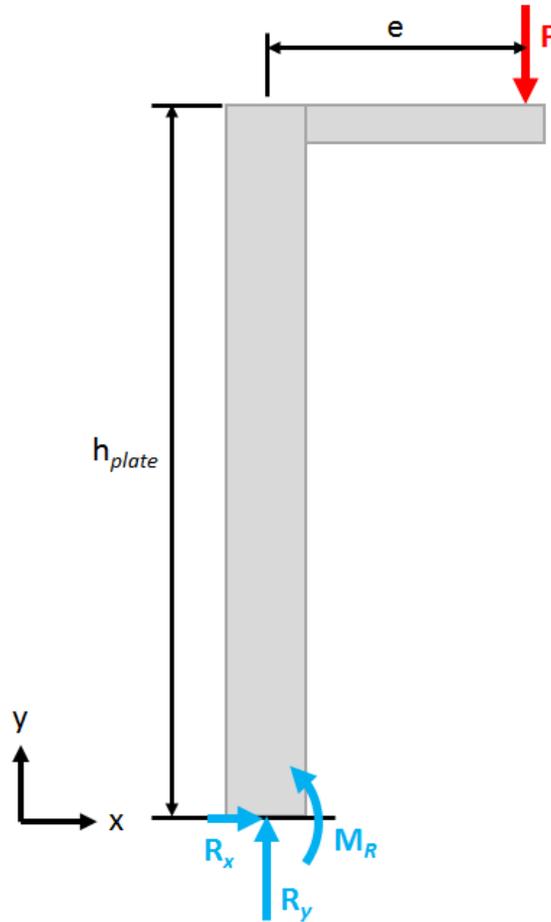


Figure 65: Simplified Free Body Diagram Showing Eccentric Buckling of the Seat Extender

F = the maximum force that can be placed on the extender before buckling occurs

h_{plate} = the length over which the buckling force acts

e = Eccentricity of applied force to column neutral axis

MathCAD was used to find the maximum possible force that would occur before the plates on the seat extender would buckle. A full derivation of the critical load can be found in Appendix H. The critical buckling load was found to be 215lbf for each plate, making the safety factor 1.72.

A summary of the factors of safety can be found in (Table 38).

Table 38: Summary of Factors of Safety in Seat Extender

Type of Failure	Factor of Safety
Shear in Bolts	89
Shear in Plates in x-directions	434
Shear in Plates in z-directions	140
Buckling in Plates	1.72

Based on the analysis, the seat extender will not fail under the weight of the user or force applied due to pedaling.

Manufacturing

With the analysis completed and the parts ordered, the manufacturing process could take place. The manufacturing began with the rear end of the MOBO Triton being assembled. The next step was to fabricate the parts which modified the MOBO from its original design, most importantly the front fork, seat extender, and the plate to hold the spring-sprocket. After the fabrication of these parts, the next step was to assemble the entire tricycle, which included attaching the fabricated parts to the MOBO, and adding the additional components, such as the brackets, gear sets, and brakes.

Machined Parts

The use of machined parts was avoided as much as possible in order to minimize the time spent manufacturing. Machined parts must be analyzed for failure, which adds complexity and time to the analysis. However, this design needed several parts which could not be ordered, and thus had to be custom made. The need for a plate to hold the bracket, handlebar extenders, and a custom seat extender to improve the ergonomics for the rider became apparent.

Spring Support Plate

An important part of the device is the plate which holds the bracket for the spring-sprocket (Figure 66). Burt Seger, who runs his own small machine shop from his home in Jefferson, MA, assisted greatly in the manufacturing of this part. This part began as a 3 x 5 x ½ inch block made from 1018 steel. The process began with drilling the holes in the part to support the bracket shell and shoulder screws. With these features in place, a fly cutter was used to create the step in the part. Finally, the outside profile of the part was machined using an end mill.

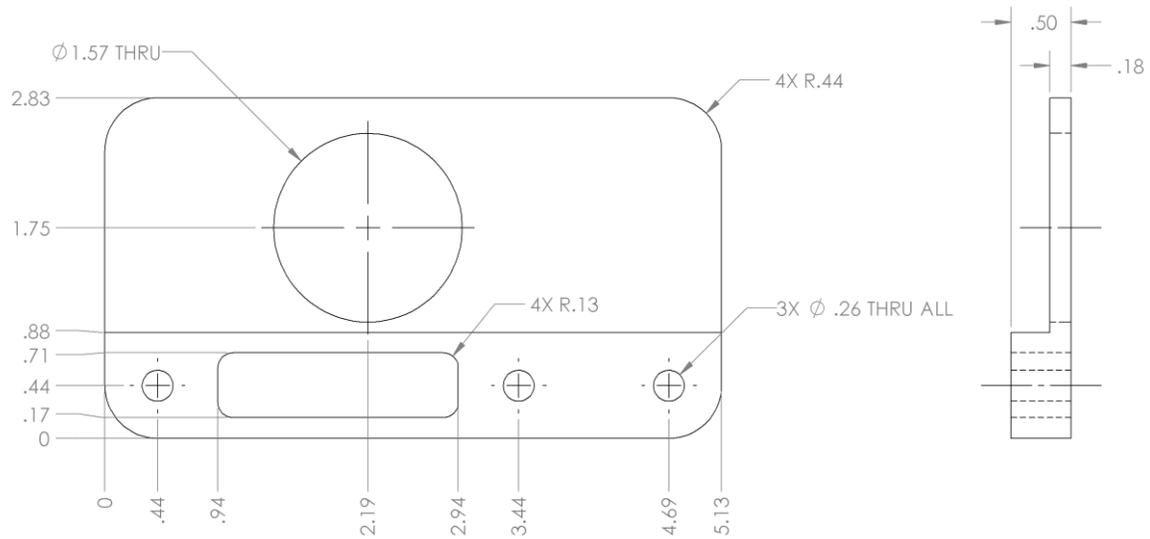


Figure 66: Plate with Tie Rod Ends

Handlebar Extender

The handlebar extenders were machined with further assistance with Burt Seger. A 2-foot length of 1 $\frac{3}{4}$ inch diameter 6061 aluminum was purchased. The stock was mounted into a lathe with 1 foot of the stock protruding into the machining area. The first step was to machine the outside profile, which has two different diameters (Figure 67). With the outer profile machined, the next step was to bore holes into each end of the handle. First, the finished surface was cut away from the stock. Then, the handlebar extender was mounted into a separate lathe and the center holes were drilled. The center hole inside the wider profile was added in order to attach the extender to the handlebar, while the center hole in the smaller profile served to reduce the weight of the part. This process was repeated identically for the other handlebar extender. The rubber grips from the original handlebars were then reattached to the smaller ends of the handlebar extender.

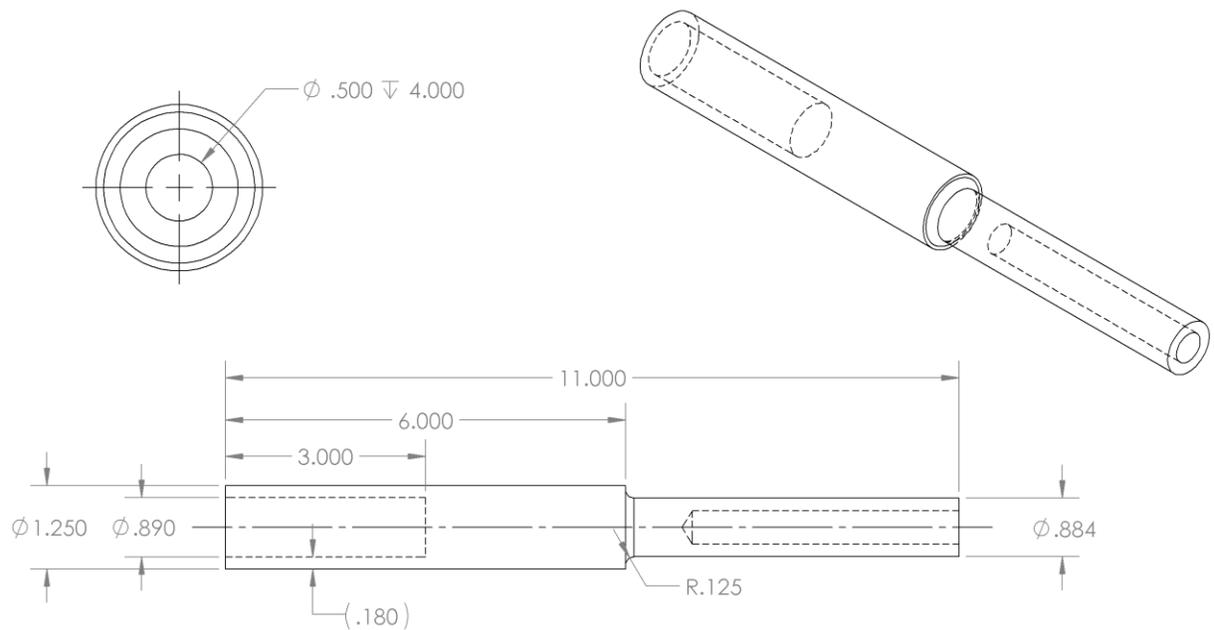


Figure 67: Outside Profile of Handlebar Extender

Welding

An important part of the manufacturing process was the use of welding. The use of welding made it possible to manufacture parts of the tricycle which would have been difficult to machine. For example, instead of machining the seat extender out of a block of material, it was made by welding two thin plates and two c-channels together. This decision reduced both cost and time, since machining the part would have resulted in a large amount of scrap material. In addition to the seat extender, the fabrication of the front fork, support plate for the spring sprocket, and connecting screws was all completed with the use of welding.

Front Fork

An important section of our design is the front fork, which is not only the front wheel of the tricycle, but where our spring sprocket mechanism is connected. This part of the manufacturing was done with the assistance of WPI alumnus Scott Guzman. Guzman provided us with access to an arc welder and assisted us in the cutting and welding of the front fork. In order to weld the necessary parts of the front

fork, a fixture was made (Figure 68). The frame allowed the parts to stay in place as they were welded together. The front fork's fixture was constructed out of wood, measuring 48 inches long, 24 inches wide, and 15 inches tall.



Figure 68: Frame with Welding Fixture

It was decided to use the seat and chain stay section of a BMX bike to act as part of the tricycle's front fork. An axle grinder was used to cut this section off from the rest of bicycle. To ensure proper welding, the square and cylindrical tubing were cut with an axle grinder so that they could have direct contact with BMX seat and pedal frame during the welding. With all parts cleaned and cut, the parts were then aligned on the fixture. First, the tubing and BMX bike frame were welded together. The threaded steel screws were then welded onto the chain stay of the BMX bike frame.

Seat Extender

To create this part, one channel piece was first welded on one end of a steel plate (*Figure 69*). Next, the second channel piece was welded on the other side of the plate, opposite to the other channel piece. Finally, the second plate was welded onto the opposite end of the channel pieces.



Figure 69: Welding of Plate to Channels

Additional Welding

The support plate and outer shell of the bottom bracket were welded together next. The outer shell was inserted into the support plate to its correct position, then welded together using the arc welder. In addition, screws for the spring attachment were welded to the front forks chain stay. The screws closest to the pedal were later shortened with a Dremel tool so that they do not interfere with the pedal crank.

Once all of the parts had been fabricated and welded, some additional modifications had to be made to the parts of the tricycle in order to allow for its functionality. These modifications were minor and easy to perform, so they were performed by hand. The modifications consisted of creating holes in the front fork assembly for adjustability, cutting the tie rods in order to attach the spring support plate, and painting the welded tubes to prevent rust.

Originally, the front end of the MOBO Triton was connected to the rear end by screwing a bolt through a hole in the rear end and any one of ten holes in the front tube. In order to preserve the adjustability of the length of the tricycle, the same feature was created in the tube of the new front fork. The holes were drilled into the tube by hand using a power drill. The holes were positioned such that the

longest setting would place the back of the seat 39 inches from the center of the crank, and the holes were each 1.5 inches apart. This positioning is nearly identical to that of the original MOBO front fork.

In order to connect the spring sprocket support plate to the frame, a truss system made of threaded tie rods was connected to the plate and the front fork using tie rod ends and screws welded to the frame. The margin of error in the length of the rods was large enough to justify cutting the rods by hand. The tie rods have 28 threads per inch, allowing for precise adjustability. In order to cut the tie rod ends to the desired length, a small circular saw was used on a Dremel tool.

Upon completion of the welding process, all of bare metal parts were painted in order to prevent rust and the loss of structural integrity.

Assembly

The first step of the assembly process was to assemble the rear end of the MOBO. Next, the seat extender and seat were bolted to the rear end of the MOBO. Then, the tie rod, plate and bracket assembly was attached to the front fork. Once these steps were completed, the next step was to attach the gear-set, chain, and spring to the front fork. Finally, the handlebar extenders were attached to the existing handlebars.

Assembling Rear End of the MOBO Triton

The MOBO was assembled according to the manufacturer's instructions. The brake was detached from the front wheel of the MOBO to allow the custom front fork to be attached to the rear end of the MOBO, and the brake to be reattached to the wheel of the custom front fork.

Attaching Seat Extender and Seat to Rear End

The seat was originally attached to the rear end of the MOBO by bolts which went through holes in the c-channel under the seat and holes in the tube of the rear end. The seat extender was designed to mimic this attachment method. Holes were drilled into the c-channel portion of the seat extender. Aligning the holes in the seat extender to those on the MOBO proved to be very difficult. Instead, holes

were drilled into the seat extender without regard to the position of the holes in the MOBO, and the holes in the seat extender were used as guides to drill new holes in the MOBO frame. Thus, the proper alignment of the bolts through both the seat extender and the tube on the rear end of the MOBO was achieved (Figure 70).



Figure 70: Fully Installed Seat Extender

Tie Rod, Plate, and Bracket Shell Assembly

The tie rod ends were bolted to the front fork using the welded screws. The tie rod ends were then attached on either end of the tie rods. The tie rod ends were then bolted into the plate using spacers and shoulder screws. Unlike the analysis predicted, the tie rod assembly was not stable, and cross-supports were eventually added to stabilize the tie rod assembly. Additionally, a problem arose when the chain between the pedals and the wheel rubbed on the tie rods. In order to prevent this interference from occurring, changing the geometry of the tie rod assembly was attempted. A longer shoulder screw and wider spacer were used to bolt the middle tie rod ends to the plate. This adjustment resolved the interference between the middle tie rod end and the chain by moving the tie rod further out from the center of the tricycle. However, the longer shoulder screw interfered with the movement of the crank.

Since changing the geometry proved to be problematic, it was decided to move the chain from the outermost sprocket of the crankset to the innermost sprocket, thus resolving the interference (Figure 71).

This solution was not ideal because it changed the kinematics of the drivetrain from those analyzed. However, it was the fastest and easiest solution to implement.

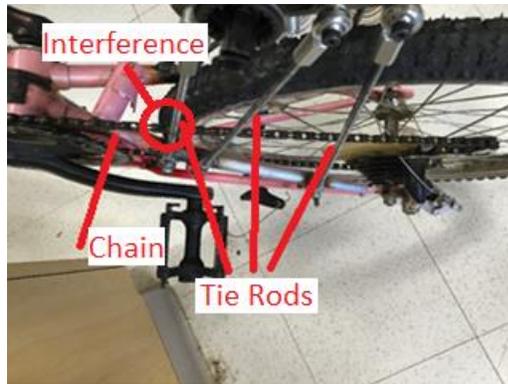


Figure 71: Chain and Tie Rod Alignment

Attaching Sprockets and Chain

With the plate secured in place, the next step was to attach the sprockets to the assembly. In order to attach the sprockets, a purchased bottom bracket was used. The bracket is designed to thread into the end of the shell. However, this task proved to be difficult because the welding process warped the bracket shell. A measurement using calipers revealed that the bracket was oval, so the bracket was clamped with a wrench to account for the warping. The presence of this wrench made it much easier to insert the bracket into the shell (Figure 72).



Figure 72: Bracket Installed into Plate Assembly

With the bracket securely installed, the next step was to attach the two sprockets. The sprockets came as part of two cranksets, which include a base connected to the crank arm. Since the crank arms were not needed, they were cut away from the base with a hacksaw. The other sprockets were unbolted from the base, leaving only one sprocket per crankset. The sprocket on the left allowed the spring to be attached, while the sprocket on the right allowed the driving crankset to be connected to the spring mechanism. The right spring sprocket was attached to the sprocket on the driving crank which had the same number of teeth (38) by using an ordinary bicycle chain. The installation of this chain allowed the tricycle drive train to work properly, by allowing the rider to drive both the forward movement of the tricycle and the rotation of the spring sprocket by simply pedaling.

Attaching the Spring

In order to attach the spring, an angled piece to attach to the screws welded to the frame was created by cutting a square tube into an L-shaped bracket with a hacksaw. Holes were drilled into the piece to allow connection to the frame and the eye bolt. The piece was then bolted to the bike frame, and an eye bolt was inserted into the top hole in order to attach the spring.

The spring was then connected to the sprocket (Figure 73). A bolt was inserted through a hole in the sprocket, and attached to the sprocket with a nut. The spring was then attached to the bolt by placing it between two bolts and two washers (Figure 74).



Figure 73: Spring Connected to Frame and Sprocket

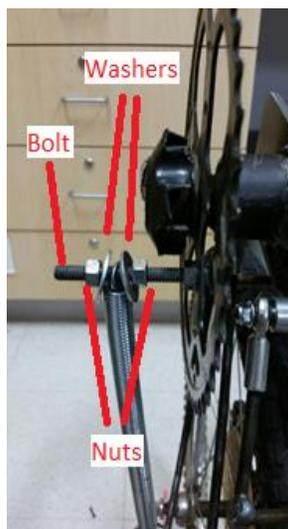


Figure 74. Spring Attached to Sprocket

Attaching the Handlebar Extenders

The handlebar extenders were mounted to the original handlebar ends using the hole in the bottom of the handlebar extender. One of the extenders had a tighter fit, and was thus press-fit onto the handlebar end. This fit was tight enough to prevent the handlebar extender from being pulled off or

rotated. The other extender was not snug on the handlebar end and was therefore fastened to the handlebar end using a strong epoxy.

Attaching the Brakes

The original brake pads from the front end of the fork were used. A new cable was purchased and measured along the bike to the proper length to allow for proper braking. The rubber jacket was then cut to its proper length, to allow about 2 inches of the wire to be exposed from the jacket. The wire was then inserted into the jacket, and bolted to the attachment point near the brake pads. The wire was then run along the length of the fork toward the rear end of the bike, and slipped through a slot on the underside of the rear end which prevents the cable from dragging along the ground when the length of the tricycle is adjusted. The wire was then properly hooked to the inside of the brake lever, thus allowing the brake pads to make full contact with the wheel when the brakes are engaged.

Testing

With manufacturing completed, the tricycle was ready to be tested. The tricycle was first inspected to ensure it was safe for the rider. The tricycle then underwent both quantitative testing with human subjects, and qualitative testing with force plates to ensure the tricycle is suitable for both recreational and rehabilitative purposes.

Safety and Functionality Testing

The first step of testing the tricycle was to ensure that the tricycle met the Consumer Product Safety Standards (Appendix A). Among the most notable standards are the needs to remove sharp edges, securely tighten all fasteners, and eliminate any protrusions from the rider's space. Upon completion of the inspection process, the tricycle was deemed safe for use by the test subjects. In addition to ensuring the tricycle met safety standards, the tricycle was tested by members of this project team to ensure that it worked properly. A group member was able to ride the tricycle on a flat surface, steer, ride and apply the brakes both up and down an inclined surface of up to 5°, and apply the brakes on level ground.

Qualitative Testing

An important part of the testing procedure was to determine whether uninitiated users could easily operate the tricycle. The test subjects were asked to perform the following test procedures, which were approved by WPI's Institutional Review Board (IRB). First, the subjects were given a pre-test to ensure that they were fit enough to ride the tricycle. The main part of the test was divided into two portions. The first portion of the test was to ride the tricycle on the level ground of WPI's quadrangle. The purpose of this test was to give the riders a feel for the pedaling, steering, and braking of the tricycle, as well as find a rough estimate of the ratio between pedaling forces from each subject. The second portion of the test was to ensure that people could effectively ride the tricycle up and down a hill, apply the brakes traveling downhill, and apply the brakes while traveling uphill at various inclines. This test was to

be performed with three different spring constants. The complete testing procedures, including the survey the subjects completed, appear in (Appendix I).

Six subjects completed the first portion of the test on the quadrangle. Only two of the subjects completed the hill portion of the test due to the time the entire test took (approximately 40 minutes). In contrast, the flat portion of the test only took 10 minutes. The subjects were all able to ride the tricycle completely through the test path. However, an ongoing issue with the spring-sprocket chain derailing prevented the test subjects from judging the difference in pedaling forces. Even without the mechanism working, the subjects were still able to ride our tricycle like a normal tricycle, and thus were able to judge all other aspects of the tricycle. The subjects gave generally favorable ratings to the tricycle. A complete overview of the results can be found in the Results and Analysis of Results sections of this report.

Quantitative Testing

In order to empirically test the amount of assistance delivered to the weak leg, sensors were used on each pedal to measure actual applied forces. Force sensors consisting of 2 pressure plates and an array of 3 load cells were attached to each pedal (Figure 75 and Figure 76). From each pedal, wires ran to the data conditioning circuits and ultimately a computer to record data.

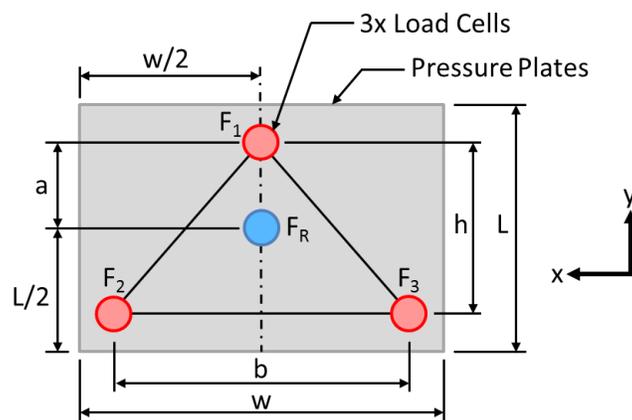


Figure 75: Force Sensor showing Load Cell Array

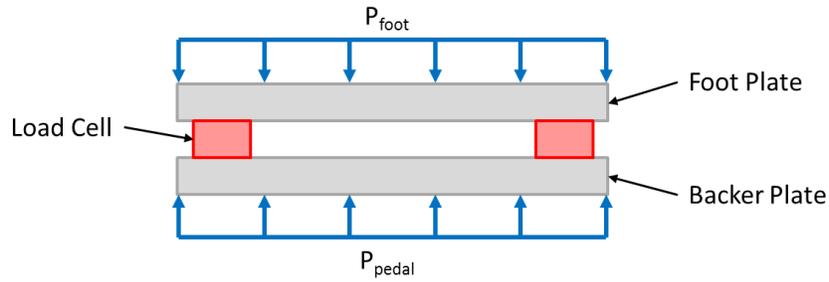


Figure 76: Force Sensor Applied Pressures

The applied foot force is represented as F_R and is the result of pressure P_{foot} taken at the centroid of the foot plate. Throughout the test, F_R was shown in real time to the test operator, as well as recorded for future use.

Force Sensor Design

The actual load cells used were “half-bridge” strain gauge load cells (Figure 77). This means they use two strain gauges in orthogonal directions to complete half of a Wheatstone bridge (Figure 78). When a force is applied the strain gauges output a change in resistance, which can be converted into a change in load.



Figure 77: Load Cell Used (Load Sensor – 50kg)

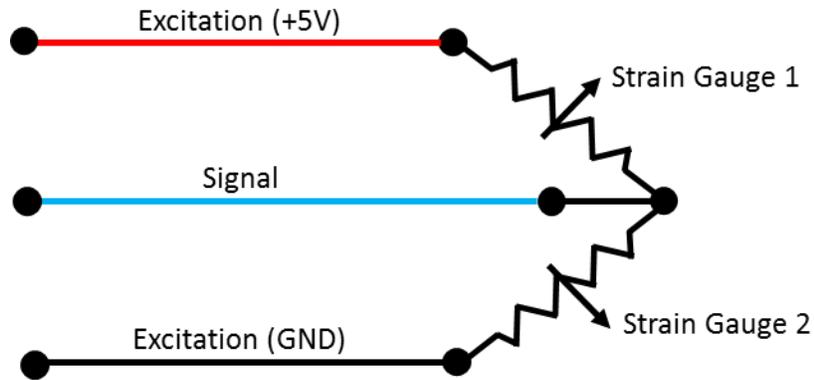


Figure 78: Load Cell Internal Wiring

In order to complete the Wheatstone bridge, two reference resistors of known resistance (330k Ohms) were inserted into the circuit. The output of all 3 load cells were wired together in parallel before running through an HX711 load cell amplifier board (Figure 79). This Analog to Digital Converter (ADC) takes the very small change in voltage due to the strain gauges and amplifies it into a digital signal that can be read by the Arduino UNO microcontroller. Finally, the digital signal is interpreted by the Arduino software and output as force data that could be saved and plotted.

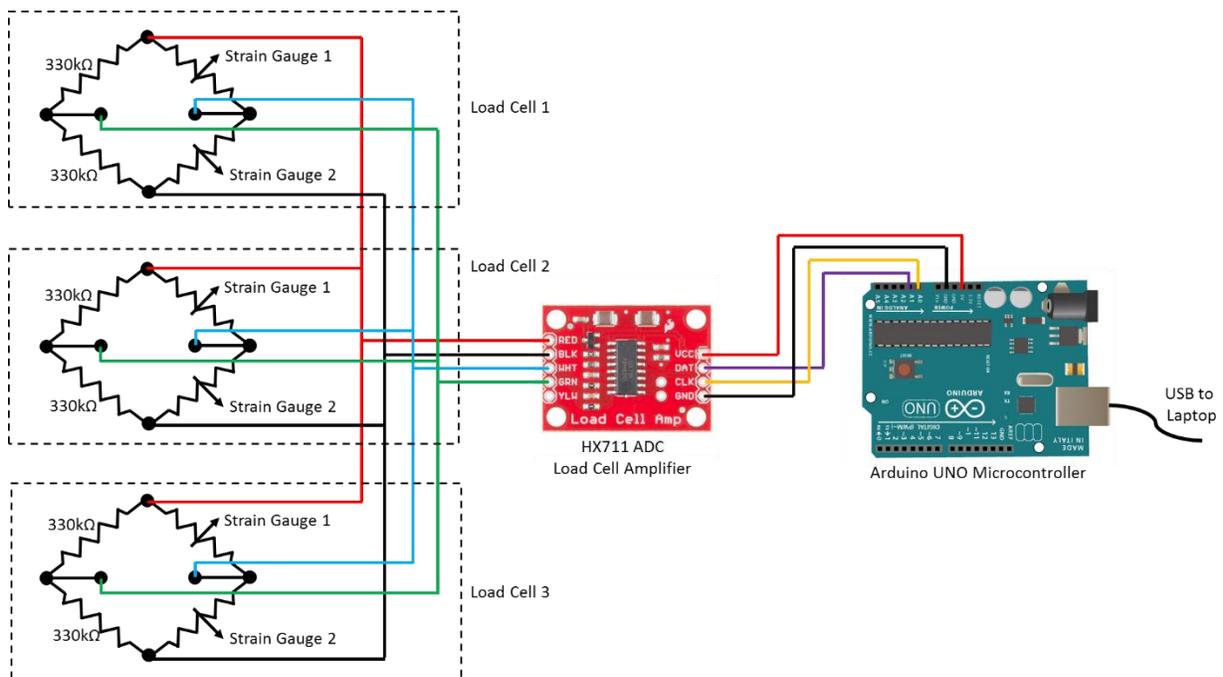


Figure 79: Load Sensor Wiring Diagram

The three wired load cells were then rigidly glued into place between the two aluminum plates. Each completed force sensor was then secured to each pedal using cable ties. During the test, a data recorder needed to follow the tricycle with a laptop to record forces. The detailed test procedure can be found in Appendix J.

Results

Qualitative Results

Due to problems with the tricycle, testing with subjects had to be modified. Many of the questions on the survey pertained to portions of the test related to the spring. Since the spring would not stay on more than one or two revolutions of the pedal, it was removed for the subject testing. The modified survey can be found in Appendix K. The test was completed on six riders with heights varying from 5 feet to 5 feet 9 inches, and weights from 100-160 pounds. The height of women and men ages 50+ are 5.0 and 5.3 cm less than the height of men and women 20-29, respectively (Gharakhanlou et al., 2012). Therefore, for the purpose of our tricycle, testing on shorter subjects corresponds to the height of riders that would typically be riding it (elderly). The results from the qualitative subject were positive overall. For the six test subjects, the average for all questions (excluding question 1) was 4.5/5. The answers to each question, for each subject, can be seen in Table 39.

Table 39: Subject Testing Results for Each Question on Survey

Question	Subject					
	1	2	3	4	5	6
What is your experience level riding bicycles?	1	5	4	5	4	4
How easily could the tricycle be adjusted to fit your height?	1	3	5	5	5	5
How comfortable did you find the recumbent pedaling position?	4	4	4	5	5	5
How easy was it to adapt to the pedaling style?	4	5	5	5	5	5
How often did the components of the device intrude into your pedaling space?	3	5	5	5	5	5
How easily was the device to steer?	3	4	5	5	4	4
How easy was the steering technique to learn?	5	4	4	5	5	5
How intuitive was the braking system to operate?	5	5	5	5	5	2
When the brakes were applied, how well did the tricycle stop?	3	5	4	5	5	4
How well did your feet remain on the pedals?	5	5	5	5	5	5
How comfortable was the seat?	4	4	4	5	5	5
How stable did you feel on the tricycle?	4	4	5	5	5	5

When the subjects finished testing, they were also asked to comment on the questions. The comments to each question can be found in Appendix L.

Quantitative Results

Force measurements were taken on each pedal simultaneously while an operator rode the tricycle along a fixed course. These tests were carried out with three different spring constants: 5.5lbf/in (963N/m), 11lbf/in (1926N/m), and 15lbf/in (2626N/m). Finally, force data were collected without the spring mechanism active in order to gain a baseline “control” sample for comparison (Figure 80). The same operator was used across all tests to maintain consistency with pedal forces so that they may be compared.

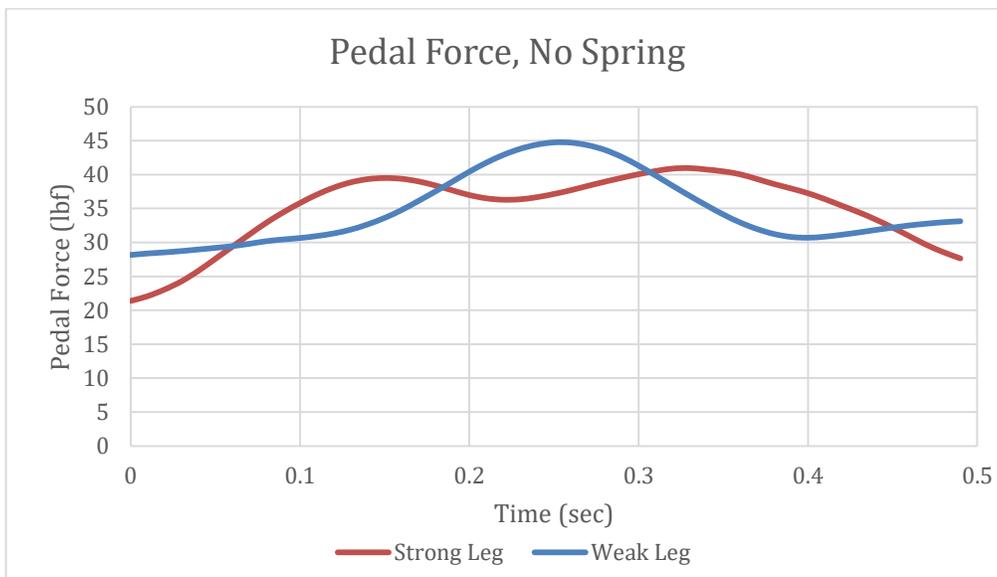


Figure 80: Pedal Force Control, No Spring

In the event of any bias between the two pedal sensors, left and right pedals were compared separately to their respective control tests. The data presented in Figure 81 and Figure 82 have been smoothed using a 15 step moving average filter in order to reduce noise and isolate power cycle peaks. Each figure depicts the isolated data pertaining to the average power stroke of each leg across all three springs, compared to the average power stroke of the control associated with that leg.

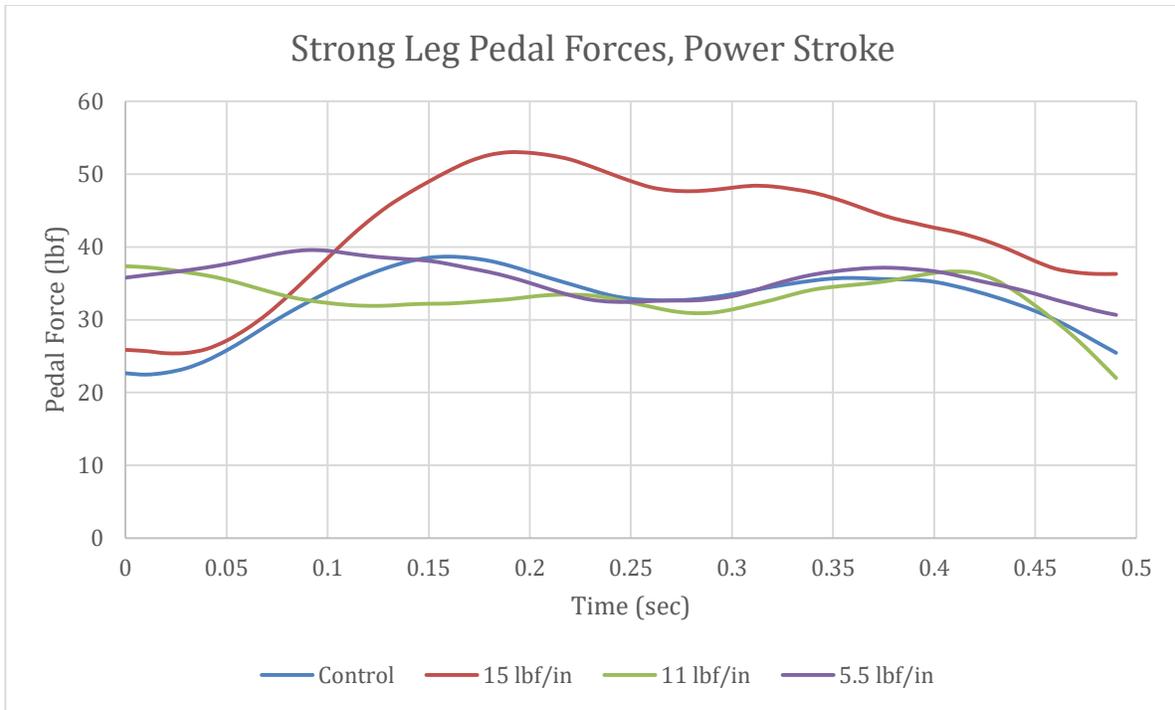


Figure 81: Strong Leg Pedal Forces with three different springs

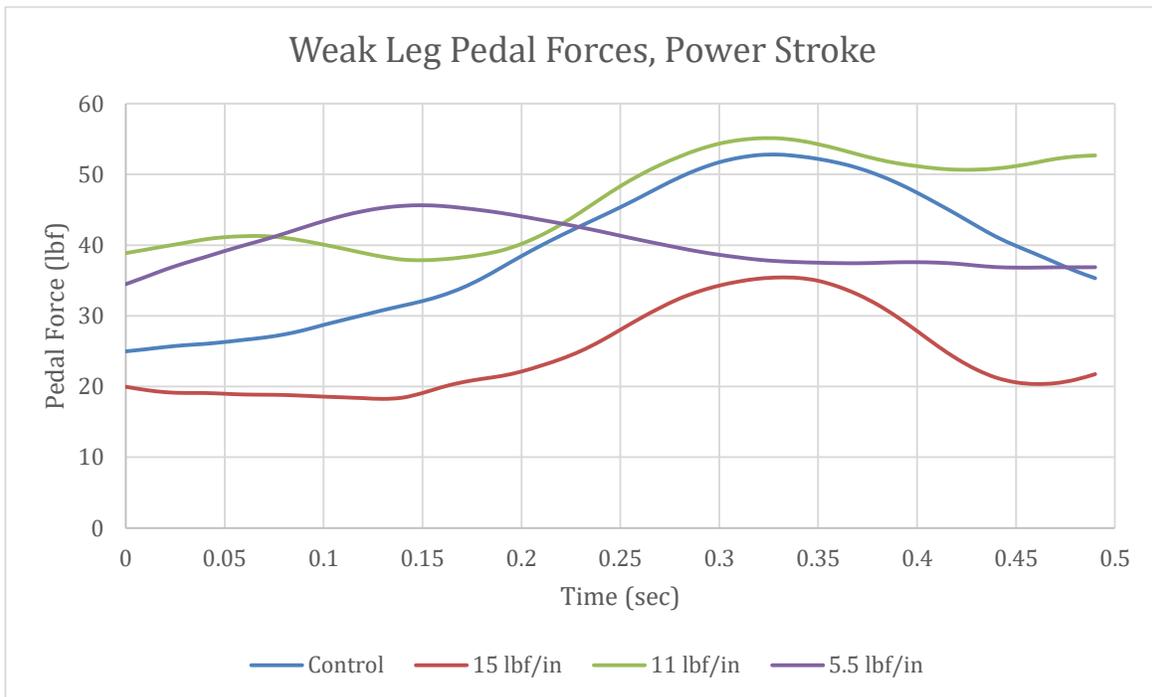


Figure 82: Weak Leg Pedal Forces with three different springs

There were a number of challenges that arose during force testing, which decreased the overall quality of the data. For instance, the Arduino Uno board could only be programmed to sample every 10ms; however, the board often got overloaded and slowed down sporadically. Additionally, the precision of the signal amplification circuits, load cells, and Arduino computer were not sufficient to produce repeatable results and thus the data may have a large error band. All things considered, the data presented still shows a clear spike in force during the power stroke of the cycle. Initial observations of the data indicate a lack of assistance or resistance in the two lighter springs.

Analysis of Results

Analysis of Qualitative Results

Since the spring was not attached for the test, the subject testing primarily tested the remaining components of the tricycle. The average values for the survey questions can be seen in Table 40.

Table 40: Average Survey Scores from 6 Test Subjects

	Question (on a scale from 1-5, with 5 being best)	5 Meaning	Average Value
1	What is your experience level riding bicycles?	Very Experienced	4
2	How easily could the tricycle be adjusted to fit your height?	Easily	4
3	How comfortable did you find the recumbent pedaling position?	Very Comfortable	4.5
4	How easy was it to adapt to the pedaling style?	Very Easy	4.8
5	How often did the components of the device intrude into your pedaling space?	Never	4.7
6	How easily was the device to steer?	Easy	4.2
7	How easy was the steering technique to learn?	Easy	4.7
8	How intuitive was the braking system to operate?	Very Easy	4.7
9	When the brakes were applied, how well did the tricycle stop?	Very Well	4.3
10	How well did your feet remain on the pedals?	Very Well	5
11	How comfortable was the seat?	Very Comfortable	4.5
12	How stable did you feel on the tricycle?	Very Stable	4.7

The remaining tricycle components that were analyzed before selection included wheel layout, tires, seat, pedals, steering mechanism, and brakes. Questions 3 and 11 indicate that the selection of 3 wheels, with one in the front allowed the users to feel comfortable and stable riding on a wheel configuration that they do not typically use. Question 3 also indicates that selecting multi-use tires created stability without making it too difficult to propel the tricycle. Questions 2 and 10 indicate that the

selection of a recumbent seat was comfortable for the rider. Question 9 indicates that the selection of pedals without clips did not create an issue for the riders. Questions 5 and 6 indicate that the steering was intuitive and easy to use. Questions 7 and 8 show that the braking system was simple to learn and made the rider feel safe in stopping when desired.

The comments indicate that the steering, seat, and braking could be slightly improved. The chain derailment is also clearly a major issue that must be addressed in future designs of the tricycle. The turning radius was very wide due to the steering design using the two back wheels. The steering design could be modified to make operating the tricycle safer and easier. The seat was slightly wobbly, so improvements could be made to the seat extender. Finally, based on the comments, the brakes posed the biggest issue for riders. Adjusting the tricycle caused the brakes to become loose, an issue that must be addressed in future iterations of the tricycle. Additionally, the brakes must be tightened so that they cannot rotate when the rider attempts to apply them.

The results show that the adjustability, comfort, pedaling style, steering, braking, and recumbent design were all well received. The subject testing indicates that the selections for the remaining design components led to a successful tricycle design. Together with the force testing, the tests of the tricycle are an indication of its overall success. With recommendations for the spring mechanism, combined with the remaining components of the tricycle design tested in the subject testing, the tricycle would well serve its purpose as a rehabilitative tricycle.

Analysis of Quantitative Results

A control test was conducted to provide a baseline without the spring in order to compare spring data. As shown in Figure 83, there is clearly a peak in each data set, indicating this was the power stroke extreme point. All data analyzed will compare these peaks in force during the power stroke. However, within the power stroke, there is also an observable “valley,” followed by a secondary peak.

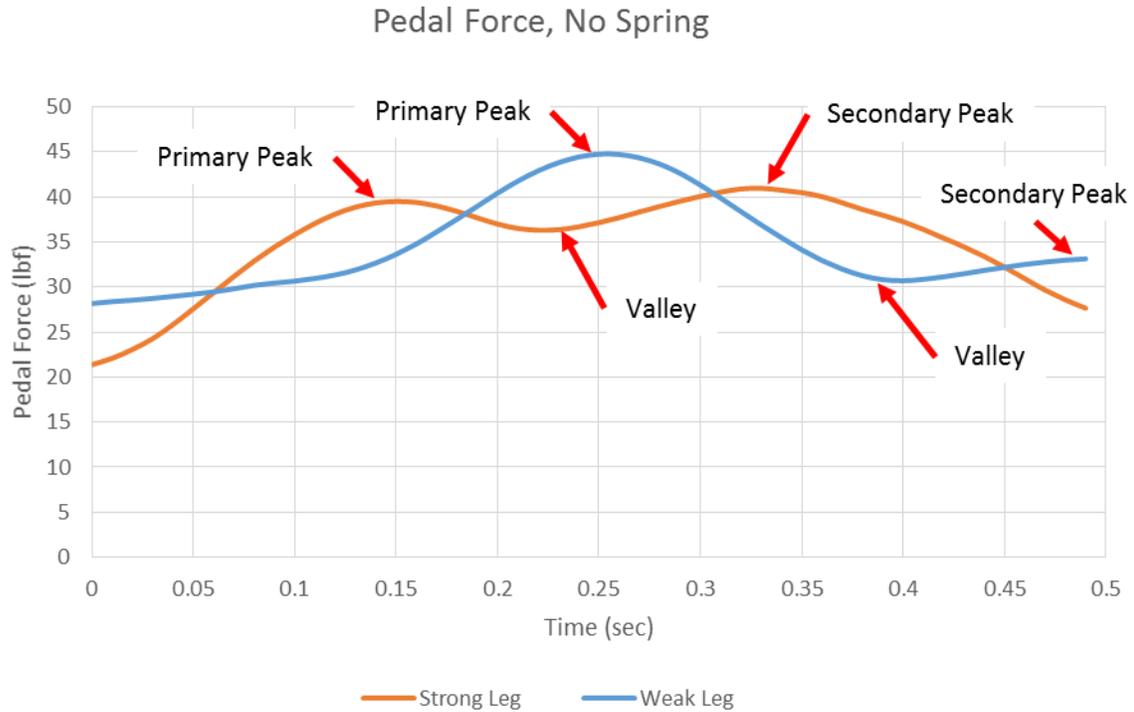


Figure 83: Peaks and Valleys of Pedal Forces

These drops in pedal forces during the power stroke have been partially attributed to a change in angle of the pedal with respect to the leg force vector. The force measurement sensors are designed to only measure forces normal to the pedal and would therefore read lower as the pedal crank reaches the $3\pi/4$ position (Figure 84); however, the change in angle between F and the pedal surface between $\pi/2$ and $3\pi/4$ is small enough to only cause slight effects to the force readings. The secondary peaks shown in Figure 84 may also be affected by the actual biomechanics of the pedaling cycle. Once the crank reaches the most extreme point away from the body (represented as π in Figure 84), the knee “locks” as the leg reaches full extension. This “locking” may temporarily cause the leg to push harder on the pedal just before it enters the recovery phase of the cycle, represented as a secondary peak in the data.

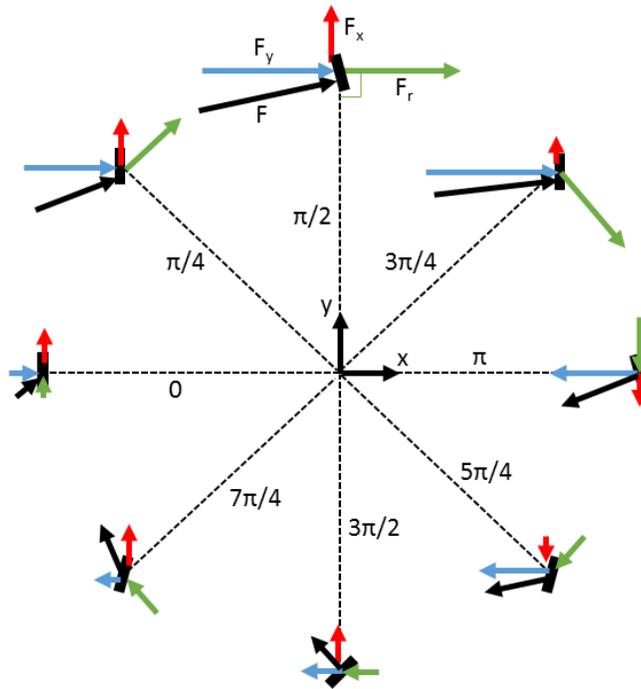


Figure 84: Recumbent Pedaling Cycle

The force phasing chart shown in Figure 84 is a modified version of the upright phasing chart shown in Figure 85. For ease of analysis, the recumbent relative pedaling cycle has been taken as the upright pedaling cycle rotated 90 degrees. Force vector \mathbf{F} represents the applied force by the rider's leg, which is broken into its constituent components, F_x and F_y . Finally, F_r represents the resultant force vector that acts normal to the crank radius. As is assumed in the upright pedaling cycle, these relative forces reflect a rider using toe clips, which would allow for slight pulling forces during the recovery phase.

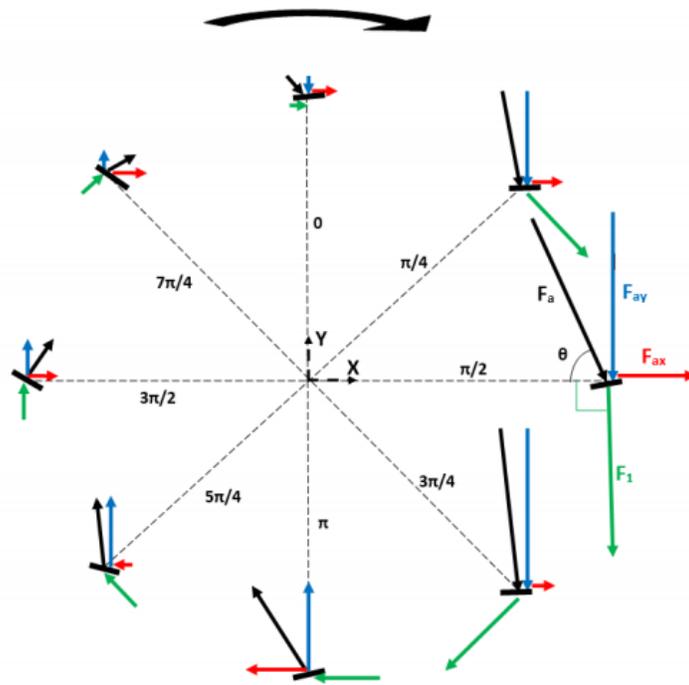


Figure 85: Upright Relative Pedal Force (Allen, Blasius & Puttre, Pp. 73)

Spring Tests Analysis

Tests were conducted using a variety of spring constants, with the middle stiffness (11lb/in) being the spring that was calculated in the preliminary analysis. Table 41 shows the percent deviation from peak force in the control test for each of the three springs.

Table 41: Pedal Force Deviation from Control, All Spring Constants

Spring Constant	Strong Leg Peak Force	Weak Leg Peak Force
15lb/in	27.06%	-49.04%
11lb/in	-3.52%	4.18%
5.5lb/in	2.27%	-15.70%

The data shows only slight differences in pedal force on the strong leg for the 5.5lb/in and 11lb/in springs, and a difference up to about 16% for the weak leg. Intuitively, the 5.5lb/in spring should not provide more assistance to the weak leg than the 11lb/in spring. This indicates that there is large error

in the data. Additionally, the data shows 49% assistance to the weak leg with the 15lbf/in spring; however, due to large error, this number is skewed and the actual assistance is probably much lower. A lack of robust data makes it impossible to draw conclusions about the exact assistance provided by the spring on the manufactured tricycle, although the deviation with the 15lbf/in spring is large enough to strongly suggest some significant assistance.

Our preliminary calculations showed that the 11lbf/in spring should provide 30% assistance in an ideal system. Testing showed this was not the case even if error is factored in. This is because our preliminary calculations estimated a tricycle weight that was much lower than what was manufactured. Pedal force calculations were performed again to reflect the properties of the actual manufactured tricycle; Figure 86 shows the updated pedal force graph. These new calculations predict that the 11lbf/in spring should only actually provide 12.6% assistance to the weak leg in the current tricycle configuration. With such a large error in test data it cannot be concluded that the 11lbf/in spring provided assistance near the calculated value.

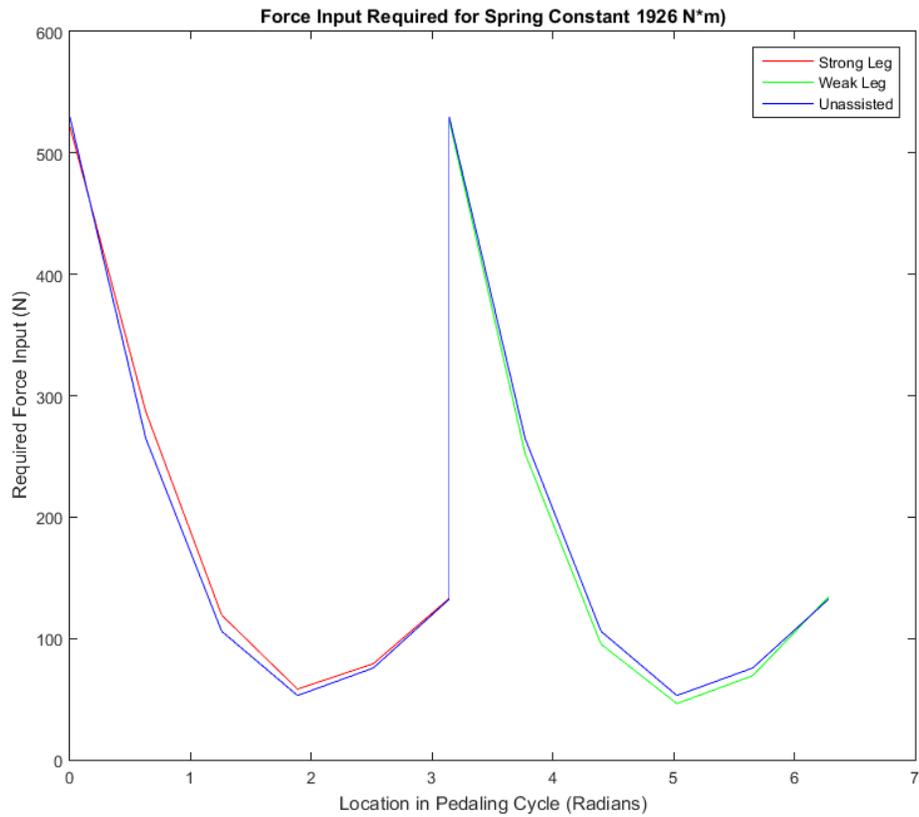


Figure 86: Pedal Force Calculations Updated for Manufactured Tricycle

Additionally, any assistance provided by the weaker springs was effectively eliminated by the user trying to keep the secondary chain from falling off. As the spring reaches its maximum extension, it has a tendency to pull the pedals around quickly. This act of pulling quickly often derailed the chain and forced the data collection to be cut short. In order to compensate, the user had to provide resistance with their opposite leg, thus applying more force back onto the pedal.

Conclusion

Strokes affect 800,000 people annually in the United States and are a common cause of disability (CDC, 2015). Strokes often result in hemiparesis, or weakness in one side of the body. This condition prevents a person from pedaling a normal tricycle, which may limit their potential to engage in beneficial recreational activities, as few devices exist for this purpose. The goal of this project was to design a rehabilitative adult tricycle to serve as a recreational and therapeutic device for stroke patients. In order to assist the weak leg, the tricycle was designed to have separate force inputs for each pedal.

Pedaling assistance was achieved through a passive spring mechanism that stores energy from the strong leg, and uses it to assist the weak leg. The extension spring in the assistance mechanism was phased with the pedal crank such that it extends on the power stroke of the strong leg, and contracts on the power stroke of the weak leg. The assistance device was designed to allow pedaling with an even cadence between each leg, making it easier for a rider to adapt to the pedaling style.

The pedaling assistance mechanism was mounted on a specially designed tricycle frame. For stability and ease of steering, the tricycle was designed with two wheels in the rear and one in the front. Through use of a commercially available tricycle for the rear end, the design and manufacturing of the steering and braking mechanisms was simplified. Modifications to the commercially available tricycle included raising the seat to the height of a standard wheelchair and extending the handlebars by an equal amount. Finally, the front end of the tricycle, which included the assistance mechanism, was constructed using a bicycle frame welded to tubing for attachment to the rear end of the tricycle.

Testing the tricycle indicated that all of the selected components received generally favorable ratings from the test subjects; however, derailment of the spring assistance chain prevented qualitative data about the tricycle being obtained from the subjects. In order to validate the assistance calculations, quantitative data were acquired using pedal force plates. These data showed that with stiffer springs, some assistance to the weak leg could be achieved.

Based on the subject and force testing, the spring mechanism support structure should be modified to improve the alignment between the sprockets and provide tension to the chain. Once these modifications are implemented, the mechanism should function as designed and allow the spring assistance mechanism to assist the weak leg during the pedaling cycle. Overall, testing proved that the tricycle was a good proof of concept, which could be optimized to serve as an effective adult rehabilitative tricycle in the future.

Recommendations

After the conclusion of the testing process, the following recommendations were made. Future iterations of the design should implement these recommendations in order to improve the operation of the tricycle.

Recommendation 1: Support the spring-sprocket mechanism with a solid part and have a tensioner in order to prevent derailment of the chain.

During testing, the chain on the spring-sprocket mechanism often derailed. This derailment made it difficult to test the tricycle, since none of the test subjects were able to complete a large portion of the test with the chain attached to the sprockets. Even the members of this project group, who were much more experienced riding the tricycle, had difficulty keeping the chain attached during portions of the force testing procedure.

This derailment was likely due to a combination of two factors: the misalignment of the two sprockets, and the lack of a method to adjust the tension of the chain. During the testing, it was apparent that the chain was at a slight angle to one of the sprockets, which would eventually lead to one of the links failing to engage with the teeth. This issue was often more pronounced with the stiffer springs, as they would bend the support structure and further misalign the sprockets. Occasionally, the chain would stay on for longer periods of time, however, this did not occur with any consistency. In order to correct the misalignment, we recommend making the support structure as one solid machined part instead of as separate tie rods. The support structure with the tie rods was extremely difficult to adjust and was never completely stable. A machined part would provide proper stability and alignment to the sprockets.

The lack of a tensioning system for the chain also exacerbated the derailing issue. Even during the tests where the chain stayed on for a sustained period of time, there was usually slack in the chain. A tensioner would have corrected this issue. However, the shape of the front fork and the support structure

cannot support a standard chain tensioner, and thus a custom tensioner would have to be created to correct the tensioning problem.

Recommendation 2: Attach the braking system to the rear end instead of the front end, which will make it easier to adjust the length of the tricycle.

The front fork of the tricycle was made using the rear end of an existing bicycle, and thus already had brakes fully installed. These brakes were used in the interest of time and ease of manufacturing. However, the brake handle had to be attached to the handlebar on the rear end of the tricycle. Therefore, every time the fork had to be repositioned to allow for a user of different height, the brake cable had to be either lengthened or shortened, which was time-consuming. If the brake pads had instead been installed on the rear wheels, the cable could have been tensioned independently of the position of the fork with respect to the rear end of the tricycle. The lack of adjustability may not be a serious problem if the tricycle were to be used for one patient. However, it should still be preserved because a therapist could purchase the tricycle for use with multiple patients.

Recommendation 3: Redesign the spring attachment to allow for multiple attachment points and easier attachment and adjustment of the spring.

The spring is attached to the front fork by connecting the loop at the end of the spring to an eye-bolt. In order to attach to the spring-sprocket mechanism, the spring is attached to a bolt by placing it between 2 nuts and 2 washers (Figure 74). Even though it successfully holds the spring, this arrangement has 2 ways it could potentially be improved. Due to the need to remove the nuts to remove the spring, this system is time-consuming to adjust. If a loop—such as another eye-bolt—could be connected to the spring sprocket mechanism, then the spring could be connected by simply hooking it on. This arrangement would save time, but would likely require great care to ensure that the spring does not wrap around the eye bolt while the sprocket rotates. One possible way to prevent this wrapping from occurring

is to use an attachment bolt with a loop, which pivots with respect to the bolt. The current setup was used primarily because it prevents the spring from wrapping around the bolt.

Another way this mechanism could be improved is by creating a way to allow the spring to be pre-loaded. By stretching the spring while the attachment point is at the bottom position of the cycle, the amount of assistance from the spring could be changed while using the same spring coefficient. This arrangement would be useful because it would negate the need for multiple springs to change the amount of assistance to the weak leg. The current mechanism lacks such a feature because the sprocket used to attach the spring has a very small amount of material in its cross-sectional area, and thus contains a limited number of attachment points for the bolt (Figure 87). A future iteration of the design should contain an attachment mechanism which could change the distance of the bolt from the center of rotation, allowing the spring to be pre-loaded to various amounts.

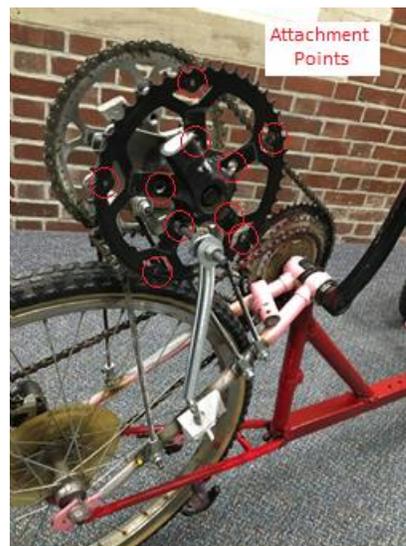


Figure 87: Attachment of spring to sprocket, detailing limited number of attachment points

Recommendation 4: Redesign the seat extender with a more rigid mounting position.

The seat extender was made using two steel plates and two steel C-channels. Due to the structure and shapes of the steel parts and how it was designed, the seat extender was not completely rigid when

attached to the tricycle's frame and seat. Due to the thickness of the steel parts, it was difficult to drill the holes into them. The inner walls of the C-channels were tapered, which made it difficult to keep the drill bit aligned. In result, some of the holes in the seat extender were misaligned with the tricycle frame's holes. When fastening the seat extender with bolts, the C-channels' tapered sides also made it difficult to fit additional spacers between the seat and seat extender. Empty spaces were then left between the fixtures, allowing small movement of the seat extender. A recommendation would be using a CNC machine when building the seat extender to remove the inner sloped sides of the C-channels. For drilling the holes, a drill press would ease the ability to drill through steel and reduce the risk of the holes being misaligned.

Recommendation 5: Move the steering mechanism to the front wheel to allow better control of the steering mechanism and create a smaller turning radius.

The MOBO Triton-Pro Tricycle has its steering mechanism attached to the back wheels. It uses two handlebars, one on each side of the tricycle, and a parallel linkage system to turn the wheels. However, due to its design, the MOBO Triton Pro would not allow turning radii under 6 feet. This arrangement makes it difficult to make turns in small spaces.

When the seat was raised using the seat extender, the turning handles were extended so that the user could reach them. However, by increasing the length of the handle, the range of motion when turning increased as well. This increase caused steering to be more sensitive than in the original MOBO Triton tricycle. A small change in handlebars' position would cause significant rotation to the wheels. When the tricycle was operated during the subject testing, it was difficult to keep the wheels straight, especially at high speeds.

One recommendation would be to extend the rear wheel axle, allowing the wheels more space to turn and not collide into the seat and turning handles. Another recommendation is to use a single rotating handlebar instead of two separate handlebars. Using the same linkage system in the rear, the user can turn the tricycle with more control since both hands will be gripping only one handlebar.

Recommendation 6: Use a more precise data acquisition system to record the pedal forces:

When recording the pedaling forces, the Arduino Uno board would record the forces at 50ms intervals. However this rate would slow down the longer the tests were. A microcontroller board that can record samples faster than the Arduino without delay should be used so this phenomenon does not occur. A National Instrument DAQ box is one alternative to replace the Arduino Uno board (Figure 88). A LabVIEW program executed with a DAQ box can both accurately record the data and automatically export it into a data sheet for analysis.



Figure 88: National Instruments X-Series DAQ Box (National Instruments, 2016)

Different hardware can also be used to improve the quality of the test. One of the HX711 analog-to-digital converters (ADC) had malfunctioned during testing, which made it necessary to purchase another. In addition, the 50kg load cells used for testing required multiple calibrations before conducting a test. In some cases, the load cells would not accurately model the pedaling cycle. The 5.5 lbf/in and 11 lbf/in springs did not show much difference between the stronger and weaker legs, and the results for all the springs showed a margin of error, based on the peak forces between the two legs. More sensitive load cells should be used for testing to eliminate or reduce the margin of error. The specific load cells

purchased for the test were favored since they were inexpensive, but they often made it difficult to measure accurate data.

Works Cited

ADA (2010, September 15). 2010 ADA Standards for Accessible Design. Retrieved September 24, 2015, from <http://www.ada.gov/regs2010/2010ADASTandards/2010ADASTandards.htm>

Allen, C., Blasius, A., & Puttre, K. (2014) Passive Assistive Pedaling Device. *Worcester Polytechnic Institute*. Retrieved April 21, 2016. Web. < https://www.wpi.edu/Pubs/E-project/Available/E-project-043014-152036/unrestricted/Passive_Assistive_Pedaling_Device_MQP_Report.pdf> Retrieved September 18, 2015, from <http://www.wpi.edu/Pubs/E-project/Available/E-project-043014-152036/>

Alterg. (2015). Anti-Gravity Treadmill. Retrieved 2015, from alterg.com

Amazon. (2015). Pedal Toe Clips. Retrieved 2015, from amazon.com

Art of Triathlon. (2015). Clipless Pedals. Retrieved 2015, from artoftriathlon.com

Aqua Creek Products (2015) Underwater Walker Instructions. Aqua Creek Products <http://www.activenable.com/assets/images/instructions/acc401-underwater-walker-instructions.pdf>

ASME. (2015). Limb Load Monitor. Retrieved 2015, from medicaldevices.asme.org

Bicycle Man. (2015). Recumbent Tricycle. Retrieved 2015, from bicycleman.com

Bike Forums. (2015). Adult Tricycle. Retrieved 2015, from bikeforums.net

Bike-Riding-Guide. (2015). Bicycle Brakes. Retrieved 2015, from bike-riding-guide.com

Body Measurements. (2012, November 2). Retrieved September 23, 2015, from <http://www.cdc.gov/nchs/fastats/body-measurements.htm>

CDC. (2015). Stroke Fact Sheet. Retrieved March 29, 2016, from http://www.cdc.gov/dhbsp/data_statistics/fact_sheets/fs_stroke.htm

Chester Cycling. (2015). Coaster Brake. Retrieved 2015, from chestercycling.wordpress.com

Consumer Product Safety Commission. (2015). Bicycle Requirements Business Guidance. Retrieved 2015, from <http://www.cpsc.gov/en/Business--Manufacturing/Business-Education/Business-Guidance/Bicycle-Requirements/>

Cornell University. Beam Deflection Formulae. (2015) Retrieved April 21, 2016, from <http://ruina.mae.cornell.edu/Courses/ME4735-2012/Rand4770Vibrations/BeamFormulas.pdf>

Coxworth, B. (2011, August 16). Flywheel Bicycle: KERS for pedal-pushers. Retrieved September 3, 2015, from <http://www.gizmag.com/flywheel-bicycle-regenerative-braking/19532/>

National Stroke Association (2015). Depression. Retrieved September 14, 2015, from <http://www.stroke.org/we-can-help/survivors/stroke-recovery/post-stroke-conditions/emotional/depression>

Energy Storage Association. (2015). Flywheels. Retrieved 2015, from <http://energystorage.org/energy-storage/technologies/flywheels>

Exercise and Depression - Harvard Health. (2009, June 9). Retrieved September 14, 2015, from <http://www.health.harvard.edu/mind-and-mood/exercise-and-depression-report-excerpt>

Exercise for Stress and Anxiety | Anxiety and Depression Association of America, ADAA. (n.d.). Retrieved September 14, 2015, from <http://www.adaa.org/living-with-anxiety/managing-anxiety/exercise-stress-and-anxiety>

Figure 1: <http://www.bankspower.com/techarticles/show/9-understanding-torque-converters>

Fonda, B., & Sarabon, N. (2010). Biomechanics of Cycling. *Sport Science Review*, 19(1-2), 187-210. Retrieved September 10, 2015, from [http://au4sb9ax7m.search.serialssolutions.com/?ctx_ver=Z39.88-2004&ctx_enc=info:ofi/enc:UTF-8&rft_id=info:sid/summon.serialssolutions.com&rft_val_fmt=info:ofi/fmt:kev:mtx:journal&rft.genre=article&rft.atitle=Biomechanics of Cycling&rft.jtitle=Sport](http://au4sb9ax7m.search.serialssolutions.com/?ctx_ver=Z39.88-2004&ctx_enc=info:ofi/enc:UTF-8&rft_id=info:sid/summon.serialssolutions.com&rft_val_fmt=info:ofi/fmt:kev:mtx:journal&rft.genre=article&rft.atitle=Biomechanics%20of%20Cycling&rft.jtitle=Sport)

Gharakhanlou, R. (2012). Anthropometric measures as predictors of cardiovascular disease risk factors in the urban population of Iran. *Arquivos Brasileiros De Cardiologia*, 98.

Google Maps. (2016). Map. Retrieved 2016, from maps.google.com

Gordon, N. F. "Physical Activity and Exercise Recommendations for Stroke Survivors: An American Heart Association Scientific Statement From the Council on Clinical Cardiology, Subcommittee on Exercise, Cardiac Rehabilitation, and Prevention; the Council on Cardiovascular." *Stroke* (2004): 1230-240. Web. 20 Sept. 2015. <http://stroke.ahajournals.org/content/35/5/1230.full>

H Therapy. (2015). Isokinetic Exercise Machine. Retrieved from htherapy.co.ca

Harris, W. (2015). How CVTs Work. Retrieved September 3, 2015, from <http://auto.howstuffworks.com/cvt.htm>

Hell Bent Cycles. (2015). OSS Joystick Style Tiller Steering. Retrieved 2015, from hellbentcycles.com

Hostelshoppe. (2015). HP Velotechnik. Retrieved 2015, from hostelshoppe.com

"How Differentials Work." *HowStuffWorks*. Web. 20 Sept. 2015.

How a Torque Converter Works. (2015). Retrieved September 18, 2015.

Huston, J., & Johnson, D. (1982). Three Wheel Vehicle Dynamics (SAE Technical Paper 820139). SAE International.

Kite, Bike, Surf, Rambling. (2015). Bicycle Brake. Retrieved 2015, from kitesurfbikerambling.wordpress.com

Koesterer, TK. (2015). Center of Gravity and Stability KINESIOLOGY. Retrieved 2015, from <http://users.etown.edu/w/wunderjt/syllabi/Chapter%2014%20REVISED%20FOR%20FYS.pdf>

Load Sensor - 50kg. (2015). Retrieved April 21, 2016, from <https://www.sparkfun.com/products/10245>

Lopes, Alexandre, Sandra Alouche, Nils Hakansson, and Moisés Cohen. "ELECTROMYOGRAPHY DURING PEDALING ON UPRIGHT AND RECUMBENT ERGOMETER." *International Journal of Sports Physical Therapy*. Sports Physical Therapy Section. Web. 20 Sept. 2015.

Old Glory Mountain Bike. (2015). Mountain Tire. Retrieved 2015, from oldglorymtb.com

Maxxis. (2015). Multi-Use Tire. Retrieved 2015, from maxxis.com

Mobo Triton Pro Ultimate Ergonomic Cruiser. (2015). Retrieved April 21, 2016, from <http://www.kohls.com/product/prd-1286210/mobo-triton-pro-ultimate-ergonomic-cruiser.jsp>

Morgancycle. (2015). Seat Back Rest. Retrieved 2015, from morgancycle.com

Mozaffarian D, Benjamin EJ, Go AS, et al. Heart disease and stroke statistics—2015 update: a report from the American Heart Association. *Circulation*. 2015 ;e29-322.

Nice, K. (2000, August 2). How Differentials Work. Retrieved September 3, 2015, from <http://auto.howstuffworks.com/differential.htm>

Pande, Reena. (2012). Yoga your way to stroke recovery. Retrieved 2015, from <http://www.reenapande.com/2012/07/29/yoga-your-way-to-stroke-recovery/>

Pearlman, A. (n.d.). 2.972 How A Differential Works. Retrieved September 3, 2015, from <http://web.mit.edu/2.972/www/reports/differential/differential.html>

Performance Bicycle. (2015). Road Tire. Retrieved 2015, from performancebicycle.com

Pratte, David. (2014). Continuously Variable Transmissions – Rubber Band Gearboxes Be Gone! Retrieved 2015, from <http://www.superstreetonline.com/how-to/transmission-drivetrain/1404-continuously-variable-transmissions/>

Pruitt, A. (2014, February 13). The Biomechanics Of The Pedal Stroke. Retrieved September 18, 2015, from <http://triathlete-europe.competitor.com/2014/02/13/the-biomechanics-of-the-pedal-stroke>

Public Health Agency of Canada. (2011). Tracking Heart Disease and Stroke in Canada. Retrieved from <http://www.phac-aspc.gc.ca/publicat/2009/cvd-avc/index-eng.php>

Quadracycle. (2015). Quadracycle 4 Wheel Adult Pedal Bicycle. Retrieved 2015, from quadracycllellc.com

Rehabmart. (2015). Adult Tricycles. Retrieved 2015, from rehabmart.com

Reisman, D., McLean, H., Keller, J., Danks, K., & Bastian, A. (2013, June 28). Result Filters. Retrieved October 2, 2015.

Rideouttech. (2015). Storm Quest Tactical Bike Saddle. Retrieved 2015, from rideouttech.com

Standard Weight Folding Wheelchairs. (2015). Retrieved September 24, 2015, from http://www.phc-online.com/Standard_Wheelchairs_s/31.htm

Singletrack. (2015). Drum Brakes. Retrieved 2015, from singletrack.com

Target. (2015). Schwinn Adult Meridian 26 Inch Three Wheel Bike. Retrieved 2015, from target.com

The Mountain Bike Encyclopedia. (2015). Platform Pedal. Retrieved 2015, from themountainbikeencyclopedia.com

Triwg. (2015). Tilt Table. Retrieved 2015, from triwg.com

Tyrx. (2015). Recumbent Tricycle. Retrieved 2015, from tyrx.com

Wikstrom, Matt. (2014). Beyond the big ring: understanding gear ratios and why they matter. Retrieved 2015, from <http://cyclingtips.com/2014/08/beyond-the-big-ring-understanding-gear-ratios-and-why-they-matter/>

Woodway. (2015). Split Belt Treadmill. Retrieved 2015, from woodway.com

Wozniak-Timmer, C. (1991). Cycling Biomechanics: A Literature Review. Retrieved September 18, 2015, from <http://www.jospt.org/doi/pdfplus/10.2519/jospt.1991.14.3.106>

Appendix A: Tricycle Safety Standards

For the purpose of the project, the team used existing bicycle safety standards from the United States

Consumer Product Safety Commission (CPSC, 2002).

What is the purpose of the requirements for bicycles?

This regulation increases the safety of bicycles by establishing, among other things, requirements for assembly, braking, protrusions, structural integrity and reflectors. Bicycles that fail any of the requirements are banned under the Federal Hazardous Substances Act.

Where can I find the requirements for bicycles?

The requirements are in the Code of Federal Regulations (CFR) in [Title 16, Part 1512](#).

What is a bicycle?

A bicycle is defined in [§1512.2](#) as either (1) a two-wheeled vehicle having a rear drive wheel solely human-powered; or (2) a two- or three-wheeled vehicle with fully operable pedals and an electric motor of less than 750 watts (1 h.p.), whose maximum speed on a paved level surface, when powered solely by such a motor while ridden by an operator who weighs 170 pounds, is less than 20 mph.

The bicycle requirements cover two different types of bicycles. Those with a seat that is more than 25 inches above the ground when the seat is adjusted to its highest position must meet all of the requirements. Sidewalk bicycles – those with a seat height of 25 inches or less – are exempt from some of the requirements or have other alternative requirements. These exemptions and alternatives are marked in bold type in this summary. Please consult [§1512.2](#) of the requirements for more information on how to measure seat height.

Are any bicycles exempt from the requirements?

Yes. Track bicycles designed and intended for use in competition that have tubular tires, a single crank–towheel ratio, and no freewheeling feature are exempt. So are one-of-a-kind bicycles made to the order of an individual without assembling stock or production parts.

How are bicycles tested in general?

Assembled bicycles must meet the requirements of the regulation in the condition in which they are offered for sale. Unassembled or partially assembled bicycles must meet the requirements after assembly according to the manufacturer’s instructions.



Figure 89: Illustration of a Bicycle and its Part

Are there any general requirements that bicycles must meet?

Yes.

- (1) Adults of normal intelligence and ability must be able to assemble a bicycle that requires assembly.
- (2) A bicycle may not have unfinished sheared metal edges or other sharp parts that may cut a rider's hands or legs. Sheared metal edges must be rolled or finished to remove burrs or feathering.
- (3) When the bicycle is tested for braking ([§1512.18\(d\) and/or \(e\)](#)) or road performance ([§1512.18\(p\) or \(q\)](#)), neither the frame, nor any steering part, wheel, pedal, crank, or braking system part may show a visible break.
- (4) Screws, bolts, and nuts used to fasten parts may not loosen, break, or fail during testing.
- (5) Control cables must be routed so that they do not fray from contact with fixed parts of a bicycle or with the ends of the cable sheaths. The ends of control cables must be capped or treated so that they do not unravel.
- (6) A bicycle may not have any protrusions within the shaded area of Diagram 1. However, control cables up to ¼ inch thick and cable clamps made of material not thicker than 3/16 inch may be attached to the top tube.

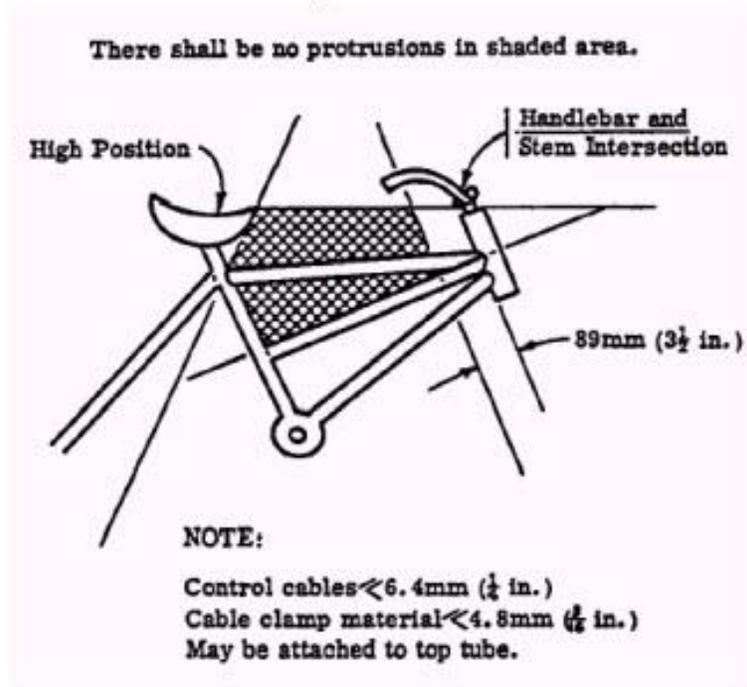


Diagram 1

Figure 90: Diagram Demonstrating Area on a Bicycle where there can be no Protrusions

What are the requirements for brakes?

Bicycles must have front and rear brakes, or rear brakes only. Sidewalk bikes may not have hand brakes only. Sidewalk bikes with a seat height of 22 inches or more when adjusted in the lowest position must have a foot brake. A sidewalk bike with a seat height of less than 22 inches need not have any brake as long as it does not have a freewheeling feature, has a permanent label saying “No brakes”, and has the same statement on its advertising and shipping cartons. Please refer to [§§ 1512.5\(e\) and 1512.18\(f\)](#) of the regulation for more detail on sidewalk bicycle brake performance and labeling.

(1) Hand brakes:

(a) When tested, hand brakes may not break, fail, or have clamps that move or parts that go out of alignment. To test the brakes, push the hand lever all the way down to the handlebar or with a force of 100 pounds (lbf) and then load test the bicycle, or rock it back and forth with a 150-pound weight on the seat. [§1512.18\(d\)\(2\)](#) contains the procedures for loading and rocking testing.

(b) Hand levers have to be on the handlebars and readily usable. The distance between middle of a hand lever and the handlebar may be no wider than 3 ½ inches (3 inches for levers on sidewalk bicycles). Unless a customer specifies otherwise, the hand lever that operates the rear brake must be on the right handlebar. The lever that operates the front brake must be on the left handlebar. A lever that operates both brakes may be on either handlebar. Please note that, if a bicycle has hand lever extensions, all tests are conducted with the extensions in place.

(c) A bicycle that only has hand brakes must stop within 15 feet when tested with a 150-pound rider riding at 15 miles per hour. See [§1512.18\(d\)](#) for more detail on this test.

(d) When the hand lever is pushed down with 10 pounds or less applied 1 inch from the end of the lever, the brake pads must contact the braking surface on the wheel. Caliper brake pads must be replaceable and adjustable. Pads must stay in their holders without movement when a 150-pound rider rocks the bicycle forward and backward. See [§1512.18\(d\)\(2\)](#) for this test.

(e) Brake assemblies must be securely fastened to the bicycle frame with locking devices such as lock washers or locknuts, and must not loosen during the rocking test, [§1512.18\(d\)\(2\)](#). Brake pad holders must be securely attached to the caliper assemblies.

(2) Foot brakes:

(a) Foot brakes must operate independently of any drive-gear positions or adjustments. Foot brakes must have a braking force of at least 40 lbf when 70 pounds of force is applied to the pedal. See [§1512.18\(e\)\(2\)](#) for the test procedure.

(b) Bicycles with foot brakes must stop within 15 feet when tested with a rider of at least 150 pounds at a speed of 10-mph. See [§1512.5\(c\)](#). A bicycle operated in its highest gear ratio at 60 pedal crank revolutions per minute that reaches a speed of more than 15 mph must stop in 15 feet when tested at a speed of 15 mph if it has a foot brake only. See [§1512.18\(e\)\(3\)](#) for the stopping test procedure.

(c) A foot brake must operate by applying force in the direction opposite to the force that drives the bicycle forward, unless the brakes are separate from the pedals and apply the braking force in the same direction as the drive force.

(d) When you hold a torque of 10 ft-lb at each point on the crank at which a rider can apply the brakes, that point cannot be more than 60 degrees away from the point on the crank at which the rider can start to pedal forward.

(e) See [§1512.18\(e\)\(2\)](#) and (f) for tests for foot brakes on sidewalk bicycles.

(3) Foot brake/ hand brake combinations: Bicycles with foot brake/ hand brake combinations must meet all the requirements for foot brakes listed above. If such a bicycle operated in its highest gear ratio at 60 pedal crank revolutions per minute reaches a speed of more than 15 mph, the bicycle must stop in 15 feet when tested at a speed of 15 mph using both types of brakes

What are the requirements for steering systems?

(1) The handlebar stem must withstand a force of 450 lbf (225 lbf for sidewalk bicycles) in a forward direction 45 degrees from the stem centerline when tested according to [§1512.18\(g\)](#). The handlebar stem must have a permanent mark or circle showing the minimum depth that the stem must be inserted into the bicycle fork. That mark must be located a distance of at least 2 ½ times the diameter of the stem from the bottom of the stem, and must not affect the strength or integrity of the stem.

(2) Handlebars should be symmetrical on either side of the stem. The handlebar ends should be no more than 16 inches above the seat when the seat is in its lowest position and the handlebars are in their highest position.

(3) The ends of the handlebars must be capped or covered. Grips, plugs, and other devices mounted on the ends must not come off when a force of 15 lbf is applied. See [§1512.18\(c\)](#) for this test.

(4) When the handlebar/stem assembly is twisted with a torque of 35 ft-lb (15 ft-lb for sidewalk bicycles), it must not move or show any signs of damage. When the handlebars are twisted with the stem being held firmly, the handlebars must support a force of 100 lbf or absorb no less than 200 inch pounds of energy while bending no more than 3 inches. During this test, the handlebars must be tight enough so that they do not turn in the handlebar clamp. After the test, they cannot show any visible sign of breaking. See [§1512.18\(h\)](#) for these tests.

What requirements must pedals meet?

(1) Pedals must have treads on both sides. However, pedals that have a definite side for the rider to use only have to have a tread on that side. Pedals intended to be used only with toe clips do not have to have treads as long as the toe clips are firmly attached to the pedals. However, if the clips are optional, the pedal must have treads.

(2) Bicycle pedals must have reflectors. See [§1512.16\(e\)](#) for this requirement. Sidewalk bicycle pedals do not have to have reflectors.

What are the requirements for chains and chain guards?

(1) A chain must operate over the sprocket without binding or catching, and must have a tensile strength of 1800 lbf (1400 lbf for sidewalk bicycles).

(2) Bicycles with a single front and a single rear sprocket must have a chain guard over the top of the chain and least 90% of the part of the front sprocket that the chain contacts. It must also extend back to within at least 3.2 inches of the center of the bicycle's rear axle. The top of the guard from the front sprocket back to the rear wheel rim must be at least twice as wide as the chain. Past that point, the top of the guard may taper down until it is ½ inch of the chain width. The guard must prevent a 3 inch long, ⅜ inch diameter rod from catching between the upper junction of the sprocket and the chain when a tester tries to insert the rod at any direction up to a 45 degree angle from the side of the bicycle that the chain is on.

(3) Derailleurs must be guarded to prevent the chain from interfering with or stopping the wheel through improper adjustment or damage.

Are there requirements for tires?

Yes. The manufacturer's recommended inflation pressure must be molded onto the sidewalls of inflatable tires in letters at least ⅛ inch high. The tire must stay on the rim when it is inflated to 110% of the recommended pressure, even when it is tested under a side load of 450 lbf. See [§1512.18\(j\)](#) for this test. Tires that do not inflate, tubular sew-up tires, and molded wired-on tires do not have to meet any of these requirements.

What requirements are there for wheels?

A wheel must have all of its spokes and be at least 1/16 inch away from each side of the fork and from any other part of the frame as the wheel turns. When the wheel is tested with a side load of 450 lbf, the tire and spokes must stay on the rim. See [§1512.18\(j\)](#) for this test. Sidewalk bikes do not have to meet the side load requirements.

What requirements must wheel hubs meet?

All bicycles (other than sidewalk bicycles) must meet the following requirements:

(1) Each wheel must have a positive locking device that fastens it to the frame. Use the manufacturer's recommended torque to tighten threaded locking devices. The locking devices on front wheels (except for quick-release devices) must not loosen or come off when a tester tries to take them off using a torque of 12.5 ft-lb applied in the direction of removal. Once fastened to the frame, the axle of the rear wheel must not move when it receives a force of 400 lbf for 30 seconds applied in the direction that removes the wheel.

(2) Quick-release devices with a lever must be adjustable to allow the lever to be set for tightness. Riders must be able to clearly see the levers and determine whether the levers are locked or unlocked. When it is locked, the clamping action of the quick release device must bite into the metal of frame or fork.

(3) Front wheel hubs that do not use a quick release device must have a positive retention feature that keeps the wheel on when the locking devices are loosened. To test this, release or unscrew the locking device, and apply a force of 25 lbf to the hub in the same direction as the slots in the fork. See [§1512.18\(j\)\(3\)](#) for this test.

Are there strength requirements for the fork and frame?

Yes. Clamp the front fork in the test fixture so it does not move and apply force until the fork bends 2 ½ inches. The fork shall have no evidence of fracture. The deflection at a force of 350-in-lbs shall be no greater than 2½ inches. Also, when the fork is mounted on the bicycle frame, the fork and frame assembly must withstand a steady force of 200 lbf or an impact force of 350 in-lbs, whichever is more severe, without breaking, or bending in a manner that would significantly limit the steering angle over which the front wheel can turn. Please see [§1512.18\(k\)\(1\) and \(2\)](#) for the tests for forks and fork/frame assemblies respectively. These requirements do not apply to sidewalk bicycles.

What are the requirements for seats?

(1) The seat post must have a permanent mark or circle showing the minimum depth that the post must be inserted into the bicycle frame. That mark must be located a distance of at least two times the diameter of the seat post from the bottom of the post, and must not affect the strength of the post.

(2) No part of the seat, seat supports, or accessories attached to the seat may be more than 5 inches above the surface of the seat.

(3) The clamps used to adjust the seat must be able to fasten the seat to the seat post in any position to which the seat can be adjusted and prevent the seat from moving during normal use. Following testing ([§1512.18\(p\) or \(q\)](#)), neither the seat nor seat post may move when subjected to a downward force of 150 lbf (75 lbf for sidewalk bicycles) or a horizontal force of 50 lbf (25 lbf for sidewalk bicycles). See [§1512.18\(l\)](#) for these tests.

Are there requirements for reflectors?

Yes. To make sure that motorists can see bicycle riders at night, bicycles (other than sidewalk bicycles) must have a combination of reflectors. Because of the complexity of these requirements, we have not attempted to include all of the tests and detail in this summary. You should carefully read the provisions of [§1512.16](#) for more specific information.

Generally, bicycles must have a colorless front reflector, recessed colorless or amber reflectors on the back and front sides of the pedals, and a red reflector on the rear. They must also have a reflector mounted on the spokes of each wheel, or reflective front and rear wheel rims or tire sidewalls. See [§1512.18\(n\)](#) for tests that measure the reflectance value of reflectors.

The front and rear reflectors must be mounted so that they do not hit the ground when the bicycle falls over. The requirements of the regulation also include specific angles for mounting the reflectors. See [§1512.18\(m\)](#) for tests that apply to front and rear reflectors.

The side reflector on a front wheel must be colorless or amber, and the rear wheel side reflector must be colorless or red. Reflective material on the sidewall or rim of a tire must go around the entire circumference, must not peel, scrape, or rub off, and must meet certain reflectance tests. See [§1512.18\(o\)](#) for these reflectance tests and [§1512.18\(r\)](#) for the abrasion test for reflective rims.

What other requirements must bicycles meet?

(1) A rider weighing at least 150 pounds must ride a bicycle at least 4 miles with the tires inflated to maximum recommended pressure. The rider must travel five times at a speed of at least 15 miles per hour over a 100 foot cleared course.

See [§1512.18\(p\)](#) for this test. During these tests, the bicycle must handle, turn and steer in a stable manner without difficulty, the frame and fork, brakes, and tires must not fail, and the seat, handlebars, controls, and reflectors must not become loose or misaligned. These requirements do not apply to sidewalk bicycles.

(2) A sidewalk bicycle loaded with a weight of 30 lb. on the seat and 10 lb. on each handlebar grip must be dropped (while maintaining an upright position) one foot onto a paved surface three times in the upright position. Without the weights, the bicycle must be dropped three times on each side in any other orientation. During these tests, the wheels, frame, seat, handlebars, and fork must not break. See [§1512.18\(q\)](#) for this test.

(3) A bicycle must be able to tilt 25 degrees to either side with the pedals in their lowest position without the pedal or any other part of the bicycle (other than tires) hitting the ground.

(4) Bicycles without toe clips must have pedals that are at least 3 ½ inches from the front tire or fender when the front tire is turned in any direction. See figure 6 of [§1512](#) for more detail about this requirement.

What requirements are there for instructions and labeling for bicycles?

(1) Every bicycle must have an instruction manual attached to its frame or included in the bicycle packaging. The manual must include operation and safety instructions, assembly instructions for complete and proper assembly, and maintenance instructions. See [§1512.19](#) for more detail.

(2) If a bicycle is sold less than fully assembled or adjusted, any advertising material and the outside of the shipping carton must include a list of tools necessary to assemble and adjust the bicycle and a drawing showing the minimum length of the leg of a rider for whom the bicycle is appropriate. That length must allow at least one inch between the top tube and the crotch of the rider when the rider's feet are on the ground.

(3) Every bicycle must have a permanent marking or label that shows the name of the manufacturer or private labeler and that the manufacturer or private labeler can use to identify the month and year the bicycle was manufactured. If the bicycle is privately labeled, the label must have information that the private labeler can use to identify the manufacturer of the bicycle.

Where can I find additional information?

For more information on the requirements for bicycles, contact the U.S. Consumer Product Safety Commission:

Office of Compliance (for specific enforcement inquires): e-mail: sect15@cpsc.gov; telephone: (301) 504-7520.

Small Business Ombudsman (for general assistance understanding and complying with CPSC regulations): e-mail: Please use our [Contact Form](#), which is the best way to get a fast response; telephone: (888) 531-9070.

Appendix B: Remaining Component Pictures



Figure 91: Three Wheel, Single in Rear (Bicycleman, 2015)



Figure 92: Three Wheel, Single in Front (Target, 2015)



Figure 93: Four Wheels (Quadracycle, 2015)



Figure 94: Road Tire (Performance Bicycle, 2015)



Figure 95: Multi-Use Bike Tire (maxxis.com)



Figure 96: Mountain Tire (Old Glory MTB, 2015)



Figure 97: Upright Seat, No Back (Rideouttech, 2015)



Figure 98: Upright Seat with Added Back (Morgancycle, 2015)



Figure 99: Once Piece Molded Seat with Back (Hostel Shoppe, 2015)



Figure 100: Handle Bars (Kite, Bike, Surf, Rambling, 2015)



Figure 101: Tiller (Hell Bent Cycles, 2015)



Figure 102: Platform Pedal (The Mountain Bike Encyclopedia, 2015)



Figure 103: Pedal Toe Clips (Amazon, 2015)



Figure 104: Clipless Bike Pedals (Art of Triathlon, 2015)



Figure 105: Upright Design (Bike Forums, 2015)



Figure 106: Recumbent Design (Rehabmart, 2015)



Figure 107: Rim Brake (Bike-Riding-Guide, 2015)



Figure 108: Drum Brakes (Chester Cycling, 2015) (chestercycling.wordpress.com)



Figure 109: Drum Brakes (Singletracks, 2015)

Appendix C: Tipping Analysis

Stability of a tricycle can vary depending on number the wheels it has, where each one is positioned on the device, and where the center of gravity is located. For a four-wheeled vehicle, as in

Figure 110, the wheel configuration is usually symmetrical from front to back and side to side, allowing the vehicle to have similar stability characteristics and equal weight distribution all around. For a tricycle, however, this is not the case.

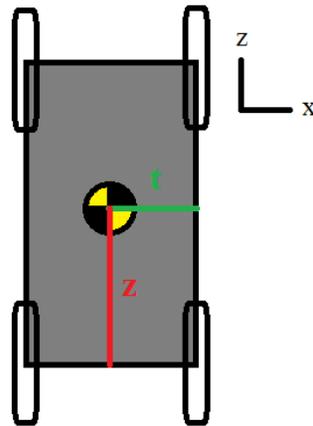


Figure 110: Drivetrain of a four-wheeled vehicle

A tricycle's stability depends on various conditions, such as the layout of the wheels and the location of the center of gravity (CG). There are two types of tricycles, distinguished based on the placement of the tricycle's wheels: delta and tadpole. A delta tricycle has one wheel in the front and two wheels in the rear. A tadpole tricycle, one the other hand, has two wheels in the front and one in the back. For the center of gravity (CG), the location of it is important to measure due to unequal weight distribution within the tricycle. This issue is caused by the layout of its wheels (mainly the critical points of contact of the wheels and the ground).

A bicycle model, as shown in the Figure 111, is modified for the layout of a delta and tadpole tricycle. For this project, the analysis focuses on a delta tricycle. Due to the placement of the wheels, the layout is in the shape of a triangle. Each corner represents the critical point of contact between the wheel

and ground. The edges of the triangle represent an axis of tipping, with one them seen as a red dotted line in Figure 111, and the yellow and black circle is the CG.

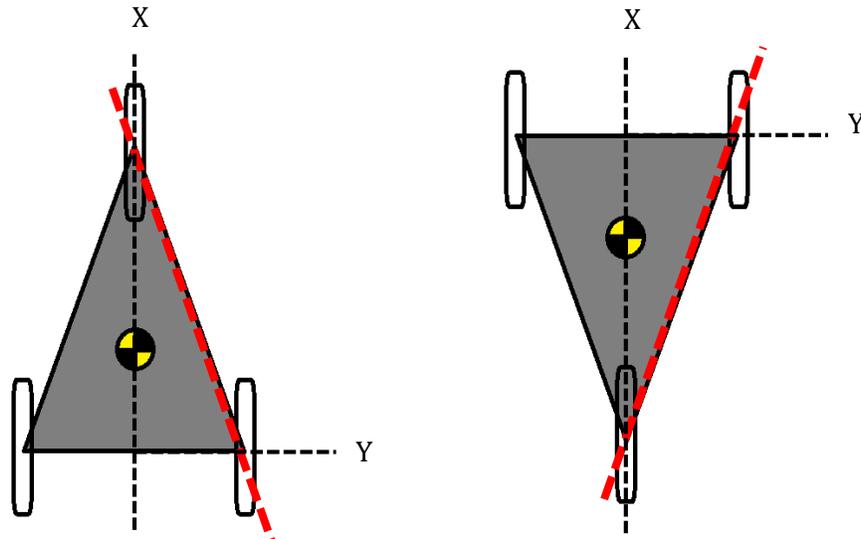


Figure 111: Bicycle Model of a Delta (left) and a Tadpole (right) Tricycle

Position and Weight of the Center of Gravity

The height of the center of gravity (CG) from the ground is an essential measurement in regards to the CG's position. The height can affect how easily the tricycle can tip (or roll) over when making a turning or riding on a sloped surface. This correlation is due to the height, combined with the CG (which acts as a mass traveling perpendicular to the height at a certain acceleration), producing a moment about the axis of tipping. If the height is high enough, the moment could be large enough flip the tricycle.

The position of the center of gravity (CG) of the tricycle is altered when someone is riding it. This change in position is varied, depending on the size, weight, and pose the rider is in while riding the tricycle. For most people, the average height of the CG for a male is 57% of their standing height, while for a female it 55%. Since the CG's height affects stability, the standing height of 57% will be used. Based on this percentage, the center of gravity is assumed to be located about the hips. For a person who is 6.25 feet, or 191 cm (the maximum height allowed to ride the device), the height of the center of

gravity is around 3.56 feet, or 109 cm. However, the user will be sitting on the tricycle, placing the human body's CG not far of the tricycle's CG (Center of Gravity and Stability KINESIOLOGY, 2014).

The CG is altered by weight, so the rider will add an additional load to the tricycle. The maximum weight a tricycle can support is 250 lbs, or 113 kg. By adding a rider's weight of 250 lbs (113 kg), with the tricycle's weight of 44 lbs, (~ 20 kg), the new CG is now 294 lbs (133 kg). It is assumed that when the masses of the rider and tricycle are combined, height of the new CG is increased by a foot, or 30.5 cm, from the tricycle's CG. The CG's position of the tricycle is based off the dimensions of a MOBO triton tricycle.

Stability from the Front and Rear

For this design, the tricycle is stable when both the front and rear wheels bear a load of more than zero Newton (or pounds force) during acceleration or braking. If the wheels ever bear no load during those phases, the wheel(s) on the front or rear axle will lose contact with the ground. If a large enough acceleration or deceleration is produced, the tricycle could flip over on its front or back. To ensure stability of the tricycle, the minimum acceleration (a_{\min}) when speeding up and braking is needed. These values depend on the center of gravity's height (h) from the ground and distance from each wheel axle (x_1, x_2). Figure 112 provides a free body diagram of the tricycle. The arrow on the bottom of the figure is the direction the tricycle is moving at a certain velocity (v). F_f and F_r are the reaction forces on the front and rear wheels from ground, respectively. The acceleration of gravity is represent as g , and measured as 9.81 m/s^2 (or 32.2 ft/s^2); m is the combined mass of the tricycle and rider.

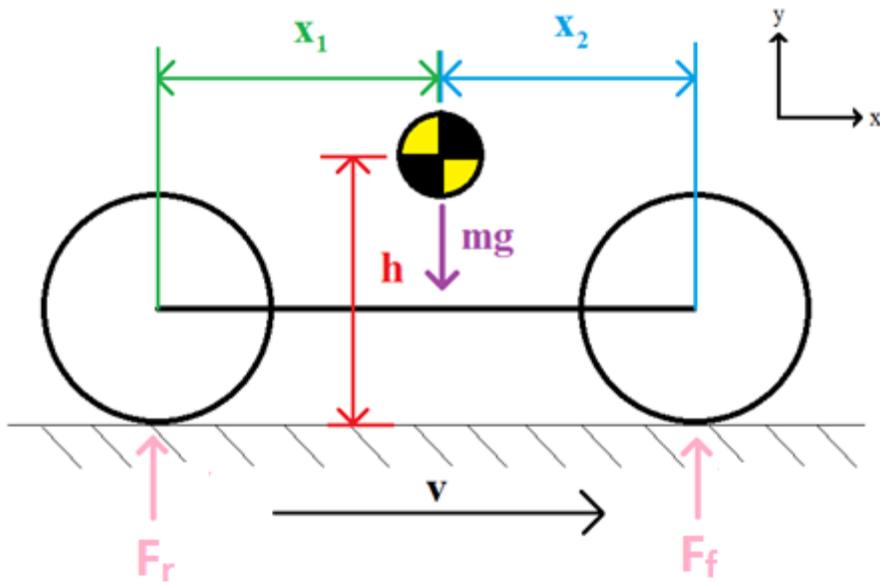


Figure 112: Free Body Diagram of the Tricycle (Side View)

When accelerating, the minimum acceleration until the front wheel(s) bear no load is based on the center of gravity's height from the ground (h), and distance from the rear wheel(s) (x_1). This can be expressed as:

$$\begin{aligned} \sum M_r = 0 &= (mg * x_1) - (ma * h) \\ (g * x_1) &= (a * h) \\ |a_{\min}| &= g * \frac{x_1}{h} \end{aligned}$$

Using the values of h and x_1 , (which are 74.2 cm and 32.3 cm, based off the dimensions of a MOBO triton-pro tricycle) the minimum acceleration is:

$$|a_{\min}| = 981 \frac{cm}{s^2} * \frac{32.3 cm}{74.2 cm} = 4.27 \frac{m}{s^2}$$

For the minimum deceleration during braking, the same equation is used, only this time the distance from the front wheel(s) to the center of gravity is used (x_2):

$$|a_{\min}| = g * \frac{x_2}{h} = 981 \frac{cm}{s^2} * \frac{x_2}{74.2 cm}$$

For this equation, x_2 depends on the wheelbase length, or the length from rear wheel axle to the front wheel axle (L). For the tricycle design, L is adjustable within a certain range (117 cm to 133 cm), allowing the tricycle to be used by people with various heights and leg lengths. Unlike x_1 , x_2 changes due to the change in length L . Figure 113 shows a graph of minimum deceleration during braking based on the wheelbase length.

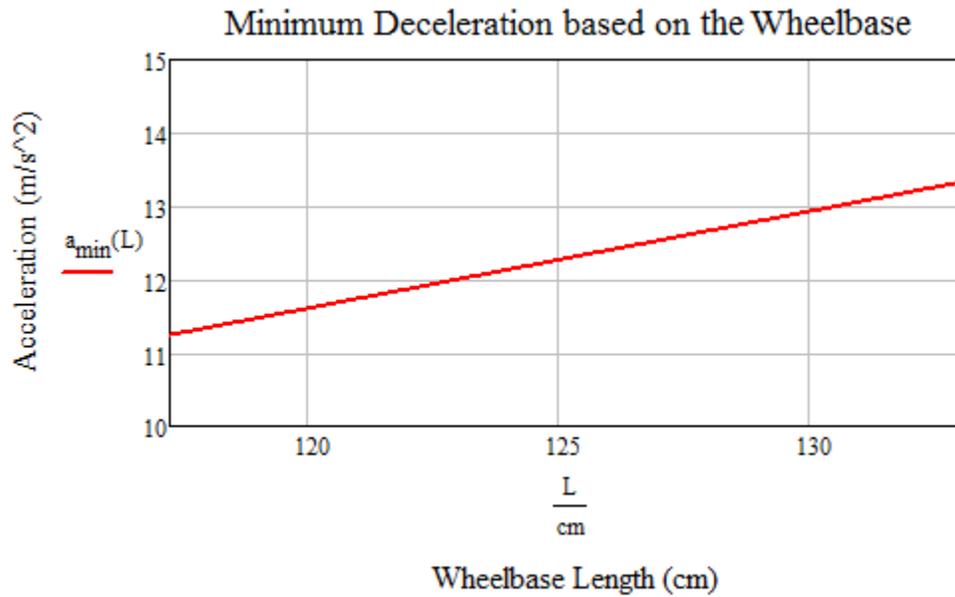


Figure 113: Minimum Deceleration during Braking based on Wheelbase Length

For $L = 133$ cm, $a_{\min} = 13.4$ m/s^2 , whereas for $L = 117$ cm, $a_{\min} = 11.2$ m/s^2 . By determining the acceleration values during accelerating and braking, the smallest ones out of the two situations will be considered. In this case, 4.27 m/s^2 is the minimum value when accelerating, and 11.2 m/s^2 is the minimum acceleration for braking (Huffman, 2010).

Uphill and Downhill Stability

The stability of the device while traveling up and down hills is an extremely important criterion to analyze. When traveling up an incline, the contact area of the device, perpendicular to the CG's direction of force, decreases, thus making it more likely that the center of gravity will fall outside of the contact area. Figure 114 shows how contact area changes over incline of the ground. The red dot with the orange

outline represents the center of gravity. The green contact area, made by the layout of the wheels, is presented perpendicular to the direction of CG's force vector (the blue arrow).

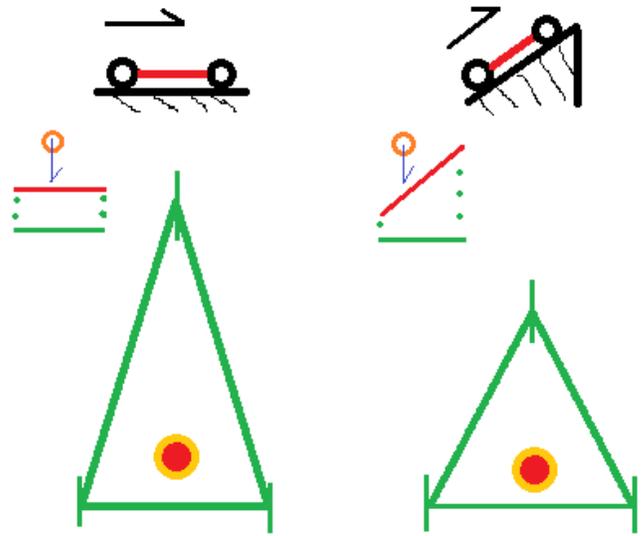


Figure 114: Change of contact area of tricycle by change of surface's incline.

Once the center of gravity falls outside the contact area, the device will tip over, thus making it unsafe for the rider. Therefore, the stability of our device on hills was carefully analyzed.

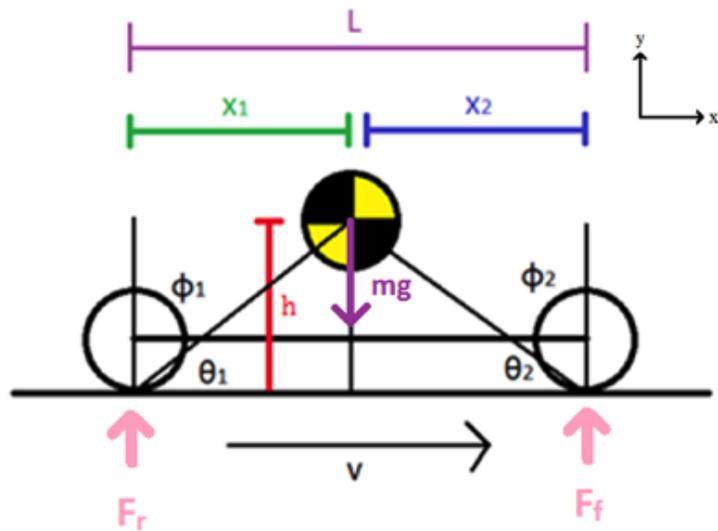


Figure 115: Diagram for Tipping Analysis

The side view of the device is shown in Figure 115. The horizontal distance between the front axle and the center of gravity is x_1 , while the horizontal distance between the back axle and the center of

gravity is x_2 . The total distance between the two axles is L , The parameter h indicates the vertical distance between the center of gravity and the ground. x_1 and h form a right triangle with an angle of θ_1 . They are related by:

$$\tan \theta_1 = \frac{h}{x_1}$$

For the design, $h = 38.9$ cm, and $x_1 = 19.3$ cm, therefore:

$$\theta_1 = \tan^{-1} \frac{h}{x_1} = \tan^{-1} \left(\frac{74.2 \text{ cm}}{32.3 \text{ cm}} \right) = 66.5^\circ$$

The angle opposite of θ is denoted as ϕ . The sum of these two angles is 90° .

$$\theta + \phi = 90^\circ$$

With the equation, ϕ_1 can be solved:

$$66.5^\circ + \phi_1 = 90^\circ \rightarrow \phi_1 = 23.5^\circ$$

For finding ϕ_2 , the length x_2 depends on the wheelbase length L :

$$\phi_2(L) = 90 - \left(\tan^{-1} \frac{h}{x_2} \right) = 90 - \tan^{-1} \left(\frac{74.2 \text{ cm}}{L - 32.3 \text{ cm}} \right)$$

Figure 116 shows a graph of ϕ_2 based on the wheelbase length.

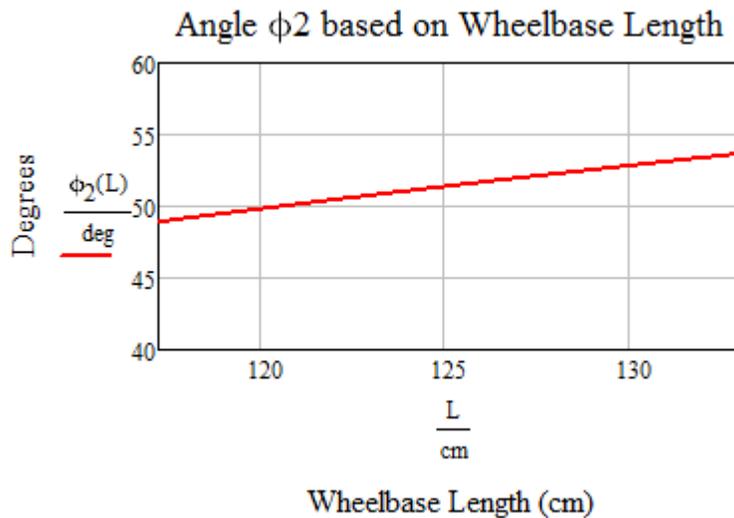


Figure 116: Angle ϕ_2 based on Wheelbase Length

If the device travels on a hill, and the center of gravity sweeps through an angle greater than ϕ , the device will begin to tip. Therefore, the device will tip when ridden on an incline above ϕ . The device will become less stable as h increases, since an increase in h will increase θ and decrease ϕ_1 and ϕ_2 . In addition, as L decreases, ϕ_2 will also decrease, thus making the device less stable going down hills. However, ϕ_1 is 23.5° when h is 74.2 cm. In order to ensure the stability of the tricycle while traveling uphill and downhill, the tricycle should neither go up an incline that causes ϕ_1 to be smaller than 24° , nor go down an incline that causes ϕ_2 to be smaller than 54° (the angle achieved at the maximum value of L , 133 cm)

If the incline of the hill only tips the device front to back, then the stability will be the same for a square or a triangular wheelbase, assuming they have the same values of h , L , x_1 , and x_2 . However, if the device is also tipped side to side, or does not travel straight up the hill, then the triangular wheelbase will be less stable than the square wheelbase. The reason for this difference in stability is explained by the side-to-side tipping analysis in this chapter.

Stability when Turning on Leveled Ground

To ensure stability of the tricycle on its sides, a clockwise moment about the axis of tipping, for this case the red dotted line in Figure 117, must be less than zero. Figure 117 provides a free body diagram of a delta tricycle turning, with the red line being the axis of tipping. At the center of gravity, a lateral force, depicted as " $W*a/g$ " in Figure 117, is formed, facing the center of the turning curvature, along its radius (Huston & Johnson, 1982).

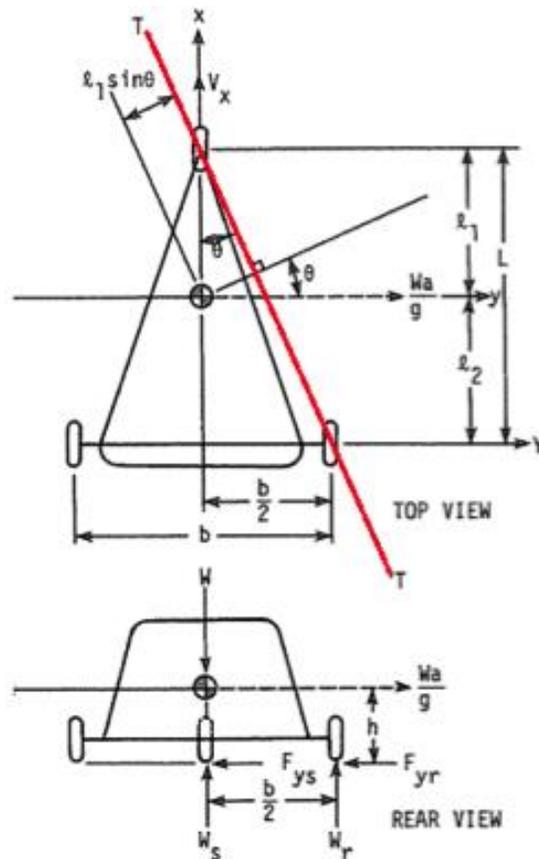


Fig. 7 - Three wheeled vehicle model with two wheels on the rear axle, lateral acceleration

Figure 117: Free Body Diagram of a Delta Tricycle (Huston & Johnson, 1982)

From Figure 117, the variables are:

L = length from rear to front axle (wheelbase length) = min: 117 cm /max: 133 cm

l_1 = length from the center of gravity to the front axle (dependent on L)

l_2 = length from the center of gravity to the rear axle = 32.3 cm

b = width of the two-wheel axle = 70.6 cm

g = acceleration of gravity = $9.81 \text{ m/s}^2 = 981 \text{ cm/s}^2$

h = height of the center of gravity from the ground = 74.1 cm

m = mass of the rider and tricycle = 133 kg

θ = angle formed by the tipping axis and reference axis (dependent on L)

a = lateral acceleration

W = weight of the rider and tricycle

The wheelbase length L and l_1 have a maximum and minimum value since they can be changed based on how much the front piece's length of the tricycle is adjusted. A moment equation, about the tipping axis, can be evaluated from the models' top view. It is assumed that counter clockwise rotation is positive.

$$\sum M_{TT} = [mg * l_1 * \sin(\theta)] - \left[\frac{W}{g} a * h * \cos(\theta) \right] = 0$$

The equation can then be simplified as:

$$\frac{a}{g} = \frac{l_1}{h} * \tan(\theta)$$

The angle θ can also be found using the wheelbase length and half of the two-wheel axle length.

$$\tan(\theta) = \frac{b}{2L}$$

By substitution, the tipping condition equation is expressed as:

$$\frac{a}{g} = \frac{l_1 b}{2hL}$$

During a turn, lateral acceleration can be expressed as:

$$a = \frac{v^2}{R}$$

With v being the velocity the tricycle is traveling, and R being the turning radius. By substituting lateral acceleration with the tipping condition equation, the rollover velocity, or the velocity (as a function of the turn radius) at which tipping occurs, can be obtained (Huston & Johnson, 1982):

$$v(R) = \sqrt{\frac{gRbl_1}{2hL}}$$

$$v(R) = \sqrt{\frac{981 * R * 66 * l_1}{2 * 43.7 * L}}$$

Figure 118 shows the curve of the maximum rollover velocity, based on the relationship between the turning radius and velocity at which the tricycle is moving. In dealing with L, both the maximum (v_{long})

and minimum (v_{short}) wheelbase length adjustments are used. If the tricycle turned about a small radius, but with a speed above the rollover velocity curve, the tricycle is at risk of rolling over (Huston & Johnson, 1982). With this case, the smallest roll-over velocity curve will be taken into account, which is when the wheelbase length is (117 cm).

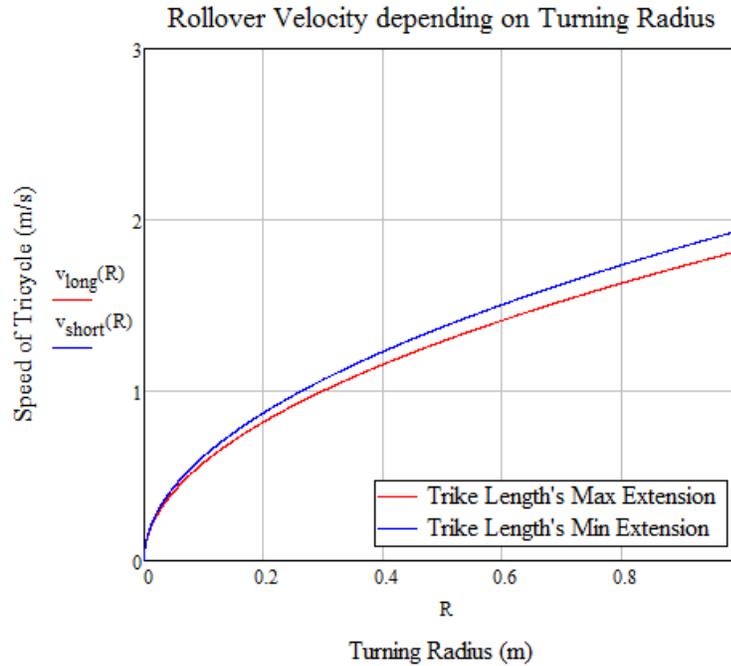


Figure 118: Plot of Rollover Velocity when Turning

Stability from the Side when on an Incline

Since the tricycle will be used in recreational environments, it will be common that this device will be ridden on hills. Depending on the angle of the inclined hill, the location of the center of gravity, and the tricycle's dimensions, instability of the tricycle could occur if the user rides the tricycle across a hill too steep. In Figure 119, a free body diagram of a delta tricycle (positioned in the most adverse orientation with respect to the slope) can be used to find the maximum angle of incline until instability. This free body diagram is the same as Figure 117, however, the lateral force due to turning is not included. Instead, the angle of the slope ϕ is used. It is also assumed that ϕ is independent from the velocity, therefore making the velocity negligible. This is considered since the tricycle is moving in a straight path and inclined on its side. (Huston & Johnson, 1982).

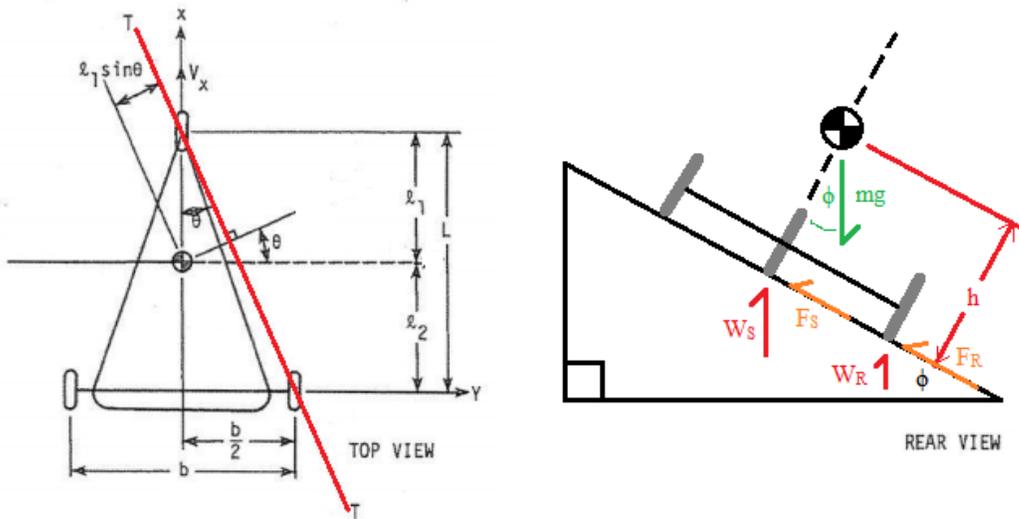


Figure 119: Free Body Diagram of a Delta Tricycle on an Incline (Huston & Johnson, 1982)

It is important to note that since the wheelbase length L can be adjusted, the angle θ is considered as a function of L .

$$\theta(L) = \tan^{-1}\left(\frac{b}{2L}\right)$$

A moment equation, about the tipping axis, can be evaluated from the model's top and rear view. It is assumed that counter clockwise rotation is positive.

$$\sum M_{TT} = - [mg * h * \sin(\phi)] + [mg * (l_1 * \sin(\theta)) * \cos(\phi)] = 0$$

It is important to note that the direction of force vector from the CG is not aligned with the reference frame of the inclined surface. Multiplying these forces by cosine and/or sine of θ will allow the alignment of these forces to the frame. The equation can then be substituted so that the maximum incline slope ϕ can be found:

$$\sum M_{TT} = - [h * \sin(\phi)] + [(l_1 * \sin(\theta)) * \cos(\phi)] = 0$$

$$[h * \sin(\phi)] = [(l_1 * \sin(\theta)) * \cos(\phi)]$$

$$\frac{\sin(\phi)}{\cos(\phi)} * h = l_1 * \sin(\theta)$$

Based on trigonometry, sine divided by cosine equals to tangent:

$$\tan(\phi) = \frac{l_1 * \sin(\theta)}{h}$$

$$\phi = \tan^{-1}\left(\frac{l_1 * \sin(\theta)}{h}\right)$$

By considering the wheelbase and fixed values:

$$\phi(L) = \tan^{-1}\left(\frac{l_1 * \sin(\theta(L))}{h}\right)$$

Figure 120 shows the maximum incline angle that the tricycle can ride across and not tip over.

This is based on the relationship between the wheelbase length and angle of the incline.

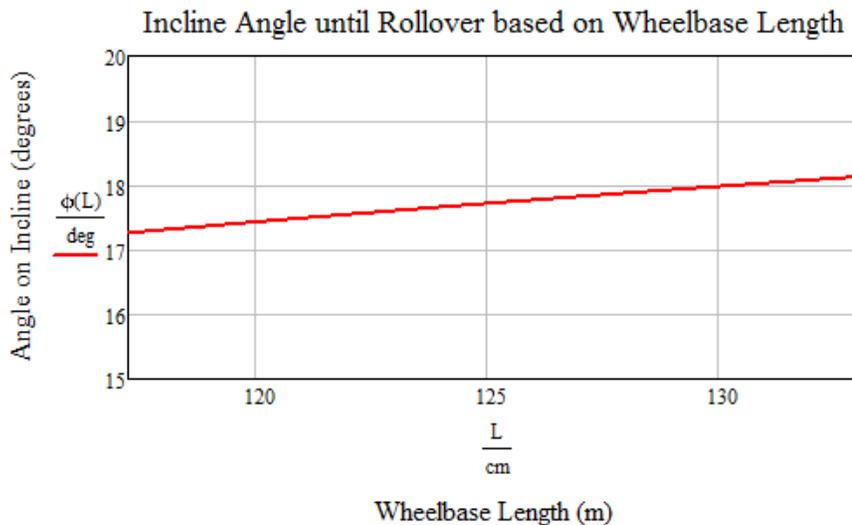


Figure 120: Maximum Incline Angle until Rollover, based on Wheelbase Length

When the wheelbase length is adjusted to 133 cm, the allowable angle of incline to ride across is 18.1°, whereas adjusted to 117 cm, it is 17.3°. For stability purposes, the tricycle should not go across a hill with an angle greater than 17°.

Stability when Turning on an Inclined Slope

Taking into account both the analysis from turning on a flat surface and going across a slope while inclined on its side, the maximum speed for any slope angle below the maximum slope to avoid tipping can be determined. Figure 121 shows a Free Body Diagram of the tricycle, taking into account the

lateral force when turning and the angle of the incline that the tricycle is turning about. From Figure 121, the variables are:

L = length from rear to front axle (wheelbase length) = min: 117 cm /max: 133 cm

l_1 = length from the center of gravity to the front axle (dependent on L)

l_2 = length from the center of gravity to the rear axle = 32.3 cm

b = width of the two-wheel axle = 70.6 cm

g = acceleration of gravity = 9.81 m/s² = 981 cm/s²

h = height of the center of gravity from the ground = 74.2 cm

θ = angle formed by the tipping axis and reference axis (dependent on L)

a = lateral acceleration

W = weight of the entire tricycle plus the maximum load it can carry (located at the CG)

Figure 121, the lateral force on the tricycle (which comes from Newton's second law) is shown as " $W*a/g$ " In order to include lateral force within the tipping moment equation (the moment about the TT Line in Figure 121), the angle θ must be included.

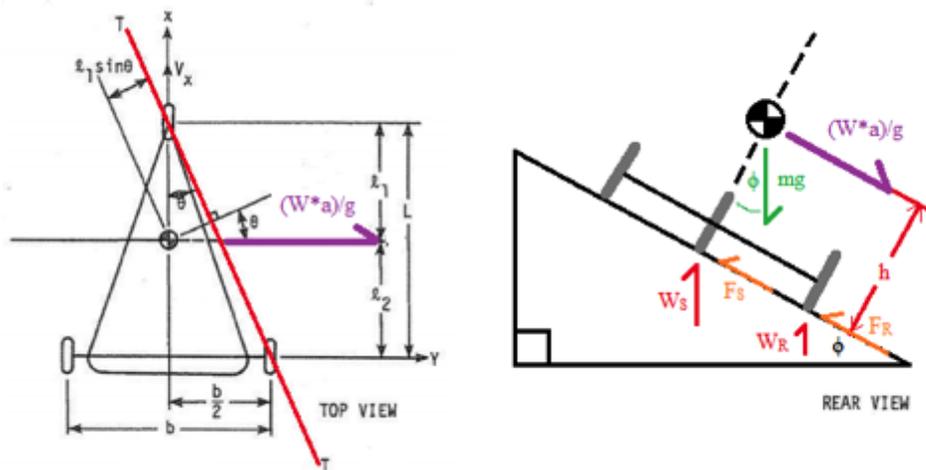


Figure 121: Free Body Diagram of Tricycle Turning on an Inclined Surface (Huston & Johnson, 1982)

A moment equation, about the tipping axis, can be evaluated from the model's top and rear view. It is assumed that counter clockwise rotation is positive and that $\phi = 17^\circ$ (since ϕ is considered independent to the change in velocity).

$$\begin{aligned} \sum M_{TT} &= - [mgh * \sin(17^\circ)] + [mg(l_1 * \sin(\theta))\cos(17^\circ)] - [mah * \cos(\theta)] = 0 \\ -[g * h * \sin(17^\circ)] + [g(l_1 * \sin(\theta))\cos(17^\circ)] - [a * h * \cos(\theta)] &= 0 \\ -[g * h * \sin(17^\circ)] + [g(l_1 * \sin(\theta))\cos(17^\circ)] &= [a * h * \cos(\theta)] \\ -\left(\frac{g \sin(17^\circ)}{\cos(\theta)}\right) + \left(\frac{g(l_1 * \tan(\theta))\cos(17^\circ)}{h}\right) &= a \end{aligned}$$

The equation for lateral acceleration “a” is:

$$a = \frac{v^2}{R}$$

Plugging in the lateral acceleration will determine the maximum velocity that tipping will occur. The velocity will depend on the wheelbase length (L) and the turning radius (R).

$$\begin{aligned} \frac{v^2}{R} &= -\left(\frac{g \sin(17^\circ)}{\cos(\theta)}\right) + \left(\frac{g(l_1 * \tan(\theta))\cos(17^\circ)}{h}\right) \\ v(R, L) &= \sqrt{R * \left[-\left(\frac{g \sin(17^\circ)}{\cos(\theta)}\right) + \left(\frac{g(l_1 * \tan(\theta))\cos(17^\circ)}{h}\right)\right]} \\ v(R, L) &= \sqrt{R * g * \left[-\left(\frac{\sin(17^\circ)}{\cos(\theta)}\right) + \left(\frac{(l_1 * \tan(\theta))\cos(17^\circ)}{h}\right)\right]} \end{aligned}$$

For L, the maximum (133 cm) and minimum (117 cm) wheelbase lengths will be used. Figure 121 shows the rollover velocity curve, using both maximum and minimum wheelbase length adjustments. These curves are based on the turning radius made with the tricycle.

Appendix D: Additional Design Considerations for Selection of Best Concepts

Table 42: Eric's Mechanism Pairwise Comparison Chart

Mechanism	Ergonomics	Safety	Conform to User Rqmts	Power Adjustability	Ease of Control	Manufacturability	Cost	Total
Ergonomics	-	1	0	0	1	1	1	4
Safety	0	-	0	0	0	1	1	2
Conform to User Rqmts	1	1	-	0.5	1	1	1	5.5
Power Adjustability	1	1	0.5	-	1	1	1	5.5
Ease of Control	0	1	0	0	-	0.5	1	2.5
Manufacturability	0	0	0	0	0.5	-	1	1.5
Cost	0	0	0	0	0	0	-	0

Table 43: Jaime's Mechanism Pairwise Comparison Chart

Mechanism	Ergonomics	Safety	Conform to User Rqmts	Power Adjustability	Ease of Control	Manufacturability	Cost	Total
Ergonomics	-	0	0.5	0	0.50	1	0	2
Safety	1	-	0.5	1	1	1	0.5	5
Conform to User Rqmts	0.5	0.5	-	1	1	0	0	3
Power Adjustability	1	0	0	-	1	1	1	4
Ease of Control	0.5	0	0	0	-	0.5	0	1
Manufacturability	0	0	1	0	0.5	-	0.5	2
Cost	1	0.5	1	0	1	0.5	-	4

Table 44: Nick's Mechanism Pairwise Comparison Chart

Mechanism	Ergonomics	Safety	Conform to User Req.	Power Adjustability	Ease of Control	Manufacturability	Cost	Total
Ergonomics	-	0	0	0	1	1	0	2
Safety	1	-	1	1	1	1	1	6
Conform to User Req.	1	0	-	1	0	0	0	2
Power Adjustability	1	0	0	-	1	1	1	4
Ease of Control	0	0	1	0	-	0	1	2
Manufacturability	0	0	1	0	1	-	0	2
Cost	1	0	1	0	0	1	-	3

Table 45: Henry's Mechanism Pairwise Comparison Chart

Mechanism	Ergonomics	Safety	Conform to User Rqmts	Power Adjustability	Ease of Control	Manufacturability	Cost	Total
Ergonomics	-	0.5	0	0	0.5	1	1	3
Safety	0.5	-	0.5	0	0.5	0	0.5	2
Conform to User Rqmts	1	0.5	-	0	0.5	0.5	1	3.5
Power Adjustability	1	1	1	-	0.5	1	1	5.5
Ease of Control	0.5	0.5	0.5	0.5	-	0.5	1	3.5
Manufacturability	0	1	0.5	0	0.5	-	0.5	2.5
Cost	0	0.5	0	0	0	0.5	-	1

Table 46: Eric's Power Mechanism Decision Matrix

Mechanisms	Criteria							Total
	Safety	Cost	Ergonomics	Ease of Control	Manufacturability	Conform to User Requirements	Power Adjustability	
Weighting Factors	18	5	11	10	5	16	35	
Piston	5	3	5	3	3	4	3	374
Motor	5	1	5	5	5	1	5	416
Planetary	5	4	3	5	3	5	3	393
Push Pedal	5	5	5	4	5	5	3	420
Spring Resistance	5	4	5	4	4	5	3	410
CVT	5	1	3	5	1	5	5	438

Table 47: Jaime's Power Mechanism Decision Matrix

Mechanisms	Criteria							Total
	Safety	Cost	Ergonomics	Ease of Control	Manufacturability	Conform to User Requirements	Power Adjustability	
Weighting Factors	18	5	11	10	5	16	35	
Piston	5	3	5	3	3	4	4	409
Motor	5	2	5	5	4	2	4	397
Planetary	5	4	3	5	3	5	4	428
Push Pedal	5	4	5	4	4	4	4	429
Spring Resistance	5	4	5	4	4	4	4	429
CVT	5	1	3	5	2	5	5	443

Table 48: Nick's Power Mechanism Decision Matrix

Mechanisms	Criteria							Total
	Safety	Cost	Ergonomics	Ease of Control	Manufacturability	Conform to User Requirements	Power Adjustability	
Weighting Factors	18	5	11	10	5	16	35	
Piston	5	3	4	3	3	4	4	398
Motor	5	2	4	5	4	2	5	421
Planetary	5	2	3	5	1	5	3	373
Push Pedal	5	3	5	3	3	4	4	409
Spring Resistance	5	3	4	3	3	4	4	398
CVT	5	1	3	5	1	5	5	438

Table 49: Henry's Mechanism Decision Matrix

Mechanisms	Criteria							Total
	Safety	Cost	Ergonomics	Ease of Control	Manufacturability	Conform to User Requirements	Power Adjustability	
Weighting Factors	18	5	11	10	5	16	35	
Piston	5	3	5	3	3	4	4	409
Motor	5	1	5	5	4	2	5	427
Planetary	5	2	3	4	2	5	3	368
Push Pedal	5	3	5	4	3	4	4	419
Spring Resistance	5	4	5	3	4	4	4	419
CVT	5	1	3	4	1	5	5	428

Table 50: Eric's Tricycle Component Pairwise Comparison Chart

Mechanism	Ergonomics	Safety	Conform to User Req.	Stability	Ease of Control	Manufacturability	Cost	Total
Ergonomics	-	0.5	0	0	1	1	1	3.5
Safety	0.5	-	1	0.5	1	1	1	5
Conform to User Req.	1	0	-	0.5	0.5	1	1	4
Stability	1	0.5	0.5	-	0.5	1	1	4.5
Ease of Control	0	0	0.5	0.5	-	1	1	3
Manufacturability	0	0	0	0	0	-	0.5	0.5
Cost	0	0	0	0	0	0.5	-	0.5

Table 51: Jaime's Component Pairwise Comparison Chart

Mechanism	Ergonomics	Safety	Conform to User Req.	Stability	Ease of Control	Manufacturability	Cost	Total
Ergonomics	-	0.5	0	0.5	0.5	1	1	3.5
Safety	0.5	-	0.5	0.5	1	1	1	4.5
Conform to User Req.	1	0.5	-	0.5	0.5	1	1	4.5
Stability	0.5	0.5	0.5	-	0.5	1	1	4
Ease of Control	0.5	0	0.5	0.5	-	1	1	3.5
Manufacturability	0	0	0	0	0	-	0.5	0.5
Cost	0	0	0	0	0	0.5	-	0.5

Table 52: Nick's Component Pairwise Comparison Chart

Mechanism	Ergonomics	Safety	Conform to User Req.	Stability	Ease of Control	Manufacturability	Cost	Total
Ergonomics	-	0.5	0.5	0	0.5	1	1	3.5
Safety	0.5	-	1	0.5	0	1	1	4
Conform to User Req.	0.5	0	-	0	1	1	0	2.5
Stability	1	0.5	1	-	0.5	0.5	0.5	4
Ease of Control	0.5	1	0	0.5	-	1	1	4
Manufacturability	0	0	0	0.5	0	-	0	0.5
Cost	0	0	1	0.5	0	1	-	2.5

Table 53: Henry's Component Pairwise Comparison Chart

Mechanism	Ergonomics	Safety	Conform to User Req.	Stability	Ease of Control	Manufacturability	Cost	Total
Ergonomics	-	0	1	0	0.5	0.5	1	3
Safety	1	-	1	0.5	0.5	1	1	5
Conform to User Req.	0	0	-	0.5	0.5	0.5	1	2.5
Stability	1	0.5	0.5	-	0.5	1	1	4.5
Ease of Control	0.5	0.5	0.5	0.5	-	1	1	4
Manufacturability	0.5	0	0.5	0	0	-	0.5	1.5
Cost	0	0	0	0	0	0.5	-	0.5

Table 54: Nick's Tricycle Component Decision Matrix

Mechanisms	Criteria							Total
	Safety	Cost	Ergonomics	Ease of Control	Manufacturability	Conform to User Requirements	Stability	
Weighting Factors	20	10	14	16	8	14	18	
1 (Rear, Tiller, Disc)	5	3	4	4	3	3	2	352
2 (Front, Handle Bars, Drum)	5	4	4	3	4	5	4	418
3 (Front, Handle Bars, Disc)	5	4	4	3	4	5	4	418
4 (Front, Tiller, Drum)	5	4	4	4	3	5	4	426
5 (Front, Tiller, Disc)	5	3	4	4	3	5	4	416
6 (Four, Tiller, Disc)	5	2	3	4	3	5	5	410

Table 55: Henry's Tricycle Component Decision Matrix

Mechanisms	Criteria							Total
	Safety	Cost	Ergonomics	Ease of Control	Manufacturability	Conform to User Requirements	Stability	
Weighting Factors	20	10	14	16	8	14	18	
1 (Rear, Tiller, Disc)	5	3	3	5	3	5	3	400
2 (Front, Handle Bars, Drum)	5	4	3	3	4	3	4	376
3 (Front, Handle Bars, Disc)	5	3	3	3	4	5	4	394
4 (Front, Tiller, Drum)	5	3	3	5	3	3	4	390
5 (Front, Tiller, Disc)	5	3	3	5	3	5	4	418
6 (Four, Tiller, Disc)	5	2	3	4	3	5	5	410

Table 56: Jaime's Tricycle Component Decision Matrix

Mechanisms	Criteria							Total
	Safety	Cost	Ergonomics	Ease of Control	Manufacturability	Conform to User Requirements	Stability	
Weighting Factors	20	10	14	16	8	14	18	
1 (Rear, Tiller, Disc)	5	3	3	5	3	5	3	400
2 (Front, Handle Bars, Drum)	5	4	3	3	4	3	4	376
3 (Front, Handle Bars, Disc)	5	4	3	4	4	5	4	420
4 (Front, Tiller, Drum)	5	4	3	4	2	3	4	376
5 (Front, Tiller, Disc)	5	3	3	5	3	5	4	418
6 (Four, Tiller, Disc)	5	2	3	2	3	5	5	378

Table 57: Eric's Component Decision Matrix

Mechanisms	Criteria							Total
	Safety	Cost	Ergonomics	Ease of Control	Manufacturability	Conform to User Requirements	Stability	
Weighting Factors	20	10	14	16	8	14	18	
1 (Rear, Tiller, Disc)	5	3	3	4	3	5	4	402
2 (Front, Handle Bars, Drum)	5	3	3	3	4	3	3	348
3 (Front, Handle Bars, Disc)	5	5	3	3	4	5	3	396
4 (Front, Tiller, Drum)	5	3	3	4	3	5	3	384
5 (Front, Tiller, Disc)	5	4	3	5	4	5	3	418
6 (Four, Tiller, Disc)	5	2	3	3	3	5	5	394

Appendix E: Propulsive Force Calculations

In order to analyze the designs, the forces required by the user to propel the device forward must be calculated. With these forces, and an assumed gear ratio, the required input torque can be found for which the user must overcome. From this required input torque, the designs can be individually analyzed to determine the assistive potential of the device. The discussion of this analysis is on Page 60.

$$\begin{aligned}
 r_{\text{wheel}} &:= 0.270\text{m} & \rho &:= 1.225 \frac{\text{kg}}{\text{m}^3} & A_{\text{cross}} &:= 1.5\text{m}^2 & \text{friction_coeff} &:= 0.004 \\
 & & & & & & \text{drag_coeff} &:= 0.8 \\
 v_1 &:= 0 \frac{\text{m}}{\text{s}} & m_{\text{trike}} &:= 115\text{lb} & \text{sprock_front} &:= 53 \\
 v_2 &:= 10 \frac{\text{m}}{\text{s}} & m_{\text{rider}} &:= 250\text{lb} & \text{sprock_rear} &:= 39 \\
 v &:= v_1, 0.1 \frac{\text{m}}{\text{s}} .. v_2 \\
 f_{\text{friction}} &:= \text{friction_coeff} \cdot 9.81 \frac{\text{m}}{\text{s}^2} \cdot (m_{\text{trike}} + m_{\text{rider}}) = 6.497 \cdot \text{N} \\
 f_{\text{wind}}(v) &:= \left(\frac{1}{2}\right) \cdot \rho \cdot v^2 \cdot \text{drag_coeff} \cdot A_{\text{cross}} \\
 f_{\text{sum}}(v) &:= f_{\text{friction}} + f_{\text{wind}}(v) \\
 \text{torque_wheel}(v) &:= f_{\text{sum}}(v) \cdot r_{\text{wheel}} \\
 \text{bike_ratio} &:= \frac{\text{sprock_front}}{\text{sprock_rear}} \\
 \text{torque_crank}(v) &:= \text{torque_wheel}(v) \cdot \text{bike_ratio} \\
 \text{torque_crank}\left(10 \frac{\text{m}}{\text{s}}\right) &= 29.353 \cdot \text{N} \cdot \text{m} \\
 \text{wheel_circ} &:= \pi \cdot (r_{\text{wheel}} \cdot 2) \\
 \omega_1(v) &:= \frac{v}{\text{wheel_circ}} \\
 \omega_2(v) &:= (\omega_1(v) \cdot \text{bike_ratio}) \cdot 360 \\
 \omega_2\left(10 \frac{\text{m}}{\text{s}}\right) &= 2.884 \times 10^3 \frac{1}{\text{s}}
 \end{aligned}$$

Appendix F: Additional Design Considerations for Selection of Final Design

Table 58: Henry's Decision Matrix for Final Mechanism Design

Criteria								
Mechanisms	Safety	Cost	Ergonomics	Ease of Control	Manufacturability	Conform to User Requirements	Power Adjustability	
Weighting Factors	18	5	11	10	5	16	35	Total
Piston	5	3	4	3	3	3	4	382
Push Pedal	5	2	4	3	2	3	4	372
Spring Resistance	5	4	4	3	4	3	4	392

Table 59: Nick's Decision Matrix for Final Mechanism Design

Criteria								
Mechanisms	Safety	Cost	Ergonomics	Ease of Control	Manufacturability	Conform to User Requirements	Power Adjustability	
Weighting Factors	18	5	11	10	5	16	35	Total
Piston	5	2	4	4	3	3	4	387
Push Pedal	5	3	4	3	4	3	4	387
Spring Resistance	5	4	4	3	4	3	4	392

Table 60: Jaime's Decision Matrix for Final Mechanism Design

		Criteria						
Mechanisms	Safety	Cost	Ergonomics	Ease of Control	Manufacturability	Conform to User Requirements	Power Adjustability	
Weighting Factors	18	5	11	10	5	16	35	Total
Piston	5	3	4	3	3	3	4	382
Push Pedal	5	2	5	3	3	3	4	388
Spring Resistance	5	4	5	3	4	3	4	403

Table 61: Eric's Decision Matrix for Final Mechanism Design

		Criteria						
Mechanisms	Safety	Cost	Ergonomics	Ease of Control	Manufacturability	Conform to User Requirements	Power Adjustability	
Weighting Factors	18	5	11	10	5	16	35	Total
Piston	5	3	4	5	3	4	4	418
Push Pedal	5	2	4	4	3	4	4	403
Spring Resistance	5	4	5	5	4	4	4	439

Appendix G: Spring Bracket Analysis

The purpose of this analysis is to determine its safety factor against failing when a spring load of 1000N is applied. The purpose of this analysis is discussed in detail on Page 92.

Input Parameters:

Geometric:

Angle Bracket Width:	$w := 0.0762\text{m}$
Angle Bracket Side Length:	$L := 0.0381\text{m}$
Bracket Thickness:	$t := 0.00635\text{m}$
Hole Location:	$a := \frac{L}{2} = 0.019\text{m}$
Hole Diameter:	$d := 0.00635\text{m}$

Material Properties (Aluminum 6061 Heat Treated):

Tensile Yield Strength:	$S_y := 27\text{MPa}$
Ultimate Tensile Strength:	$S_{ut} := 31\text{MPa}$

Loading:

Applied Force:	$F := 1000\text{N}$
Moment at Point B:	$M_B := F \cdot (a) = 168.607\text{lb}\cdot\text{in}$

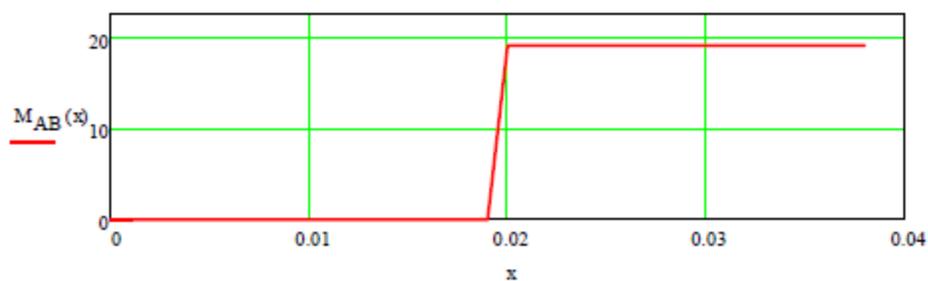
Static Analysis (AB):

Singularity Function: $S(x, z) := \text{if}(x \geq z, 1, 0)$

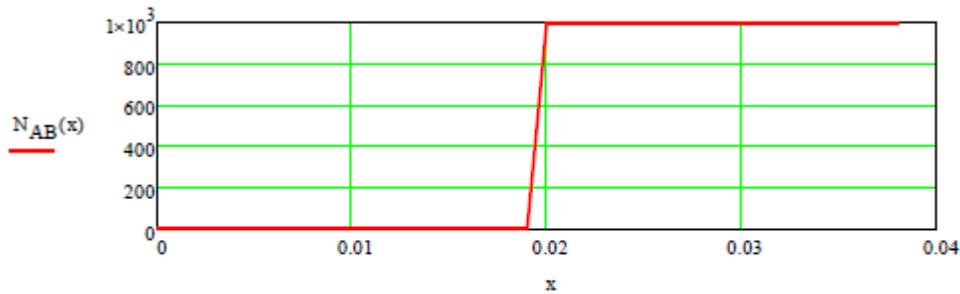
Domain of X: $x := 0\text{m}, 0.001\text{m}..L$

Moment Reaction: $M_R := M_B = 19.05\text{N}\cdot\text{m}$

Moment Function: $M_{AB}(x) := M_R \cdot (x - a)^0 \cdot S(x, a) - M_R \cdot (x - L)^0 \cdot S(x, L)$



Normal Force: $N_{AB}(x) := F \cdot (x - a)^0 \cdot S(x, a) - F \cdot (x - L)^0 \cdot S(x, L)$



Geometric Properties of Critical Section:

$$\frac{A}{w} := \frac{(w - d)}{2} \cdot t = 2.218 \times 10^{-4} \text{ m}^2$$

$$I := \frac{1}{12} \cdot \frac{w - d}{2} \cdot t^3 = 7.452 \times 10^{-10} \text{ m}^4$$

$$r_x := \frac{t}{2} = 3.175 \times 10^{-3} \text{ m}$$

Loading At Critical Section:

$$M_{\text{crit}} := M_{AB}(a) = 168.607 \cdot \text{lb} \cdot \text{in}$$

$$N_{\text{crit}} := N_{AB}(a) = 1 \times 10^3 \text{ N}$$

Stress Concentration Factors at Critical Section:

Discontinuity Ratio: $\frac{R}{w} := \frac{d}{w} = 0.083$

Axial Stress Concentration Factor:

$$K_{\text{axial}} := 3.0039 - 3.753 \cdot R + 7.9735 \cdot R^2 - 9.2659 \cdot R^3 + 1.8145 \cdot R^4 + 2.9684 \cdot R^5 = 2.741$$

Bending Stress Concentration Factor:

$$K_{\text{bend}} := 2.9947 - 3.4833 \cdot R + 5.8268 \cdot R^2 - 4.1986 \cdot R^3 = 2.742$$

Stresses at Critical Point:

$$\sigma_{\text{axial}} := \frac{N_{\text{crit}}}{A} \cdot K_{\text{axial}} = 12.361 \cdot \text{MPa}$$

$$\sigma_{\text{bend}} := \frac{M_{\text{crit}} \cdot c}{I} \cdot K_{\text{bend}} = 222.588 \cdot \text{MPa}$$

$$\sigma_x := \sigma_{\text{axial}} + \sigma_{\text{bend}} = 234.949 \cdot \text{MPa}$$

$$\sigma_z := 0 \cdot \text{MPa}$$

$$\tau_{xz} := 0 \cdot \text{MPa}$$

Principle Stresses:

$$\tau_{\text{max}} := \sqrt{\left(\frac{\sigma_x - \sigma_z}{2}\right)^2 + \tau_{xz}^2} = 117.475 \cdot \text{MPa}$$

$$\sigma_1 := \frac{\sigma_x + \sigma_z}{2} + \tau_{\text{max}} = 234.949 \cdot \text{MPa}$$

$$\sigma_2 := 0 \cdot \text{MPa}$$

$$\sigma_3 := \frac{\sigma_x + \sigma_z}{2} - \tau_{\text{max}} = 0 \cdot \text{Pa}$$

Von-Mises Equivalent Stress:

$$\sigma'_{\text{AB}} := \sqrt{\sigma_1^2 - \sigma_1 \cdot \sigma_3 + \sigma_3^2} = 234.949 \cdot \text{MPa}$$

Static Safety Factor:

$$\text{Distortion Energy Theory: } N_{\text{DST}} := \frac{S_y}{\sigma'_{\text{AB}}} = 1.175$$

Bearing Analysis at Pt. A:

$$\text{Bearing Area: } A_{\text{bearing}} := \frac{\pi}{4} \cdot t \cdot d = 3.167 \times 10^{-5} \cdot \text{m}^2$$

$$\text{Bearing Stress: } \sigma_{\text{bearing}} := \frac{F}{A_{\text{bearing}}} = 31.576 \cdot \text{MPa}$$

$$\text{Bearing Safety Factor: } N_{\text{bearing}} := \frac{S_y}{\sigma_{\text{bearing}}} = 8.741$$

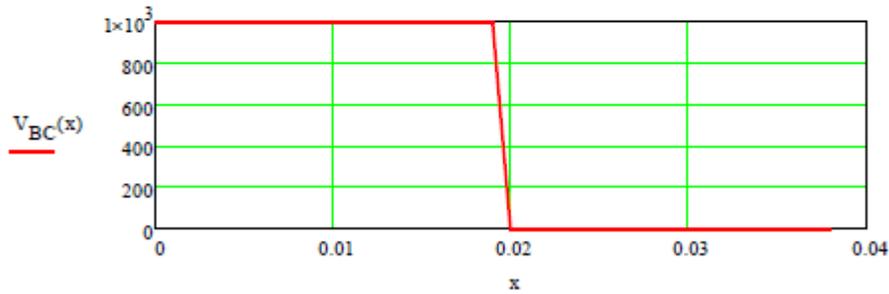
Static Analysis (BC):

Reactions: $M_{RB} := F \cdot a = 19.05 \text{ N}\cdot\text{m}$

$$R_B := F = 1 \times 10^3 \text{ N}$$

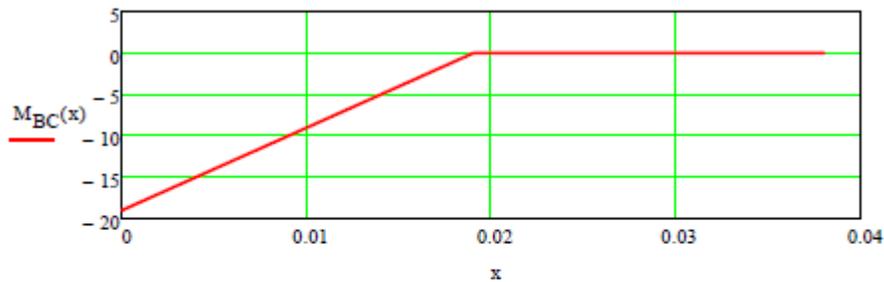
Shear Function:

$$V_{BC}(x) := R_B \cdot (x - 0)^0 \cdot S(x, 0) - F \cdot (x - a)^0 \cdot S(x, a)$$



Moment Function:

$$M_{BC}(x) := -M_{RB} \cdot (x - 0)^0 \cdot S(x, 0) + R_B \cdot (x - 0)^1 \cdot S(x, 0) - F \cdot (x - a)^1 \cdot S(x, a)$$



The Critical Section Occurs at $X = 0$

Fretting Concentration Factor: $K_t := 2$

Applied Stresses:

Max Bending Stress: $\sigma_{xBC} := \frac{M_{BC(0m)} \cdot c}{I} \cdot K_t = -162.328 \text{ MPa}$

$$\sigma_{zBC} := 0 \text{ MPa}$$

Max Shear Stress: $\tau_{BC} := \frac{V_{BC}(0in)}{A} \cdot K_t = 9.018 \cdot \text{MPa}$

Principle Stresses:

$$\tau_{\max BC} := \sqrt{\left(\frac{\sigma_{xBC} - \sigma_{zBC}}{2}\right)^2 + \tau_{BC}^2} = 81.663 \cdot \text{MPa}$$

$$\sigma_{1BC} := \frac{\sigma_{xBC} + \sigma_{zBC}}{2} + \tau_{\max BC} = 0.499 \cdot \text{MPa}$$

$$\sigma_{3BC} := \frac{\sigma_{xBC} + \sigma_{zBC}}{2} - \tau_{\max BC} = -162.827 \cdot \text{MPa}$$

Von Mises Stress:

$$\sigma'_{BC} := \sqrt{\sigma_{1BC}^2 - \sigma_{1BC} \cdot \sigma_{3BC} + \sigma_{3BC}^2} = 163.077 \cdot \text{MPa}$$

Safety Factor Using Distortion Energy: $N_{BC} := \frac{S_y}{\sigma'_{BC}} = 1.692$

Appendix H: Seat Extender Buckling Analysis Calculations

Eccentric Buckling Analysis

The purpose of this analysis is to identify the critical eccentric buckling load applied to each side plate within the seat extender. Eccentricity, e , has been taken as the distance from the neutral axis (z) of the column cross section (Figure 2) to the axis of applied load equidistant from each plate in the extender. The free body diagram for this analysis is shown in Figure 1.

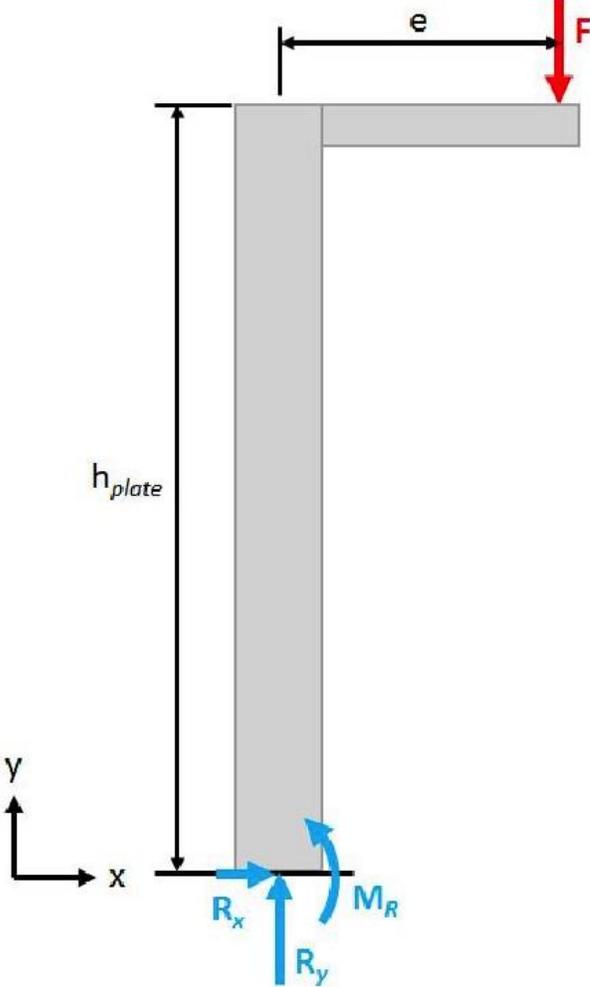


Figure 1

Note that the methodology for this analysis does not require that the reaction forces and moments be applied. The bottom section which is attached to the tricycle frame is considered rigid and the appropriate boundary condition has been applied within the Secant equation.

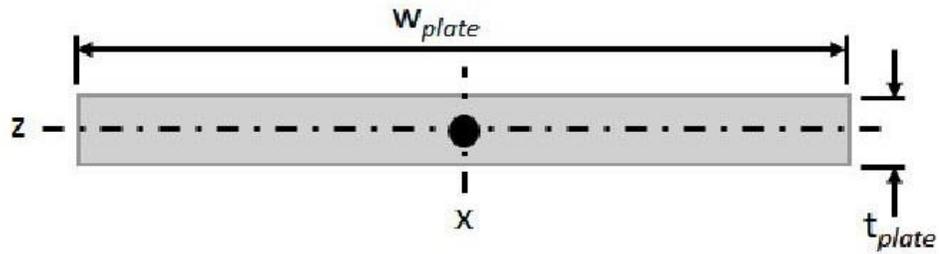


Figure 2

Geometric Parameters:

Width of Plate:	$w_{plate} := 5.5\text{in}$	
Height of Plate	$h_{plate} := 8\text{in}$	
Plate Thickness:	$t_{plate} := 0.1046\text{in}$	12G Steel Sheet
Eccentricity:	$e := 1.125\text{in}$	

Material Properties (AISI 1010 - Cold Rolled):

Modulus of Elasticity:	$E := 30 \cdot 10^6 \text{psi}$
Tensile Yield Strength:	$S_y := 44\text{ksi}$

Loading Parameters:

Applied Vertical Load:	$F := \frac{250}{2} \text{lbf}$
------------------------	---------------------------------

Properties of Cross Section:

Area:	$A := w_{plate} \cdot t_{plate}$	$A = 0.575 \cdot \text{in}^2$
Moment of Inertia:	$I := \frac{w_{plate} \cdot t_{plate}^3}{12}$	$I = 5.245 \times 10^{-4} \cdot \text{in}^4$
Max Fiber Distance:	$c := \frac{t_{plate}}{2}$	$c = 0.052 \text{in}$

Column Properties:

Radius of Gyration: $k := \sqrt{\frac{I}{A}}$ $k = 0.03 \text{ in}$

Eccentricity Ratio: $E_r := \frac{e \cdot c}{k^2}$ $E_r = 64.532$

Effective Length: $l_{\text{eff}} := 2.1 \cdot h_{\text{plate}}$ $l_{\text{eff}} = 16.8 \text{ in}$

Slenderness Ratio: $S_r := \frac{l_{\text{eff}}}{k}$ $S_r = 556.376$

Critical Buckling Force:

Initial Guess Value: $P := 1000 \text{ lbf}$

Given

$$P = \frac{S_y \cdot A}{1 + E_r \cdot \sec\left(S_r \cdot \sqrt{\frac{P}{4 \cdot E \cdot A}}\right)}$$

Secant equation for eccentrically loaded columns.

Critical Buckling Force: $P_{\text{crit}} := \text{Find}(P)$ $P_{\text{crit}} = 215.596 \text{ lbf}$

Safety Factors:

Safety Factor for Column: $N := \frac{P_{\text{crit}}}{F}$ $N = 1.725$

Appendix I: Qualitative Testing Procedures

Locations:

1. WPI's Quadrangle (In Red, *Figure 122*). The test will occur on the paved path along the outside of the quadrangle. This section of the quadrangle is level, and is not open to vehicular traffic.

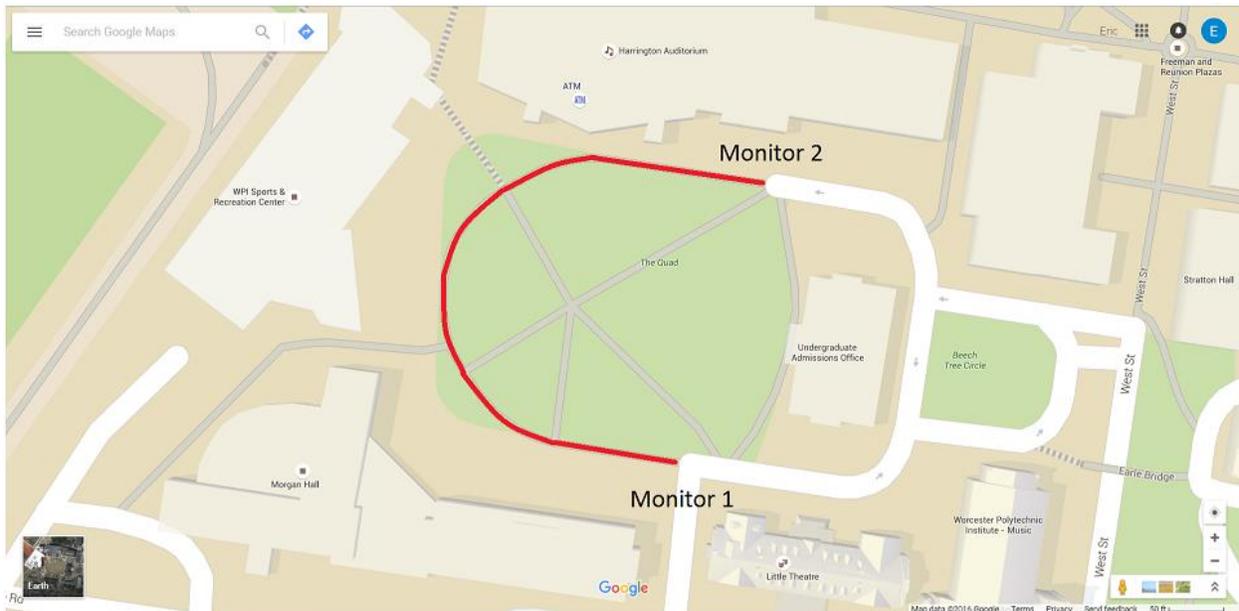


Figure 122: Test Path Along the Quadrangle (Google, 2016)

Testing Procedure: The test subjects will be asked to complete the following tasks:

1. Pass a pre-test which will ensure the subject is fit to take part in the study. The pre-test will consist of the successfully accomplishing the following tasks:
 - i. Stand on one foot for 5 seconds (to demonstrate balance).
 - ii. Bend the hip so the thigh is horizontal and the calf is vertical while standing (with each leg, to demonstrate range of motion).
 - iii. Walk heel-to-toe for 10 steps (to demonstrate coordination).
 - iv. Walk normally for 10 steps (to demonstrate strength)
 - v. Apply the brake on the tricycle while stationary (to ensure the subject can apply the brake while the tricycle is in motion)
 - vi. The subjects will also be asked their height and which weight category they fall into: 100-125, 125-150, 150-175, 150-175, 175-200, 200-225, or 225-250 pounds

2. Ride the tricycle through a pre-determined length of the course in a given time. This procedure will ensure that the subjects can achieve and maintain the desired 5 MPH speed.
3. Ride the tricycle along the test path around WPI's Quadrangle (a spotter will be at both ends of the course).
4. Complete a survey detailing the operation of the tricycle (see below).

Survey:

On a scale of 1 to 5, please rank how well the tricycle fulfills each category. The specific meaning of 1, 3, and 5 are provided for each question. After providing a numerical score for each question, please provide additional comments for why you chose this value.

1. What is your experience level riding bicycles?

Inexperienced		Somewhat Experienced		Very experienced
1	2	3	4	5

Comments:

2. How easily could the tricycle be adjusted to fit your height?

Could Not Adjust to My Height		Somewhat Difficult		Easily
1	2	3	4	5

Comments:

3. How comfortable did you find the recumbent pedaling position?

Not at All		Somewhat		Very
1	2	3	4	5

Comments:

4. How easy was it to adapt to the pedaling style?

Challenging		Neutral		Easy
-------------	--	---------	--	------

1 2 3 4 5

Comments:

5. How often did the components of the device intrude into your pedaling space?

Frequently Occasionally Never
1 2 3 4 5

Comments:

6. How easy was the device to steer?

Difficult Neutral Easy
1 2 3 4 5

Comments:

7. How easy was the steering technique to learn?

Difficult Neutral Easy
1 2 3 4 5

Comments:

8. How intuitive was the braking system to operate?

Not at All Somewhat Very
1 2 3 4 5

Comments:

9. When the brakes were applied, how well did the tricycle stop?

Not Well at All Somewhat Well Very Well
1 2 3 4 5

Comments:

10. How well did your feet remain on the pedals?

Not Well at All Somewhat Well Very Well
1 2 3 4 5

Comments:

11. How comfortable was the seat?

Not at All Somewhat Very
1 2 3 4 5

Comments:

12. How stable did you feel on the tricycle ?

Not at All

Somewhat

Very

1

2

3

4

5

Comments:

General Questions:

13. What did you think was the best feature about the tricycle ?

14. What did you think was the worst feature of the tricycle ?

15. Do you have any other comments or suggestions?

Appendix J: Quantitative Testing Procedure

Setting up the Force Sensors

Prior to conducting the test, it was important to ensure that it was set up properly. Each of the two force sensors must be properly assembled with 3 load cells glued to the backer plate and foot plate in the proper triangular configuration. Next, one force sensor was fixed to the top of each pedal using cable ties in between the backer and foot plate. It was ensured that the wires from the force sensors to the conditioning circuits were long enough to avoid getting tangled during a pedaling cycle. Finally, the system was powered up to make sure it recorded data correctly.

Setting up the Test Course

The tests described herein required both a straight length of dry, flat pavement, and a straight length of inclined, dry pavement between 3 and 5 degrees. The test course (Figure 123) consisted of 2 zones, the acceleration zone and the sustained speed zone. Zones were discretized using 3 lines, made up of lengths of tape on the pavement, including the “Start” line, the “Sustain” line, and the “Brake” line. In between each line there were tape markers evenly spaced every 1m apart. The purpose of these lines is described in further detail in the test procedure.

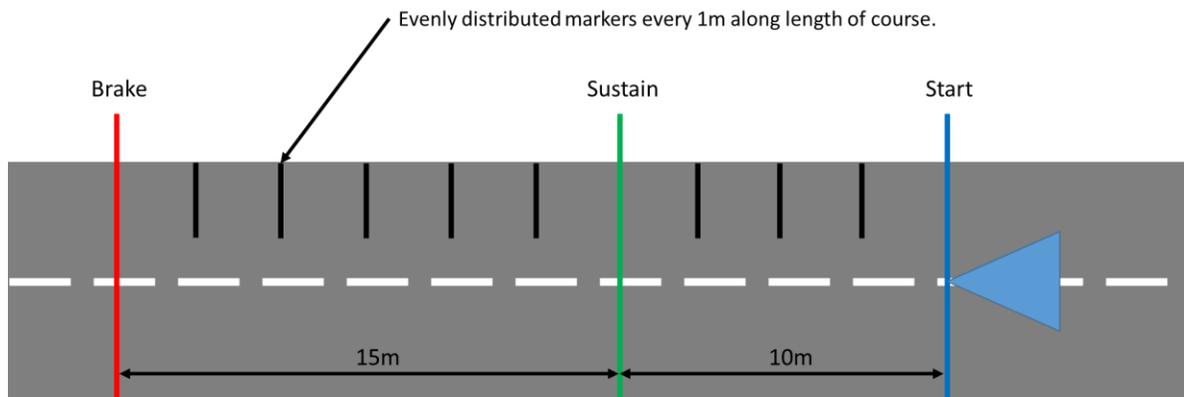


Figure 123: Test Course Diagram

Calibration

The load cells used for testing employ strain gauges to determine applied force. This outputs to a computer as a change in resistance. Values recorded by the computer without proper calibration will not reflect the actual force applied. However, because strain gauges output change in resistance linearly with change in strain, only two known applied loads were necessary for calibration. The following steps outline how the force sensors were calibrated:

1. With the computer constantly displaying the current strain force sensor output, a 10lbf weight was placed on top of the foot plate while taking note of the output value.
2. Similarly, a 20lbf weight was placed on the sensor while taking note of the output value.
3. The calibration constants were then adjusted in the weight sensing code with the actual values output from the two weights.
4. The code was then re-uploaded to the Arduino.
5. The calibration was validated by placing the weights back on the sensor and recording the output and checked with several other known weights.

Combined Transient and Steady State Testing

The combined transient and steady state test was intended to evaluate the assistance performance of the tricycle under both “pedaling to accelerate” and “pedaling to sustain” conditions. With data being recorded for the entire test, the operator accelerated the tricycle from rest to a constant and smooth pedaling motion, and maintained this for 15m before braking to a stop. The same operator was used for every test, ensuring they stayed consistent with their pedaling, this allowed the data to still be comparable even without knowing the exact traveling speed. Using data from the duration of the test it was possible to determine the transient and steady state force profiles. These curves were then be analyzed for performance characteristics. This test was first performed on dry, flat pavement and then repeated on dry, inclined pavement of between 3 and 5 degrees. The following steps outline the procedure for this test:

1. The front of the tricycle was positioned on the “Start” line. The front wheel was then lifted, allowing it to spin freely, and the pedals rotated so they are horizontal and the spring was in its nominal position.
2. The test operator then sat in the tricycle and a secondary operator was ready to guide any power/data cables along while the tricycle moved so they did not get tangled.
3. The load sensor system was then powered up.
4. Data recording was started.
5. From rest at the “Start Line” the operator began pedaling up to 1.5m/s, ensuring to reach this speed by the time the “Sustain” line was reached.
6. Once the “Sustain” line was reached, a constant speed was maintained until the “Brake” line was reached.
7. The operator broke to a complete stop.
8. Data recording was stopped and the file saved while taking note of the spring used in the test.
9. Steps 1 through 9 were then repeated with all 3 available springs.

Once all data are collected, force curves vs time can be generated for each foot and spring constant. By comparing the results from one foot to the other, it will be possible to determine the actual assistance level provided by the spring mechanism.

Appendix K: Updated Subject Testing Procedure

Locations:

2. WPI's Quadrangle (In Red, *Figure 124*). The test will occur on the paved path along the outside of the quadrangle. This section of the quadrangle is level, and is not open to vehicular traffic.

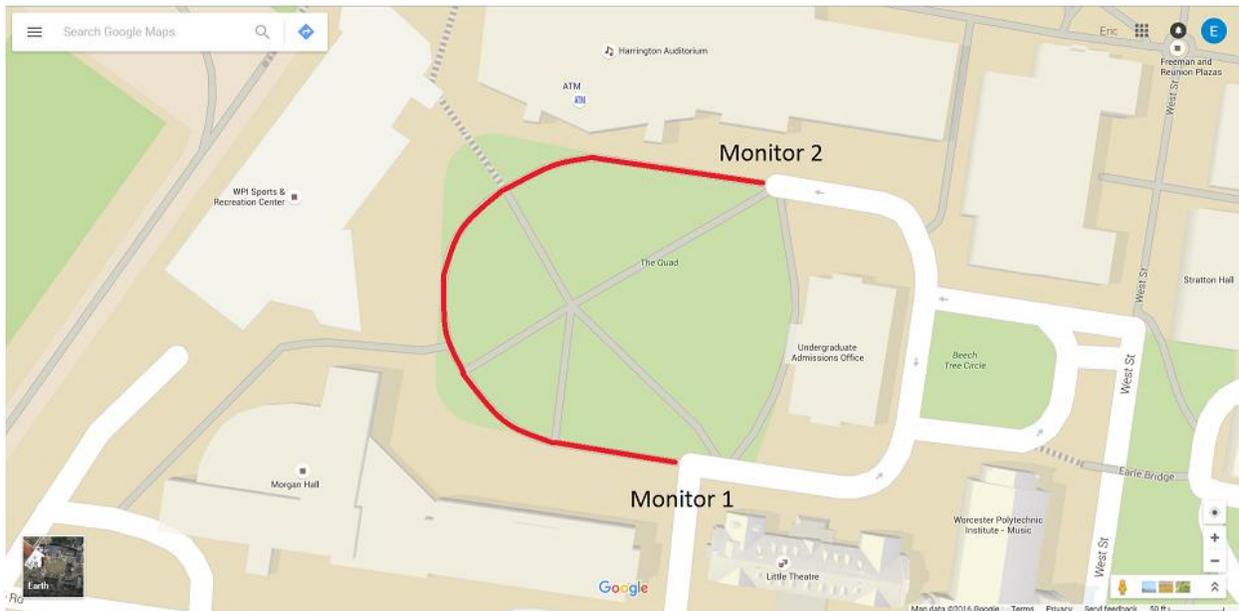


Figure 124: Test Path along the Quadrangle (Google, 2016)

Testing Procedure: The test subjects will be asked to complete the following tasks:

5. Pass a pre-test which will ensure the subject is fit to take part in the study. The pre-test will consist of the successfully accomplishing the following tasks:
 - i. Stand on one foot for 5 seconds (to demonstrate balance).
 - ii. Bend the hip so the thigh is horizontal and the calf is vertical while standing (with each leg, to demonstrate range of motion).
 - iii. Walk heel-to-toe for 10 steps (to demonstrate coordination).
 - iv. Walk normally for 10 steps (to demonstrate strength)
 - v. Apply the brake on the tricycle while stationary (to ensure the subject can apply the brake while the tricycle is in motion)
 - vi. The subjects will also be asked their height and which weight category they fall into: 100-125, 125-150, 150-175, 150-175, 175-200, 200-225, or 225-250 pounds

6. Ride the tricycle through a pre-determined length of the course in a given time. This procedure will ensure that the subjects can achieve and maintain the desired 5 MPH speed.
7. Ride the tricycle along the test path around WPI's Quadrangle (a spotter will be at both ends of the course).
8. Complete a survey detailing the operation of the tricycle (see below).

Survey:

On a scale of 1 to 5, please rank how well the tricycle fulfills each category. The specific meaning of 1, 3, and 5 are provided for each question. After providing a numerical score for each question, please provide additional comments for why you chose this value.

1. What is your experience level riding bicycles?

Inexperienced		Somewhat Experienced		Very experienced
1	2	3	4	5

Comments:

2. How easily could the tricycle be adjusted to fit your height?

Could Not Adjust to My Height		Somewhat Difficult		Easily
1	2	3	4	5

Comments:

3. How comfortable did you find the recumbent pedaling position?

Not at All		Somewhat		Very
1	2	3	4	5

Comments:

4. How easy was it to adapt to the pedaling style?

Challenging		Neutral		Easy
-------------	--	---------	--	------

1 2 3 4 5

Comments:

5. How often did the components of the device intrude into your pedaling space?

Frequently Occasionally Never
1 2 3 4 5

Comments:

6. How easy was the device to steer?

Difficult Neutral Easy
1 2 3 4 5

Comments:

7. How easy was the steering technique to learn?

Difficult Neutral Easy
1 2 3 4 5

Comments:

8. How intuitive was the braking system to operate?

Not at All Somewhat Very

1 2 3 4 5

Comments:

9. When the brakes were applied, how well did the tricycle stop?

Not Well at All		Somewhat Well		Very Well
1	2	3	4	5

Comments:

10. How well did your feet remain on the pedals?

Not Well at All		Somewhat Well	Very Well	
1	2	3	4	5

Comments:

11. How comfortable was the seat?

Not at All		Somewhat		Very
1	2	3	4	5

12. How stable did you feel on the tricycle ?

Comments:

Not at All		Somewhat		Very
1	2	3	4	5

Comments:

General Questions:

13. What did you think was the best feature about the tricycle ?

14. What did you think was the worst feature of the tricycle ?

15. Do you have any other comments or suggestions?

Appendix L: Subject Testing Results

Table 62: Subject's Comments to Subject Testing Questions

Question	Comments
1	<ul style="list-style-type: none"> • Never learned to ride a bike • I can ride pretty well
2	<ul style="list-style-type: none"> • I have short legs so it worked perfectly without adjustment • adjusting height affected brake cable
3	<ul style="list-style-type: none"> • None
4	<ul style="list-style-type: none"> • It was smooth
5	<ul style="list-style-type: none"> • No obstruction • Toes were slightly touching spring screw
6	<ul style="list-style-type: none"> • Turning radius was wide • Sudden turns at high speeds
7	<ul style="list-style-type: none"> • None
8	<ul style="list-style-type: none"> • Brakes loosened frequently
9	<ul style="list-style-type: none"> • Just needs to be tightened; otherwise perfect • 1 sec delay
10	<ul style="list-style-type: none"> • The position of the pedals paired with the position of my seat made it easier
11	<ul style="list-style-type: none"> • Slightly wobbly; otherwise fine
12	<ul style="list-style-type: none"> • can't really fall off a tricycle • as stable as any 3 wheel vehicle can be,
Best Feature of the Tricycle	<ul style="list-style-type: none"> • Intuitive to use • Really easy to sit and pedal and it was comfortable • Easy to operate even having never ridden a bike before • Flame graphic • Turned very well, great pedal positioning • Ease of use
Worst Feature of the Tricycle	<ul style="list-style-type: none"> • Brakes could have been more responsive • Chain fell off • Chain kept coming off • Wobbly seat
Other Suggestions:	<ul style="list-style-type: none"> • Responsive brakes • Add a chain guard • Fix the alignment on the sprockets